

General Disclaimer

One or more of the Following Statements may affect this Document

- This document has been reproduced from the best copy furnished by the organizational source. It is being released in the interest of making available as much information as possible.
- This document may contain data, which exceeds the sheet parameters. It was furnished in this condition by the organizational source and is the best copy available.
- This document may contain tone-on-tone or color graphs, charts and/or pictures, which have been reproduced in black and white.
- This document is paginated as submitted by the original source.
- Portions of this document are not fully legible due to the historical nature of some of the material. However, it is the best reproduction available from the original submission.

PROCEEDINGS OF THE SPACE OPTICAL TECHNOLOGY CONFERENCE VOL. I

(H.C.) \$7.00
(M.F.) \$1.65

APRIL 1966

N 68-31759
(ACCESSION NUMBER)

N 68-31773
(THRU)

156
(PAGES)

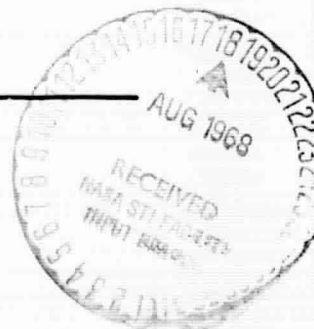
(CODE)

TMX-61037
(NASA CR OR TMX OR AD NUMBER)

07
(CATEGORY)



MARSHALL SPACE FLIGHT CENTER
HUNTSVILLE, ALA.

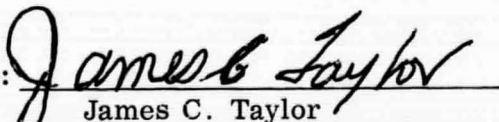


NASA-GEORGE C. MARSHALL SPACE FLIGHT CENTER

SPACE OPTICAL TECHNOLOGY CONFERENCE
HELD NOVEMBER 2-4, 1965, AT
GEORGE C. MARSHALL SPACE FLIGHT CENTER
VOLUME I

George C. Marshall Space Flight Center
Huntsville, Alabama

APPROVED:


James C. Taylor
Chief, Applied Research Branch

PRECEDING PAGE BLANK NOT FILMED.

TABLE OF CONTENTS

	Page
PARTICIPATION OF AMES RESEARCH CENTER IN THE MSC-4 EXPERIMENT by Norman S. Johnson, Ames Research Center	1 ✓
RADOT, 60.96-CM (24-IN.) MULTIMODE TELESCOPE AND FUTURE FACILITIES by Walter J. Carrion, Goddard Space Flight Center	9 ✓
ANALYSIS OF A TEN-MICRON COMMUNICATION SYSTEM by Nelson McAvoy, Goddard Space Flight Center	17 ✓
SPHERICAL MIROS by P. O. Minott, Goddard Space Flight Center	33 ✓
THE OPTICAL IMAGING SYSTEMS FOR RANGER, MARINER, AND SURVEYOR TELEVISION by E. P. Martz, Jr., Jet Propulsion Laboratory	43 ✓
ADVANCED COMPUTER DESIGN TECHNIQUES FOR OPTICAL SYSTEMS by John M. McLaughlan, Jet Propulsion Laboratory	51 ✓
FEASIBILITY STUDIES OF OPTICAL SPACE COMMUNICATIONS AND TRACKING AND OTHER ACTIVITIES OF THE JPL QUANTUM ELEC- TRONICS GROUP by Willard H. Wells, Jet Propulsion Laboratory	59 ✓
TECHNOLOGY FOR A MANNED ORBITING TELESCOPE by W. E. Howell, Langley Research Center	67 ✓
OPTICAL COMMUNICATIONS EXPERIMENTS ON GEMINI VII by D. S. Lilly, Manned Spacecraft Center	81 ✓
MANNED SPACECRAFT CENTER LASER PROGRAMS AND PLANS by W. L. Thompson, Manned Spacecraft Center	91 ✓
WHITE SANDS MISSILE RANGE STATION OF MSC-4 by R. W. Ward, Manned Spacecraft Center	99 ✓
THE OPTICAL GUIDANCE SYSTEM FOR RENDEZVOUS by Charles L. Wyman, Marshall Space Flight Center	103 ✓

TABLE OF CONTENTS (Concluded)

	Page
OPTICAL TECHNOLOGY EXPERIMENTS FOR APOLLO APPLICATIONS PROGRAM by E. J. Reinbolt and J. L. Randall, Marshall Space Flight Center	115 ✓
SOME ASTROPHYSICAL INSTRUMENTATION CONSIDERATIONS RELATED TO SPACE OPTICAL TECHNOLOGY by G. A. Vacca, NASA Headquarters	131 ✓

PARTICIPATION OF AMES RESEARCH CENTER IN THE MSC-4 EXPERIMENT

Norman S. Johnson
Ames Research Center

N 68-31760

Ames Research Center is engaged in a specific laser research project to determine whether the backscattered light from the turbulent region can be used to detect clear-air turbulence. To solve this problem, it is essential first to understand the effect of the atmosphere and atmospheric variations on laser propagation. This has led Ames to initiate an additional research program to study the effect of the atmosphere on laser transmission. Specifically, the study will consist of comparing the signal propagated from the ground station to that reflected from an earth-orbiting satellite with corner reflectors.

The laser transmitter and receiver, and the tracking equipment for accomplishing this task, have been developed by an Ames Research Center contractor, Electro-Optical Systems, Inc., Pasadena, Calif. Although this equipment was developed independently of the MSC-4 experiment, with minor modifications it will be able to receive the laser signal to be transmitted by the astronaut from the Gemini 7 spacecraft. When the modifications have been completed, it is planned to locate the Ames propagation experimental equipment at Kauai, Hawaii, for the purpose of participating in the MSC-4 experiment.

The objectives of Ames' participation in the Gemini 7 laser experiment are listed in Figure 1. The first two, which are in direct support of the MSC-4 experiment, are intended to increase the probability of obtaining the basic data of the voice communication signal. The third, fourth, and fifth objectives, which are independent of the MSC-4 experiment, are slanted toward obtaining basic data on the effect of the atmosphere on a transmitted laser signal.

A sketch of the experimental setup for the Ames propagation experiments is shown in Figure 2. The equipment will be mounted on two NIKE-AJAX tracking mounts. Both mounts will be slaved to a predetermined pointing command so that the equipment can be pointed along a predetermined trajectory. A laser signal will be directed toward a satellite that has corner reflectors, such as Explorer 22, Explorer 27, and Geos 1. The signal will be reflected and directed toward its source. The velocity of the satellite will cause the position of the signal to shift slightly, and this is the reason for the two tracking mounts. The transmitter will be mounted on one and the receiver on the other in position appropriately to the first.

Both continuous wave and pulse transmission characteristics will be evaluated. For this purpose a continuous wave (argon) and a pulsed (ruby) laser will be mounted on one pedestal. The other pedestal will contain the receiver equipment.

The experiment will give two-wave transmission data at 4880 Å, 5300 Å, and 6943 Å. These are the primary laser wavelengths and are related generally to high-power gas and solid-state laser systems.

The equipment is a modification of the Ames propagation experimental setup. The GT-7 experimental setup is shown in Figure 3. Again, the equipment consists of two tracking pedestals on which are mounted the laser transmitter and receiver, as described previously. The transmitter is used as a visible beacon to enable the astronaut to detect the location of the receiver and to direct his transmitter toward it. The receiver is, therefore, mounted on the same pedestal as the ground transmitter. Because the second pedestal is available, a separate receiver will be mounted upon it in the hope that a comparison of the two signals will provide additional pointing information.

It is planned to retain the argon laser from the propagation experiment for the ground transmitter. The pulsed laser will be removed. Since the transmitted signal from the spacecraft is from a gallium arsenide laser transmitting at about 9000 Å, some modification to the receiver was required to make it compatible with this laser. The equipment includes a 40.64-cm (16-in.)-dia. mirror, a 7102 photomultiplier, and a 117-Å bandpass filter.

It is planned to slave the pedestal containing the transmitter-receiver combination to the FPS-16 Gemini track radar at the Kauai site. The pedestal containing only the receiver will be slaved to the other pedestal. Total tracking errors are expected to be less than 40 seconds of arc, which is less than the transmitting laser beamwidth. It is planned to obtain data on the basic experiment by recording the audio signal that will be transmitted over the laser beam. It is also planned to film the trace of the fast rise-time pulses on a high-frequency oscilloscope. A tape recorder will be used to record the pointing angle, time, range, laser demodulated audio signal, Gemini communication audio signal, and argon laser power output.

The geographical location of the island of Kauai is shown in Figure 4. It is apparent that the Hawaiian Island chain is a readily identifiable landmark from orbit and affords a very early identification of the ground-based laser experiment site. The island of Kauai is large enough to be easily identified from orbit and should give the astronaut a readily identifiable target at which to generally point the laser in preparation for the fine pointing task.

The Kauai site is very advantageously located in latitude and affords coverage of a maximum number of orbits. This also allows the spacecraft to appear significantly above the horizon, and thus data can be obtained for a wide variation in zenith angles. Data for high zenith angles will have a lower signal-to-noise ratio, and if only this type of data is received, chances of mission success are diminished.

The Kauai site has additional advantages other than its geographical location. These are listed in Figure 5. The first two are concerned with geometrical location and have been discussed. The next three are concerned with the manner in which the natural attributes of the site contribute toward idealized sighting conditions. Because it is located away from any metropolitan area, there will be little interference from extraneous light sources, and thus there will be an optimum opportunity for laser pointing and communication with the Gemini spacecraft during orbital passes at night. Investigations have shown that because of the atmospheric conditions near the island of Kauai, turbulence is not a problem. Without this undesirable parameter, the probability of the success of the experiment is increased.

Initially there was some concern over the cloud cover known to be common over the Hawaiian Islands, but it was found that during the months of December and January the cloud cover is a minimum. Consequently, there is an excellent chance that the site will be free of cloud cover during the GT-7 experiment.

Kauai, furthermore, is a readily accessible NASA site containing some of the equipment necessary for the experiments. Because of the potential changes in orbit due to astronaut-initiated maneuvers, the only method of obtaining tracking data accurate enough for laser pointing is to slave the experiment to a radar that is actually tracking the vehicle. The FPS available on Kauai is therefore a requirement. Also, a voice link is required for one of the Ames experiments, and direct voice communication to the space vehicle is available from Kauai.

The experiments that Ames Research Center plans in connection with its participation in the Gemini 7 laser experiment are shown in Figure 6. The basic experiment is to determine whether the astronaut aboard the Gemini spacecraft can point a laser at a ground receiver and communicate by voice. The experimental setup for accomplishing this task has already been discussed in detail.

The Gemini 7 experiment offers Ames Research Center the opportunity to gain additional data on the effect of the atmosphere on laser transmissions. For the Gemini 7 experiment signal variations will be caused by errors in

pointing and variations in the far-field pattern of the transmitting laser. However, it is felt that if the higher amplitude pulses are used to represent signal propagation, the effect of the atmosphere on one-way transmission may be deduced. In addition, data on the effect of the atmosphere on laser propagation at a wavelength of 9000 Å is desired, and the Gemini experiment offers an opportunity to obtain it. It is expected that this information will be extremely valuable in laser propagation research and will augment the existing Ames Laser Propagation Research Program.

The most critical part of the planned MSC-4 experiment is the pointing of the spacecraft laser transmitter at the ground-based receiver within its 3-milliradian beamwidth. Data will be obtained on quality of transmission only if this task is performed successfully. It is desirable, however, to plan the experiment to obtain data when a pointing error exists.

To accomplish this it is planned to place the two pedestals of the laser propagation research equipment several hundred feet apart. As outlined previously, each will be equipped with an optical receiver. The signals from each receiver will be recorded to increase somewhat the chance of obtaining significant data and to estimate the astronaut's pointing error.

The final experiment is proposed because the 100-nanosecond optical pulse from the injection laser aboard the spacecraft is well above the highest frequency refractive index fluctuations in the atmosphere. Therefore, there are no changes in refractive indices during the time the laser pulse travels through the atmosphere. Because the laser pulse does not change shape due to refraction, it can be focused sharply on a film and will trace a series of dots as a function of time. Because of changes in the refractive index of the atmosphere, however, the line will not be straight. But a mean straight line can be obtained statistically, and a measure of the variation in the refraction index can be obtained from the deviations of the actual dot from this line. The statistical data on frequency and amplitude of these deviations thus obtained can be correlated with theory. It should be noted that a laser offers a unique opportunity for this experimentation, since the requirement of a pulsed intense source rules out a natural celestial environment.

- PROVIDE A BACK-UP RECEIVER FOR THE MSC-4 EXPERIMENT
- PROVIDE AN ADDITIONAL COMMUNICATION OPPORTUNITY TO THE ASTRONAUT
- COLLECT PROPAGATION DATA AT 9010 \AA FOR A.R.C. LASER PROPAGATION STUDIES
- PROVIDE DATA FROM ANOTHER LOCATION FOR A.R.C. LASER PROPAGATION STUDIES
- PERFORM ADDITIONAL EXPERIMENTS ON LASER BEAM SIGNATURE AND ATMOSPHERIC REFRACTION

FIGURE 1. OBJECTIVES OF THE A.R.C. GEMINI 7 LASER EXPERIMENT

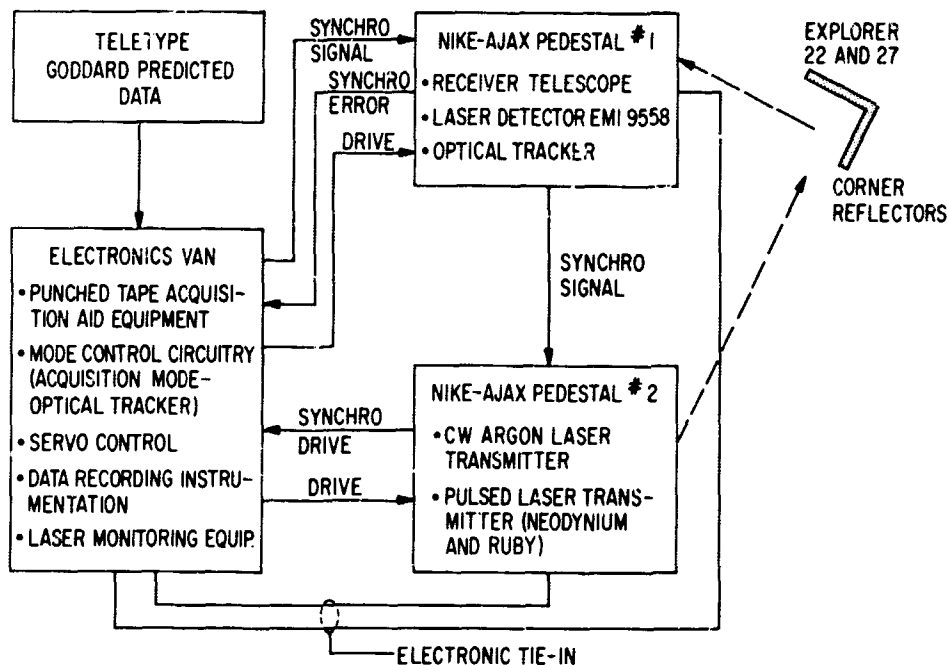


FIGURE 2. LASER PROPAGATION RESEARCH EXPERIMENT

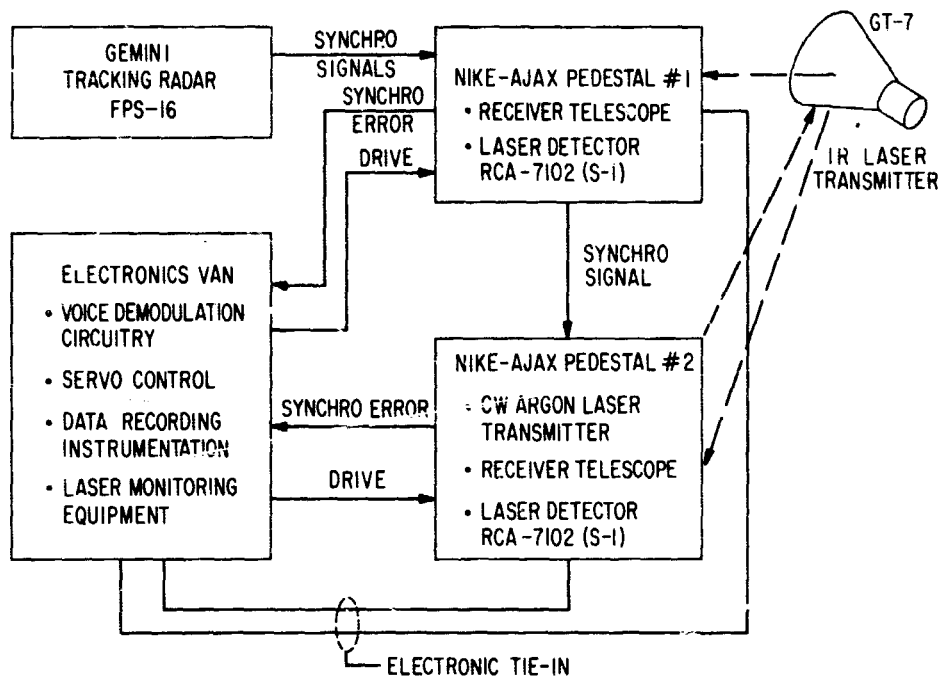


FIGURE 3. A.R.C. EQUIPMENT TO PERFORM MSC-4 EXPERIMENT

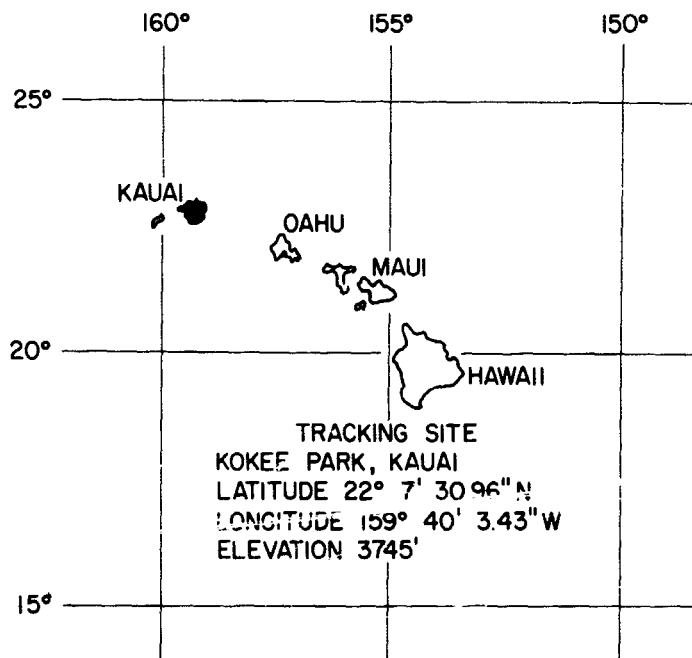


FIGURE 4. THE GEOGRAPHICAL LOCATION OF THE ISLAND OF KAUAI

- EASILY IDENTIFIED FROM ORBIT
- LATITUDE IS CENTRALLY LOCATED
RELATIVE TO THE GEMINI-7 ORBIT
- LOW ATMOSPHERIC TURBULENCE
- LOW SKY ILLUMINATION
- MINIMUM CLOUD COVER IN DECEMBER
AND JANUARY
- EASILY ACCESSIBLE
- NASA SITE
- GEMINI TRACKING RADAR (FPS - 16) AVAILABLE
- DIRECT COMMUNICATION LINK AVAILABLE

FIGURE 5. ADVANTAGES OF KAUAI SITE

- BASIC EXPERIMENT OF VOICE COMMUNICATION
- OBTAIN DATA IN ONE-WAY LASER
PROPAGATION AT 9010 Å
- EVALUATION OF LASER POINTING ACCURACY
- MEASUREMENT OF REFRACTION INDEX

FIGURE 6. PLANNED A.R.C. LASER EXPERIMENTS FOR GEMINI 7

PRECEDING PAGE BLANK NOT FILMED.

RADOT, 60.96-CM (24-IN.) MULTIMODE TELESCOPE AND FUTURE FACILITIES

Walter J. Carrion
Goddard Space Flight Center

N 68-31761

As optical communication technological advances and practical deep-space communication systems become a reality, the present tracking instrumentation becomes obsolete. No longer can we think in terms of precision cinetheodolite angle measurements obtained by accurately reading out the tracking error and correcting the angle data information. To transmit and/or receive at data rates in the order of 10^7 bits per second at interplanetary distances, laser communication techniques may employ diffraction-limited optics that will need to be pointed with an accuracy equal to or better than the diffraction beam spread.

Precision computer steering will be required to take into account the earth's rotation about its axis and the earth's orbit about the sun as well as the velocity of the satellite because the transit time to send information from interplanetary distances can no longer be neglected. Precision tracking instrumentation will move into a new era, from passive data to real-time data to the era where instrumentation will have to be at least one step ahead of real time; that is, we need precision predicted position pointing. The Optical Systems Branch of the Tracking and Data Systems Directorate of the Goddard Space Flight Center has pioneered in precision laser tracking of spacecraft. The actual field experience in tracking the S-66 satellite, being directly associated with the field problems of acquisition, tracking, and data handling, has enabled the Optical Systems Branch to modify instrumentation under development as well as plan future instrumentation to meet the research and development program and operational requirement for a deep-space optical communication network.

To meet the immediate requirements for the laser tracking experiment, a Nike-Ajax system was modified by adding shaft angle encoders, water cooled laser, telescope receiver, programmer, and the guiding scopes (Fig. 1). This system in the program mode tracks the satellite well within the laser beam divergence angle and is successfully tracking the S-66, receiving as much as 92 percent return of the transmitted pulses during a single pass.

The Real-time Automatic Digital Optical Tracker (RADOT) is a precision computer controlled optical tracker (Fig. 2). The x-y mount has been developed and fabricated to an accuracy of two seconds of arc. The system has been delivered and installed in the Goddard Optical Research Facility. Field evaluation tests are currently being set up.

Figure 3 is a block diagram of the RADOT system. An image orthicon sweeps the focal plane of the optical system and, in conjunction with the computer, measures the position of the centroid of the image as well as the image offset. Simultaneously, the shaft angle position is fed into the computer. The computer in real time converts the angle information to develop a tracking error signal as well as corrects the angle information for the amount of tracking error measured by the image orthicon.

The multimode mount system has been developed as a research tool to support the R&D programs of the Optical Systems Branch (Fig. 4). The mount has an equatorial and an x-y mode. The mount and optics for this system have just been completed and installed in the observatory. Integration of the mount and drive system is currently under way and is scheduled for operational use by February of 1966. The optical system consists of four different configurations.

Figure 5 shows the Cassegrain system, which has a primary Cassegrain focal length of 1270 cm (500 in.) with amplification in steps of 1270 cm (500 in.) to a maximum of 6350 cm (2500 in.). Provisions have been designed for the main tube to carry two experimental packages weighing up to 90.6 kg (200 lbm) each. These packages can be mounted on the top and bottom of the main trunnion support casting.

Figure 6 shows the optical system converted to a 335.28-cm (132-in.) focal length Newtonian system.

Figure 7 shows the optical system converted to 254-cm (100-in.) focal length, Baker reflector-corrector system having a corrected 6° field of view.

The described instrumentation provides the research tools to conduct controlled optical communication experiments as well as field evaluate newly developed systems. New advances in laser technology like the 10.6 micron and the argon ion laser with several watts output promise a laser communication system within a few years.

To fully support NASA's planned R&D programs, a Southwestern Optical Research Facility is needed. This facility will consist of a large aperture telescope and associated instrumentation designed specifically for conducting communication experiments in conjunction with interplanetary missions in addition to supporting NASA's planetary studies and investigation. Integrated in the GSFC tracking network, it will serve as an operational station when high data rate communication systems become a reality.

Under an established OART/SRT task, "Southwestern Optical Research Facility," the Optical Systems Branch of the Goddard Space Flight Center is conducting a site survey in southern California. From weather records of the past 10 years, geological data, observatory seeing studies, etc. three tentative sites have been selected. A Goddard team is presently investigating the sites from a construction and facility point of view. Specifications have been written for the instrumentation required to conduct on-site seeing studies. A contract will be made for a team to conduct the seeing studies while the facility design criterion document is being prepared for man-power and budgetary purposes.

This facility, in conjunction with the present Goddard Optical Research Facility, and any other available facility, will give us the instrumentation and facility necessary to conduct earth-to-satellite-to-earth experiments, station switchover experiments, high data rate transmission and receiving experiments, and allied experiments such as precision pointing, field evaluation of modulating and demodulating techniques, and many others.

Present astronomical observatories cannot support our optical communication programs. Besides being overcommitted for astronomical studies, the astronomical telescope differs in tracking rates and precision pointing. In general, it lacks computer servo control capabilities to position instrumentation to predicted position rather than pointing at a specific target.

A Southwestern Optical Research Facility is an important research and operational station to all NASA Centers. To carefully study NASA's requirements to determine the type of instrumentation to be developed and plan the facility for future operational requirements to support the deep-space optical communication mission, it is suggested that a NASA space optical research working group be formed. The working group should consist of representatives from each NASA Center who are actively engaged in optical communication R&D programs from which future requirements are generated.

It is realized that we are several years from having an operational deep-space optical communication system but I feel certain it will become a reality. It will require some five to seven years to design and construct an operational facility such as the Southwestern Optical Research Facility. We feel that the program is vital to NASA's future deep-space missions.

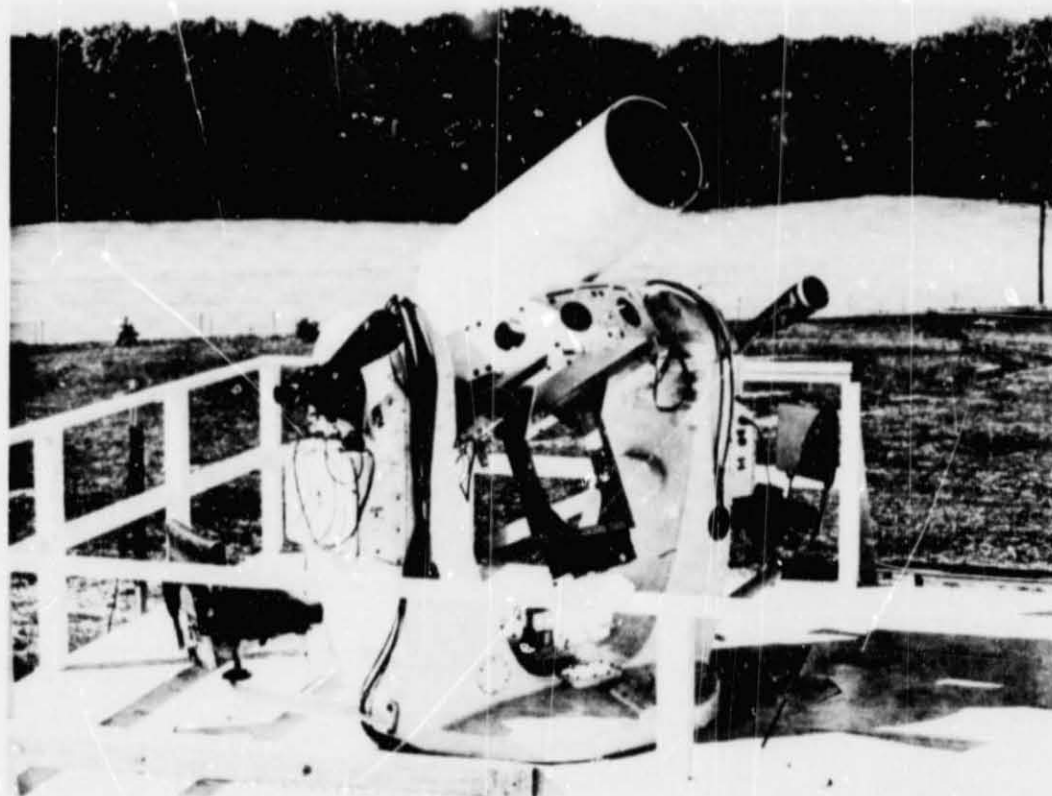


FIGURE 1. TRANSMITTING LASER AND RECEIVING TELESCOPE,
MOUNTED ON A MODIFIED NIKE-AJAX RADAR PEDESTAL

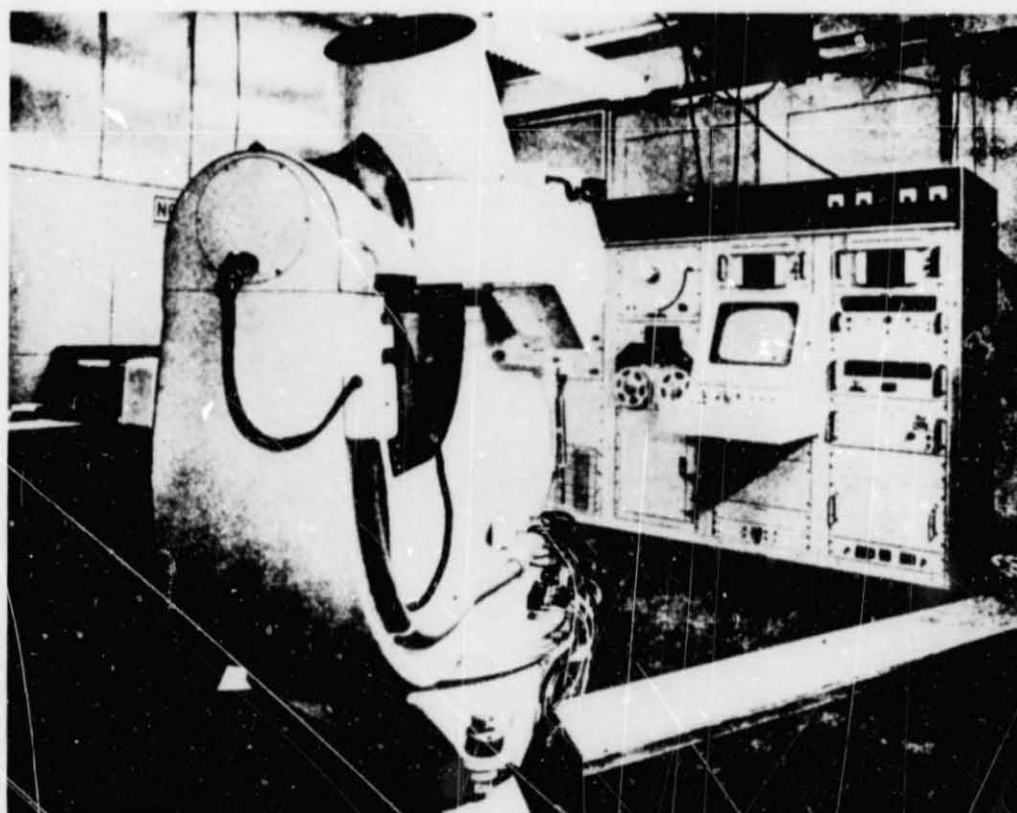


FIGURE 2. REAL-TIME AUTOMATIC DIGITAL OPTICAL TRACKER

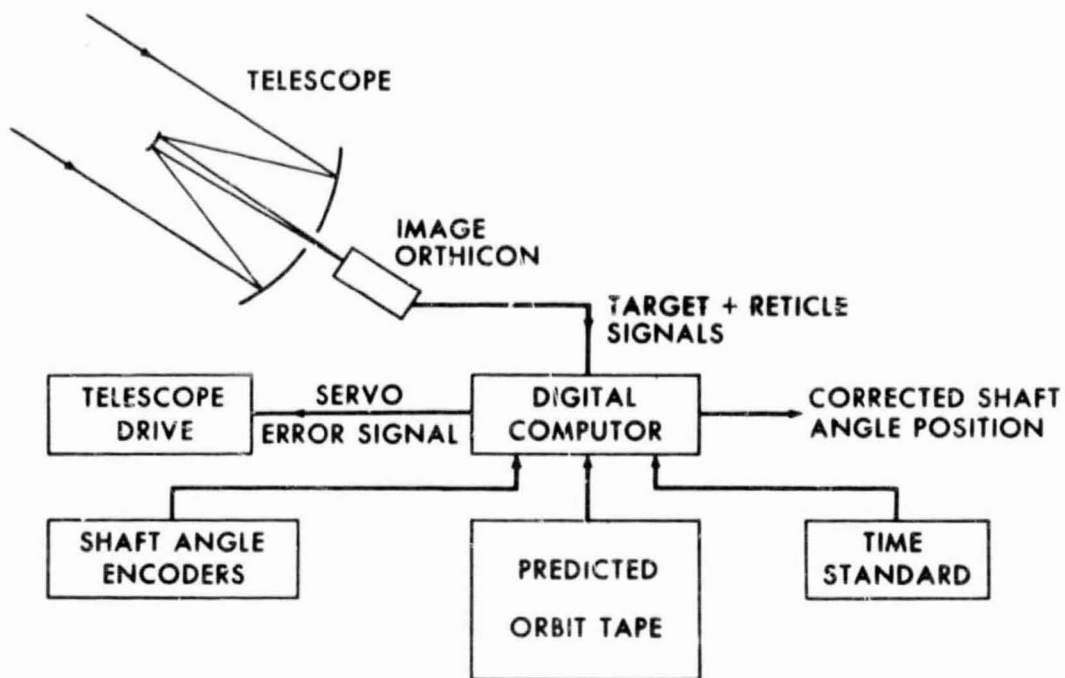


FIGURE 3. REAL-TIME AUTOMATIC DIGITAL OPTICAL TRACKER

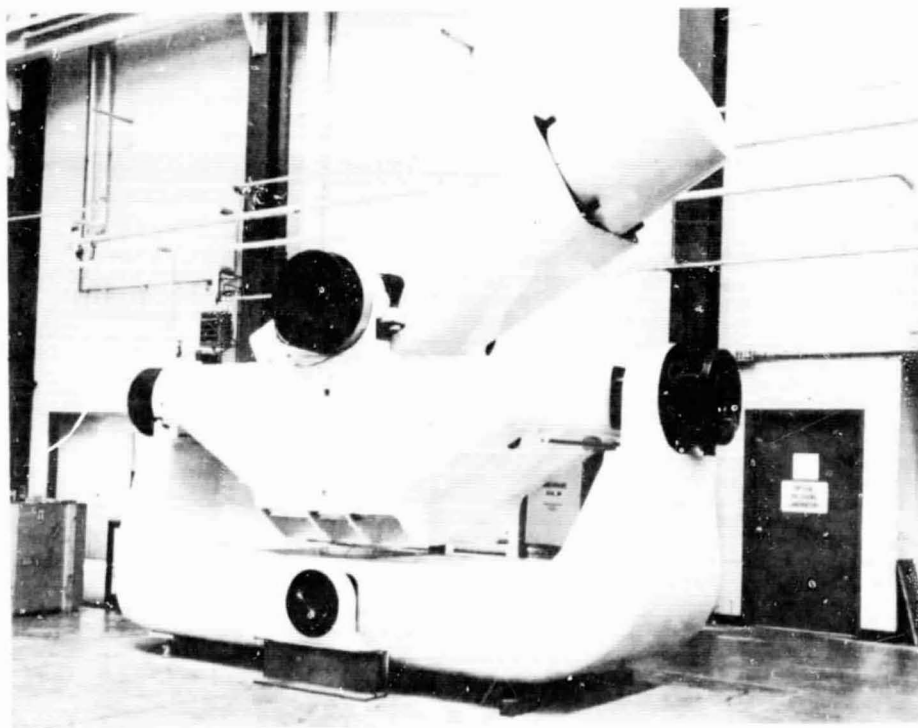


FIGURE 4. THE MULTIMODE MOUNT

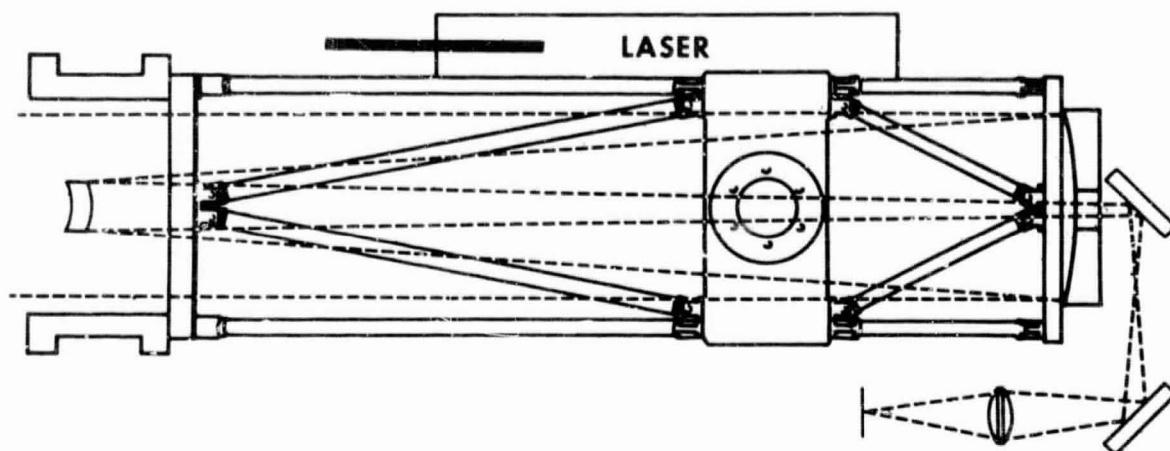


FIGURE 5. CASSEGRAINIAN, PRIMARY FOCAL LENGTH 1270 CM (500 IN.)

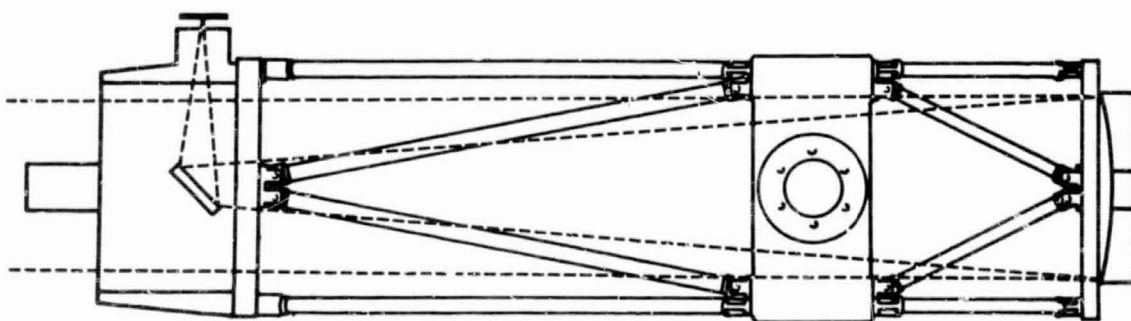


FIGURE 6. NEWTONIAN, FOCAL LENGTH 335 CM (132 IN.)

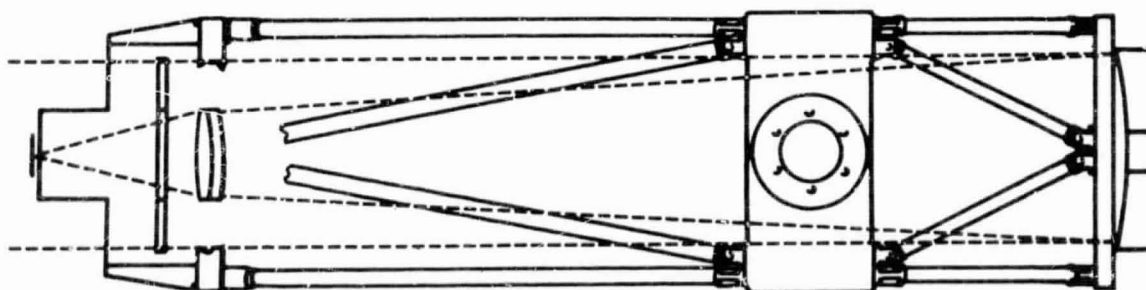


FIGURE 7. BASIC BAKER REFLECTOR CORRECTOR, FOCAL LENGTH 254 CM (100 IN.), 6° FIELD OF VIEW

PRECEDING PAGE BLANK NOT FILMED.

ANALYSIS OF A TEN-MICRON COMMUNICATION SYSTEM

Nelson McAvoy
Goddard Space Flight Center

N 68-31762

Extensive investigation has been made by industrial concerns and NASA personnel on the use of lasers for NASA deep-space communication requirements. Most of this analysis has been speculative in that it has been made on projected development of new lasers, new optical receivers, new modulators, improved tracking telescopes, and large diffraction-limited optics. The analysis made herein and the resulting proposed communication system is based on either equipment that is presently available or equipment that is to be modified by tried and proven methods. It is felt that the experiment to be discussed in conjunction with similar experiments on the optical technology satellite now being studied under contract NAS8-20115 can result in sufficient know-how to design a communications transmitter and auxiliary equipment for a Mars probe that will transmit a real-time TV signal to earth.

It is first necessary to establish the capability of optical receivers. This is done in the Appendix, which shows that the minimum detectable signal power is

$$P = \frac{R h \nu B}{\eta} \quad , \quad (1)$$

in which R is the signal-to-noise ratio, η is the quantum efficiency of the detector, B is the receiver bandwidth, and $h\nu$ is the energy per quanta. The limit shown in equation (1) results from fluctuation in the number of quanta in the local oscillator in case of heterodyne reception and fluctuation in the number of signal quanta in the case of envelope reception. The minimum detectable signal of equation (1) is a practical limit for heterodyne reception and a theoretical unattainable limit for envelope detection [1, 2, 3]. Shannon's law requires

$$P = \frac{R' h \nu B'}{\eta} \quad (2)$$

watts of signal power for an information bit rate B' . In practice it is convenient to have R' photons per bit approximately equal to ten to eliminate sophisticated data processing. It is interesting to note that obtaining equation (2) does not require the assumption of boson statistics while equation (1) does not require the assumptions of information theory. From information theory, one can establish that the bit rate B' of equation (1) requires at least a bandwidth B .

It is seen from equation (1) that for a given power incident on the receiver and a given receiver bandwidth, one will have a larger signal-to-noise ratio, R , for lower frequency lasers. It should be noted that equation (1) and the latter statement do not hold when

$$e^{\frac{h\nu}{kT}} \approx 1 + \frac{h\nu}{kT},$$

i. e., not in the rf microwave or millimeter wave range. Parenthetically, neither does equation (2) remain valid in the rf microwave and millimeter range. This is illustrated in Figure 1, which shows receiver capability over the useful spectral range.

One can conclude from equation (1) that, neglecting availability of lasers, transmitter pointing accuracy, transmitter antenna gain, atmospheric absorption, and atmospheric coherence disturbance, one is better off working at frequencies in the range $h\nu \approx kT$ or $\nu = 6 \times 10^{12}$ Hz ($\lambda = 50$ microns). At this wavelength thermal noise begins to predominate.

We next concern ourselves with the two practical parameters: (1) practical telescope apertures and consequently laser transmitter antenna gains and (2) practical limitations of pointing laser transmitters. It is reasonable to assume that pointing apparatus presently exists to either track from the ground or a satellite to within two arc seconds. We also assume that presently existing fabrication methods permit the use of infrared diffraction-limited telescopes with apertures of at least one meter. Still neglecting the practical limitation of the availability of lasers throughout the spectral range, we are forced to ask the question: To how low a frequency can one go with one-meter aperture telescopes and have laser transmitter antenna gains equivalent to two arc seconds beam divergence? The answer, from the diffraction-limit equation, is a laser transmitter in the ten-micron region. I would like to stress that the preceding analysis is not an ipso facto result from recent startling laser developments in the ten-micron region--the carbon dioxide lasers which are capable of high power efficiency and monochromaticity [4].

There are three major remaining problems with which to be concerned: (1) atmospheric absorption and scatter, (2) distortion of the plane isophase surface of the transmitted beam by the atmosphere and (3) Doppler shift of the transmitted beam causing large difference frequency in the optical mixer. The first of these problems can be dismissed from the results of the many DOD infrared propagation studies which have shown the ten-micron range to exhibit less absorption and scatter than the visual range. As to the second of these

problems, it has been shown theoretically [5] and verified experimentally [6, 7] that the coherence aperture of a beam propagated through the atmosphere varies with the 6/5th power of the wavelength. This results in a projected coherence area at ten microns larger than the one-meter aperture telescopes to be proposed. The third of these problems, but the most stringent, is the requirement on response time of optical mixers. In the experiments that will be discussed, Doppler shifts up to 500 MHz will be experienced. Bulk photodetectors do exist in the ten-micron range which have sufficiently fast minority carrier mobilities to obtain 450 MHz bandwidth photomixers [8]. It is theoretically possible, although it has not been verified in the infrared range, to generate optically tracking local oscillators from Brillouin scattering (parametric interaction) by rotating the interaction crystals [9, 10]. This will alleviate the problem of needing photomixers with response times higher than 10^{-8} seconds.

In brief summation, the reasons for choosing the ten-micron range for optical communication experiments in contradistinction to the visual range are: (1) better lasers, (2) large coherence areas, (3) coherence areas compatible with diffraction limit of scopes, (4) diffraction limit of scopes compatible with their tracking accuracy, (5) high quality (accuracy) optics are not needed, (6) best atmospheric window, (7) smaller Doppler shifts, and (8) less power per information bit required at the receiver.

The following parameters are within the realm of realization for telemetry links between a Mars-probe-borne laser and receivers on the earth:

Transmitter:

pointing accuracy of laser - two arc seconds

laser output power at 10.6 microns - 100 watt cw

electrical power input to the laser - 2000 watts

laser modulator power - 50 watts

laser modulator bandwidth - 2 MHz

laser transmitter gain antenna - 1 meter aperture

Receiver:

receiver antenna - 1 meter aperture (Cassegrainian)

receiver tracking accuracy - two arc seconds

optical mixer quantum efficiency - 20 percent

optical mixer mismatch - VSWR of 5

optical mixer bandwidth - 1 GHz

optical local oscillator power - 20 dBm

i. f. tracking bandwidth - 10 MHz

information bandwidth - 5 MHz

base bandwidth - 1 kHz (laser short term stability of 3×10^{10})

Figure 2 shows the parameters of the range equation for a typical 10.6-micron laser system and receiver capability.

In order to develop equipment for and establish the practicality of the previously discussed telemetry link, we propose to transmit signals to Echo II and to receive the echo of these signals at various locations on the earth. The first experiments will be done using a receiver superimposed with the transmitter and with only audio modulation of the transmitted signal. In this mode of operation, a portion of the transmitted, unmodulated signal can be used for a local oscillator. Thus, phase, frequency, and amplitude fluctuations caused by laser instability, atmospheric perturbations, and nonspecularity of Echo II can be established.

Although extensive development is required in general for the instrumentation discussed, equipment is presently almost ready to do the first phase of the Echo II experiment, i. e., the transceiver mode of operation.

Figure 3 shows the return signal power from Echo II for tracking conditions that will be expected. Figure 4 shows the transceiving equipment which has already been designed for coherent receiver studies with helium-neon lasers. With only slight modification, this equipment can be used with 10.6-micron lasers. Figure 5 shows a block diagram of a possible configuration of the equipment needed.

Figure 6 shows the thermal effects in the infrared spectra of Echo II.

In the receiving system, one has a choice between (1) using a 450-MHz-wide i. f. amplifier and detector, (2) tuning sidebands of part of the transmitted signal for a tracking L. O. and consequently having a fixed i. f. , or (3) tuning i. f. of the optical mixer from 0 to 450 MHz. The three choices are in order of increasing difficulty and will be tried in that order.

Appendix

Signal and Noise Relations in Optical Detectors

A detector, such as a photoemissive diode, photo-junction diode, or an extrinsic photoresistor, gives off an electron for an absorbed photon. An ideal detector is one which produces at the output terminals of the detector one electron for every photon incident.* The basic circuit used in the detection process is shown in the following diagram.

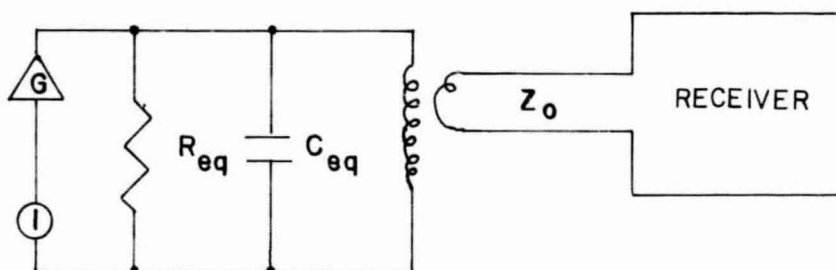


FIGURE 7. BASIC CIRCUIT FOR CURRENT SOURCE DETECTOR

"i" is the current source equivalent to the current generated in the photoemission process. "G" is an equivalent amplifier for the photomultiplication. "R_{eq}" and "C_{eq}" are the equivalent capacitance and resistance of the photodetector.

It will be assumed that the frequency of the current, ω , will satisfy

* Those who approach detection from the quantum electrodynamic point of view where detection electrons are obtained from the creation and annihilation of photons also put the restriction on the ideal detector that its dimensions be less than the photon wavelength. We chose to deal with the practical detector sizes and degrade our output signal power by the phase difference between the current generated at two points on the detector separated by an appreciable part of a photon wavelength.

$$\frac{1}{\omega} \gg R_{eq} C_{eq} ,$$

i. e. , we are not limited by the time constant of the detector.

Photoresistive detectors such as the metal doped germanium cannot be represented with the equivalent circuit of Figure 7. There is no diode effect, and a bias is required since the resistivity is changed by the incident light. The minimum detectable signal for coherent detection and the noise analysis is only slightly different from that for diodes [11, 12].

Suppose a steady stream of photons is incident on a detector at an average rate \bar{n} photons/sec. The root mean square deviation of the number of photons from the average, at a rate between ν and $\nu + \delta\nu$ is [13, 14]

$$n_{\delta\nu} = \sqrt{2 \bar{n} \delta\nu} . \quad (3)$$

The same statistics apply for photoelectrons emitted from the photocathode. The current resulting from a flux of $n(t)$ photons/sec on the photosurface before amplification is

$$i(t) = e n(t) \eta . \quad (4)$$

"e" is the electronic charge and η is the quantum efficiency.

In terms of current, expression (3) is

$$n = \sqrt{2 \frac{\bar{i}}{e\eta} \delta\nu} . \quad (5)$$

Again applying equation (4) , the root mean square deviation of the current at a rate between ν and $\nu + \delta\nu$ is

$$i_{\delta\nu} = e\eta \sqrt{2 \frac{\bar{i}}{e\eta} \delta\nu} . \quad (6)$$

With proper matching to the receiver, the power input to the receiver between frequencies ν and $\nu + \delta\nu$ will be

$$\frac{1}{2} i_{\delta\nu} R_{eq} G^2 = R_{eq} G^2 e\eta \bar{i} \delta\nu .$$

The current may be caused by several sources: i_s due to the laser signal; i_{lo} due to a laser local oscillator (if any); i_b due to background illumination; or i_d due to dark current. The total shot noise power to be expected in the receiver with bandwidth B is

$$P_{\text{shot noise}} = G^2 R_{\text{eq}} e \eta B (\bar{i}_s + \bar{i}_{lo} + \bar{i}_d + \bar{i}_b) . \quad (7)$$

Another contribution to the noise is the current arising from the beating of the local oscillator with the background radiation having the same isophasels and wavelength as the signal. In practice this contribution is too small to consider further here.

Finally, we must include the thermal contribution to the noise. The noise out of the receiver of Figure 7 due to thermal effects is

$$P_{\text{th}} = K T_{\text{eq}} B, \quad (8)$$

where K is Boltzman's constant and B is the bandwidth of equation (7). " T_{eq} " is the temperature of a fictitious resistor with value Z_0 of Figure 7. The noise power within the bandwidth B at RF from a resistor R delivered to a matched load is KTB . Therefore, the T_{eq} is defined as the temperature of a fictitious resistor on the input terminals of the receiver that will simulate the noise generated inside the receiver, plus the actual thermal noise of the detector [15]. The receiver thermal noise will be the dominant thermal source in most cases except, perhaps, when liquid helium cooled masers and parametric amplifiers in the the UHV range are used. Notice that this noise appears at the output of the detector and, therefore, is not acted upon by its gain.

For establishing the current due to the signal we consider first a situation in which the detector is illuminated simultaneously by a signal and local oscillator; they are plane polarized in the same direction and have the same isophasel surface. The power absorbed by the detector is

$$P(t) = [E_s(t) + E_{lo}(t)]^2 A \sqrt{\frac{\epsilon}{\mu}}, \quad (9)$$

where E_s is the signal electric field at the detector,

E_{lo} is the local oscillator electric field at the detector,

$\sqrt{\frac{\epsilon}{\mu}}$ is the admittance of free space, and

A is the detector area.

This is equivalent to the arrival of photons at a rate $\frac{P(t)}{h\nu}$ photons per second, and the resultant generated current would be

$$i(t) = e\eta \left| \frac{P(t)}{h\nu} \right|. \quad (10)$$

Equations (9) and (10) give

$$i(t) = \frac{e\eta}{h\nu} A \sqrt{\frac{\epsilon}{\mu}} [E_s^2(t) + E_{lo}^2(t) + 2 E_s(t) E_{lo}(t)]. \quad (11)$$

Only the last term in the brackets contributes to signal current at the i. f. frequency, $|\omega_s - \omega_{lo}|$. If the electric field at the various frequencies is represented as

$$E = E_o \sin(\omega_i t + \frac{\omega_i}{c} X + \theta_i),$$

$$i(t) = i_s(t) + i_{lo}(t) + i_{if} \cos |\omega_s - \omega_{lo}| t \quad (12)$$

where

$$i_{if} = \sqrt{2 I_s I_{lo}}. \quad (13)$$

The average output power delivered to a matched load, after the tube gain acts upon the current, would be

$$\overline{P}_{if} = \frac{1}{2} i_{if}^2 R_{eq} G^2. \quad (14)$$

The signal-to-noise ratio can now be obtained by combining equation (14), equation (7), and equation (8).

$$S/N = \frac{\frac{1}{2} i_{if}^2 G^2 R_{eq}}{K T_{eq} B + e G^2 B R_{eq} (i_s + i_{lo} + i_b + i_d)} \quad (15)$$

or, from equation (13),

$$S/N = \frac{\bar{i}_s \bar{i}_{lo} G^2 R_{eq}}{K T_{eq} B + e G^2 B R_{eq} (\bar{i}_s + \bar{i}_{lo} + \bar{i}_b + \bar{i}_d)} \quad (16)$$

This is the general expression usually seen for photodetector S/N [16, 17, 18].

The usual conditions of heterodyne detection require that the L. O. be sufficiently intense that

$$i_{lo} > i_s + i_b + i_d$$

and

$$e G^2 R_{eq} B \bar{i}_{lo} > K T_{eq} B.$$

Under these conditions, equation (16) reduces to

$$S/N = \frac{\bar{i}_s}{e B} \quad (17)$$

Incorporating equation (10),

$$S/N = \frac{\eta \bar{P}_s}{n \nu B} \quad (18)$$

The incident power that results in a S/N of unity is

$$\bar{P}_{min} = \frac{h \nu B}{\eta} \quad (19)$$

The results are very similar for the extrinsic semiconductor for photoresistive detectors. When the detector time constants are taken into consideration, one will get [11]

$$S/N = \frac{\eta \eta_a P_s}{h \nu \Delta B (1 + \omega_{if} \tau_o)} \quad (20)$$

Where τ_o is the carrier lifetime, η_a is fractional absorption by the detector.

This treatment also includes the case of direct (or incoherent) envelope detection, in the absence of a local oscillator. Instead of an i. f. signal, we consider detecting a signal at a modulation frequency, within a bandwidth B. In equation (15), we should replace i_{if}^2 with $m^2 \bar{i}_s^2$, where m is the modulation index, and set $i_{lo} = 0$. The expression for S/N becomes

$$S/N = \frac{\frac{1}{2} m^2 \bar{i}_s^2 G^2 R_{eq}}{K T_{eq} B + 2 e G^2 B R_{eq} (\bar{i}_s + \bar{i}_b + \bar{i}_d)} \quad (21)$$

In the absence of a local oscillator, we cannot arbitrarily neglect terms in the denominator. If the detection process were limited by thermal noise,

$$K T_{eq} B \gg 2 e G^2 B R_{eq} (\bar{i}_s + \bar{i}_b + \bar{i}_d). \quad (22)$$

Equation (21) becomes

$$S/N = \frac{\frac{1}{2} m^2 \left(\frac{e\eta}{h\nu} \bar{P}_s \right)^2 G^2 R}{K T_{eq} B} \quad (23)$$

The power which is equivalent to the noise in this case is

$$P_{nep} = \frac{h\nu}{m e G \eta} \sqrt{\frac{2 K T B}{R}} \quad (24)$$

This is the common parameter used for a figure of excellence in IR detectors.

REFERENCES

1. McMurtry, B. J. : Lecture Notes Prepared for the AGARD Lecture Series on Orbit Optimization and Advanced Guidance Instrumentation. Proc. IEEE, vol. 51, no. 4, Apr. 1963.
2. McAvoy, N. : Advanced Development Division. GSFC Quart. Rep. , no. 6, Mar. 1965, p. 2.
3. Arams, F. ; and Wung, Marie: Proc. IEEE, vol. 53, Mar. 1965, p. 329.
4. Patel, C. K. N. : CW Higher Power $N_2 - CO_2$ Laser. Appl. Phys. Lett. , vol. 7, no. 1, July 1, 1965.
5. Fried, D. L. : Optical Heterodyne Detection of an Atmospherically Distorted Signal Waveform. NAA Electro-Optical Laboratory, Tech. Memo 118, July 1964.
6. Harwit, M. : Phys. Rev. , vol. 120, 1960, p. 1551.
7. Low, Frank, Dr. : Private Communications. National Radio Astronomy Observatory, Greenbank, W. Va.
8. Yardley, J. T. ; and Moore, C. B. : Response Time of Ge:Cu Infrared Detectors. Appl. Phys. Lett. , to be published.
9. Chico, R. Y. ; Stoichett, B. P. ; and Townes, C. H. : Phys. Rev. Lett. vol. 12, May 25, 1964, p. 592.
10. Sealer, D. A. ; and Hsu, H. : Parametric Interaction of Light and Hypersonic Waves. Ohio State University Research Foundation Report 1579-16, Oct. 15, 1964.
11. Lucovsky, G. ; Schwarz, R. F. ; and Emmons, R. B. : Photoelectric Mixing of Coherent Light in Bulk Photoconductors. Proc. IEEE, vol. 51, no. 4, Apr. 1963.
12. Levinstein, H. : Extrinsic Detectors. Appl. Optics, vol. 4, June 1965, p. 639.

REFERENCES (Concluded)

13. Spangenberg, K. R.: Vacuum Tubes. McGraw-Hill Book Co., Inc., 1948.
14. Ross, M.: Optical Receivers. John Wiley and Sons, Inc., to be published.
15. See Noise Figure Standards, Proc. I. R. E.

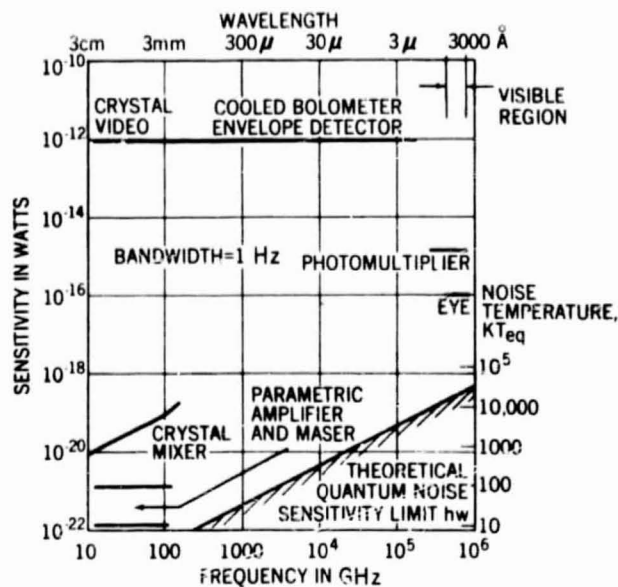


FIGURE 1. SENSITIVITY OF RECEIVERS FROM RF TO VISUAL RANGE

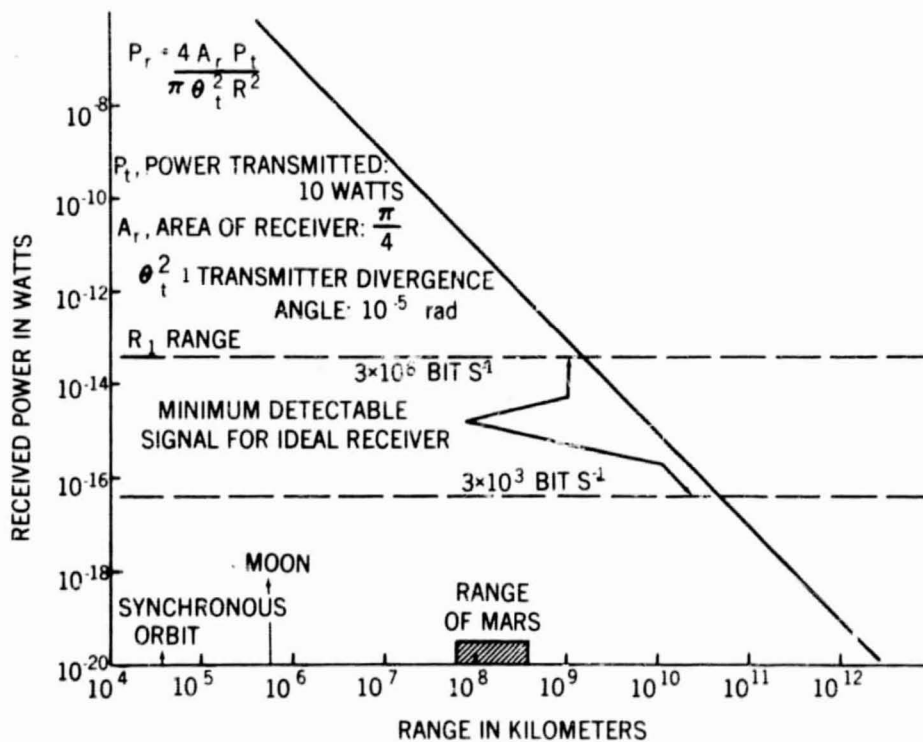


FIGURE 2. 10.6-MICRON ONE-WAY COMMUNICATION CAPABILITY

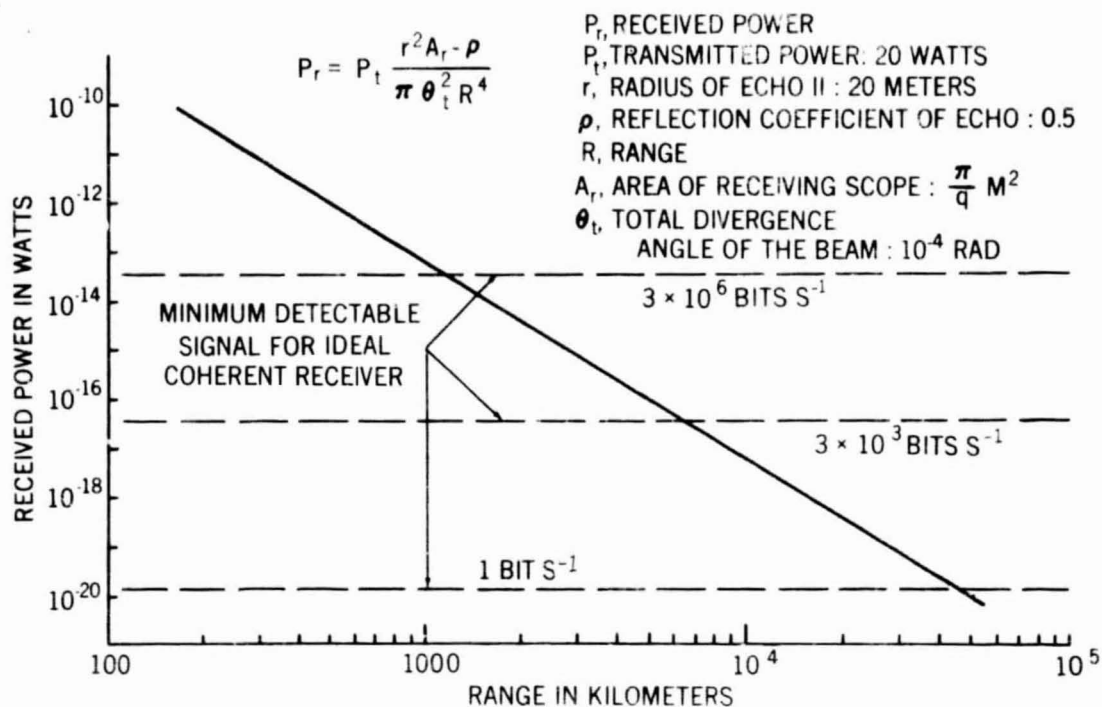


FIGURE 3. POWER RECEIVED IN A REFLECTED BEAM FROM ECHO II USING A 10.6-MICRON TRANSCEIVER

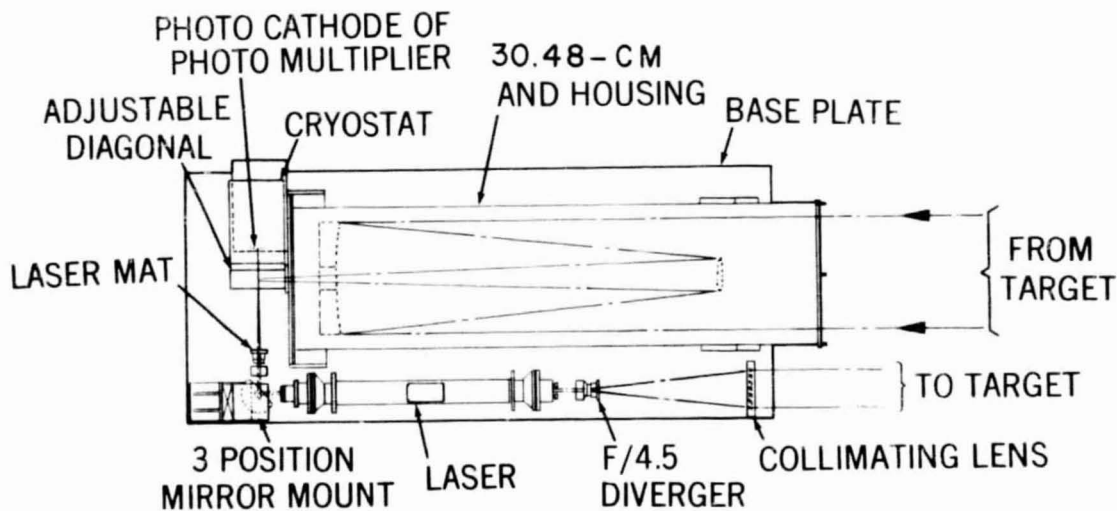


FIGURE 4. HOMODYNE TRANSCEIVER FOR 6328-Å LASER WITH 30.48-CM APERTURE RECEIVER TELESCOPE

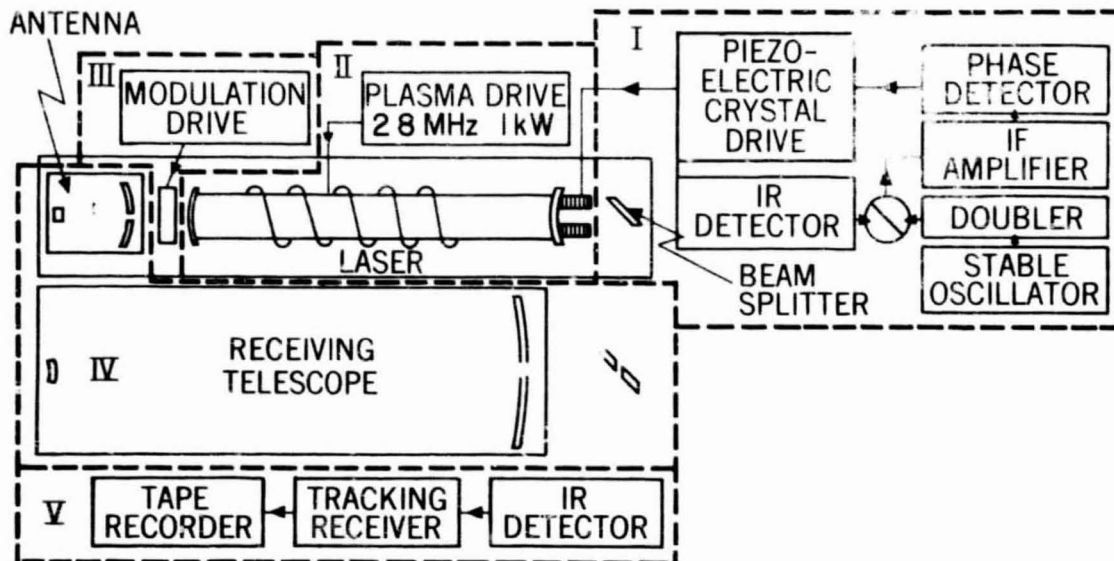


FIGURE 5. BLOCK DIAGRAM OF 10.6-MICRON HOMODYNE TRANSCEIVER.
THE MODULES ARE: I LASER STABILIZER, II LASER, III LASER MODULATOR, IV MIRRORS AND PLATFORM, V OPTICAL HETERODYNE RECEIVER.

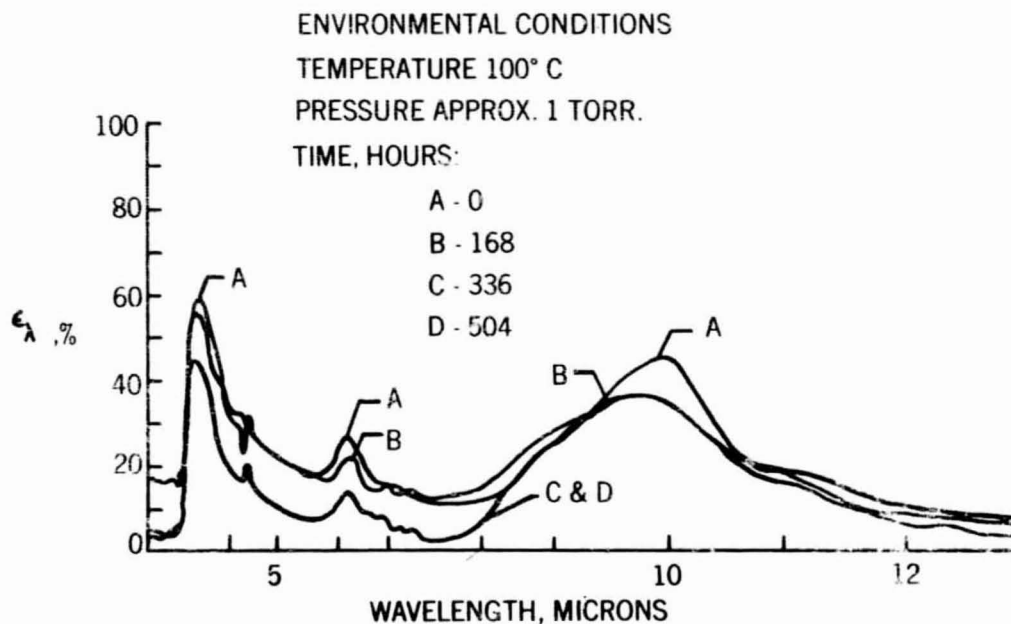


FIGURE 6. THERMAL EFFECTS IN THE INFRARED SPECTRA OF ECHO II.

PRECEDING PAGE BLANK NOT FILMED.

SPHERICAL MIROS

P. O. Minott
Goddard Space Flight Center

N 68-31763

MIROS stands for Modulation Inducing Retrodirective Optical System. The system described in this paper is an outgrowth of the original MIROS concept and is called Spherical MIROS. The intended application for Spherical MIROS is as a means of laser communication relay via satellite. The system may be considered as an optical analog to the Echo satellites. That is, the Spherical MIROS system relays communications from one ground station to another distant station via reflection of electromagnetic radiation from a passive satellite.

Figure 1 illustrates the system concept for a communication link from an orbiting satellite to a ground station. As shown, the ground station, which consists of a laser mounted on an optical tracking theodolite, directs a narrow cw gas laser beam at the satellite. The satellite, which is equipped with a retrodirective optical system, reflects some of this radiation back to the ground station. The ground station is equipped with a telescope that collects the reflected radiation and focuses it on a photomultiplier. Up to this point, the system is quite similar to the S-66 and Geos laser satellite tracking systems. However, the pulsed ruby laser has been replaced by a cw gas laser, and the cube corner panels of S-66 have been replaced by a new type of retrodirective system.

Figure 2 shows the configuration of this new retrodirector. The panels of hundreds of small cube corners are replaced by a single Bouwer's corrected concentric optical system. Basically, the system performs very much the same as a spherical mirror with a second concentric spherical mirror placed in its focal plane. The two corrector plates are used only to correct for the spherical aberration of the primary mirror. The dotted lines indicate the paths of rays passing through the system. Optically, the system performs identically to an optical cube corner; that is, a ray directed into it is reflected in a direction parallel to but opposite in sense to its original direction. It has approximately the same optical efficiency as a cube corner and can be designed to operate over wide angles of acceptance. One important difference should be noted; the radiation must always strike the focal plane mirror. Therefore, if the reflectivity of the focal plane could be controlled, the effective reflectivity of the entire entrance pupil of the system can be controlled. Because the area of the focal plane mirror is much smaller than the entrance pupil, there is an effective

magnification of controlled area over controlling area. This magnification for most of the designs considered is on the order of six to eight times.

By varying the reflectivity of the system, the amount of light reflected back to the ground receiver will be amplitude modulated. If a sinusoidal modulation is imposed on the reflected radiation, the output of the receiver photomultiplier will respond accordingly and can be handled in the same manner as the voltage generated on a radio antenna.

The manner in which the reflectivity of the focal plane mirror is varied is shown in Figure 3. The modulator consists of two closely spaced concentric elements. The first element is a spherical beam splitter whose rear surface is coated to transmit $2/3$ and reflect $1/3$ of the light incident. The second element is a mirror whose surface is spherical and concentric to the beam splitter. The initial separation of the elements is a few wavelengths of light. On the rear surface of the mirror, a piezoelectric element is mounted and connected to the modulator frame in such a manner that the piezoelectric crystal thickness controls the separation of the elements. By applying voltages to the crystal the element spacing may be varied, causing the phase lag between the wavefronts reflected from the beam splitter and mirror to change correspondingly. The effect is to create interference between the wavefronts, thereby effectively changing the reflectivity of the system.

Figure 4 shows a cross section of the first prototype of this system. The aspheric corrector was not included in this unit. The prototype was first successfully operated late in 1964 and has been modulated at all frequencies between 10 kHz and 500 kHz. The depth of modulation, however, is poor at most frequencies, and the system performs best at its resonant frequency (60 kHz). At resonance, the depth of modulation is about 30 to 35 percent. Because the resonance is not sharp the carrier modulation may be amplitude modulated at frequencies up to about 10 kHz with reasonable success. Satisfactory music has been picked up by reflecting a laser beam from the prototype.

Figure 5 shows the test setup used. Pulse frequency modulation telemetry signals have also been successfully imposed on a beam reflected from the Spherical MIROS retrodirector. Power consumption for the system including all of the losses in the driver amplifier, signal generator, etc., is approximately 1.75 W by measurement. Less than 200 mW are actually dissipated in the modulator.

To further illustrate capabilities of the Spherical MIROS system, the equation for energy received by the ground receiver will now be discussed.

Figure 6 shows the equation for energy received by the ground receiver and describes the terms involved in the calculation. A greater insight to the design of the system is obtained by factoring the equation into groups of terms, each group pertaining to a single design problem. As shown in Figure 6, five basic groups may be obtained. These groups pertain to transmitter design, satellite design, receiver design, atmospheric transmission, and orbit parameters, in that order.

To maximize the first term, the laser power must be maximized and the transmission beam divergence minimized. Because transmission beam divergence is limited to 4 arc seconds or greater by obtainable tracking accuracy and laser power is limited to about 10 W by present laser technology, this group of terms cannot be modified greatly. The third term indicates that the only important parameter of the receiver telescope is its area, and the fourth term, atmospheric transmission, is fixed by station location. The fifth term is determined by the orbit selected for the satellite.

The second group is the most important group in the equation. It is this group that must be controlled to make up for the fixed values of the other four. I have chosen to call this group of terms "Retromittance" and denote it by the Greek letter Ψ (Psi). Figure 7 shows the Retromittance term. The area may be replaced by a function of the diameter. The beam divergence may also be replaced by a function of the diameter. When these values are substituted into the equation we find that Retromittance is proportional to the diameter of the system to the fourth power, and inversely proportional to the wavelength squared. For this reason, it is essential that the diameter be as great as possible and that as short a wavelength as possible be used. To illustrate this, let us compare the performance of an array of 2.54-cm (1-in.) diameter modulators to one 50.8-cm (20-in.) diameter modulator. Because the Retromittance is the fourth power of the ratio of diameters, the 50.8-cm (20-in.) diameter is $20^4 = 160\,000$ times as effective, or alternately 160 000 2.54-cm (2-in.) modulators would have to be assembled to equal the single 50.8-cm (20-in.) diameter modulator.

A sample power calculation for a synchronous orbiting Spherical MIROS is shown in Figure 8. With this power level, a bandwidth of approximately one MHz should be possible. The modulators presently available do not permit modulation of this bandwidth, but it is expected that better modulation techniques developed in the future may be able to utilize a greater portion of this bandwidth than is presently possible. A Pockel's cell modulator is under study for higher modulation capability. As the available power increases, bandwidth should increase to at least tens of MHz.

To use the Spherical MIROS system as a ground-to-ground relay system, further equipment must be added to the satellite. As shown in Figure 9, Station A transmits a modulated information carrying laser beam to the satellite. The receiver aboard the satellite senses the laser beam, amplifies the modulation, and uses it to drive the Spherical MIROS retrodirector modulator. Station B sends a cw laser beam to the satellite. The reflected radiation from Station B's beam will now be modulated with the same modulation as Station A's transmitted beam. Station B receives the reflected radiation and converts it into electrical signals photoelectrically. By this method Station A may transmit information to B. In a similar manner, Station B may transmit information to A.

Some possible applications of the Spherical MIROS system are:

1. As a telemetry link from satellite to ground, reducing data loading on radio tracking stations
2. As a ground-to-ground communication link
3. To transmit telemetry signals from a moon station back to earth
4. As a secure means of transmitting military information from one continent to another
5. To transmit telemetry signals from planetary expeditions. This requirement, however, would require a moon-based or orbiting transmitter station
6. To determine atmospheric effects upon laser communications to and from space stations

In summary, the Spherical MIROS laser communication system differs from other laser communication schemes in that it does not require a laser transmitter at each end of the communication link. Because of its simple construction and retrodirective properties, it would have an extremely long life-time and would not require accurate stabilization of the satellite. Its passive nature requires only minimal power supplies, thereby reducing weight and cost. Spherical MIROS presents a novel and effective means of communication via laser beams without any of the complexity or low reliability associated with systems employing lasers aboard satellites.

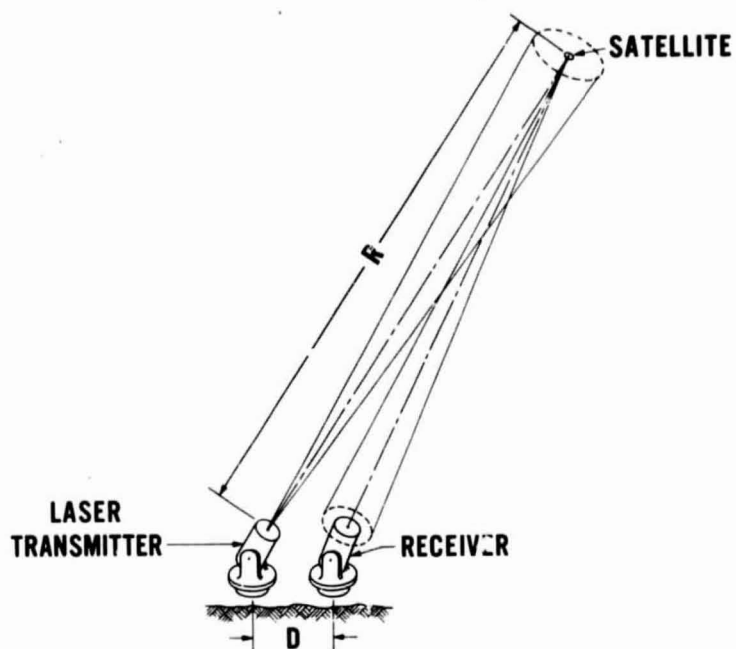


FIGURE 1. TYPICAL SATELLITE-TO-GROUND MIROS COMMUNICATIONS LINK

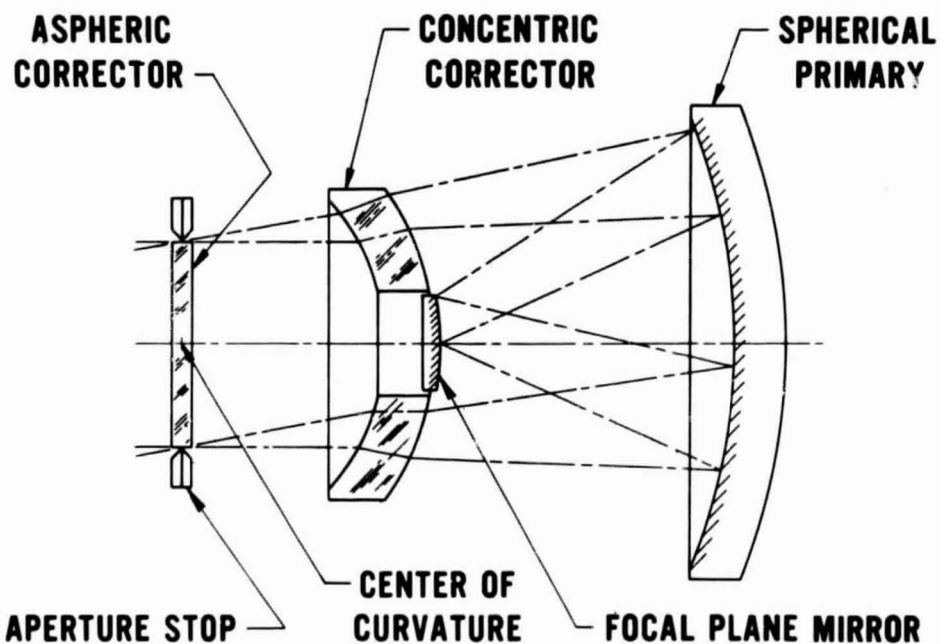


FIGURE 2. BOUWER'S CORRECTED CONCENTRIC OPTICAL SYSTEM

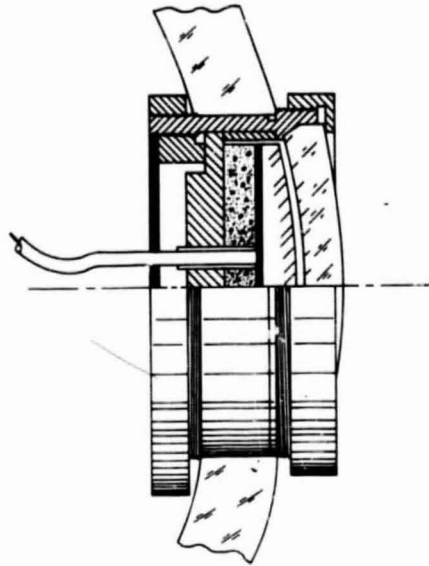


FIGURE 3. PIEZOELECTRIC INTERFEROMETER MODULATOR

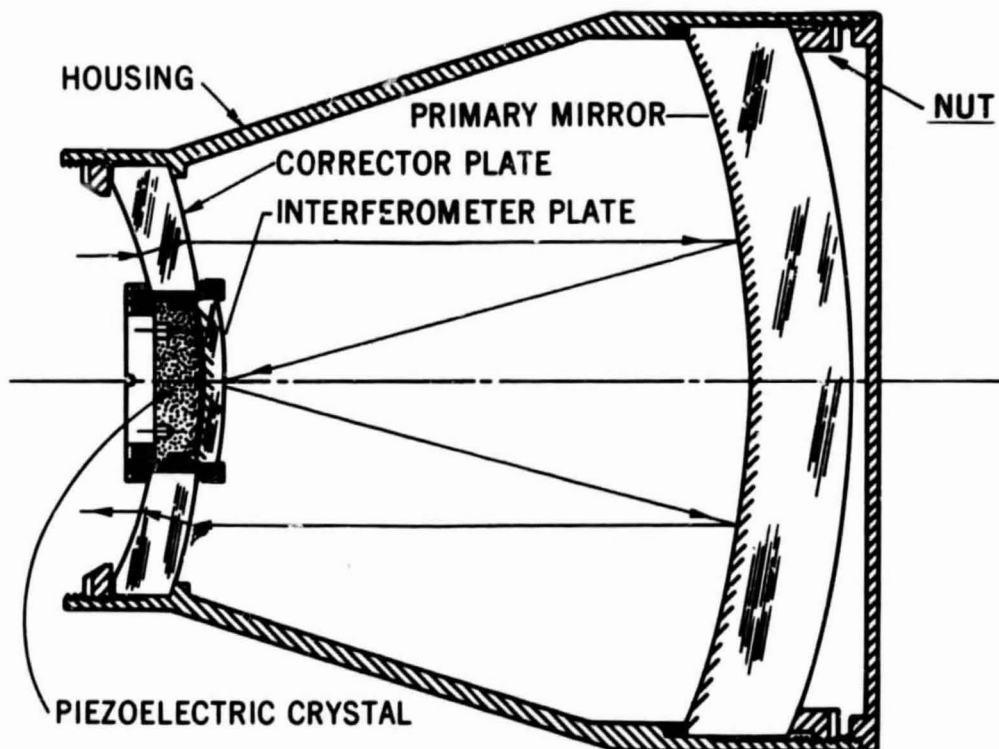


FIGURE 4. CROSS SECTION OF FIRST PROTOTYPE OF MIROS

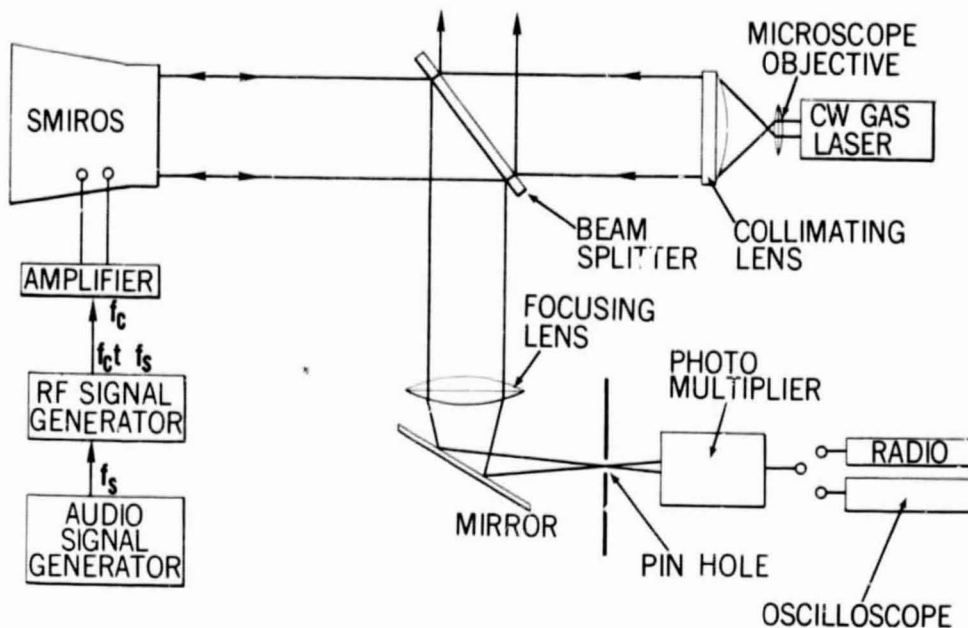


FIGURE 5. TEST SETUP

$$W_R = \frac{P_t A_C A_R \tau^2}{\pi^2 \theta_c^2 \theta_t^2 R^4}$$

$$= \left\{ \frac{P_t}{\pi \theta_t^2} \right\} \cdot \left\{ \frac{A_C}{\pi \theta_c^2} \right\} \cdot \left\{ A_R \right\} \cdot \left\{ \tau^2 \right\} \cdot \left\{ \frac{1}{R^4} \right\}$$

W_R = POWER RECEIVED BY GROUND RECEIVER

P_t = TRANSMITTED LASER POWER

A_C = AREA OF SATELLITE RETRODIRECTOR

A_R = AREA OF RECEIVER

τ = ATMOSPHERIC TRANSMISSION

θ_t = HALF ANGLE OF TRANSMITTED LASER BEAM

θ_c = HALF ANGLE OF REFLECTED LASER BEAM

R = RANGE FROM TRANSMITTER TO SATELLITE

FIGURE 6. EQUATION FOR ENERGY RECEIVED BY THE GROUND RECEIVER

$$\text{RETROMITTANCE} = \psi = \frac{A_c}{\pi \theta_c^2}$$

$$\text{BUT } A_c = K_1 \pi D_c^2 \quad \text{WHERE } K_1 = 0.75$$

$$\theta_c = \frac{K_2 \lambda}{D_c} \quad \text{WHERE } K_2 = 1.22$$

THEREFORE

$$\begin{aligned} \psi &= \frac{K_1 \pi D_c^2}{\pi \left[\frac{K_2 \lambda}{D_c} \right]^2} = \frac{K_1 D_c^4}{K_2^2 \lambda^2} \\ &= K_3 \frac{D_c^4}{\lambda^2} \quad \text{WHERE } K_3 = \frac{K_1}{K_2^2} = 0.50 \\ &= \frac{D_c^4}{2 \lambda^2} \end{aligned}$$

FIGURE 7. RETROMITTANCE TERM

$$W_R = \frac{P_t A_c A_R \tau^2}{\pi^2 \theta_c^2 \theta_t^2 R^4} = \frac{P_t A_R \tau^2 D_c^4}{2 \pi \theta_t^2 \lambda^2 R^4}$$

$$P_t = 1 \text{ WATT}$$

$$A_R = 1 \text{ METER}^2$$

$$\tau = .707$$

$$D_c = 0.5 \text{ METERS} \approx 20 \text{ INCHES}$$

$$\theta_t = 20 \mu \text{ RADIANS} \approx 4 \text{ ARC SECONDS}$$

$$\lambda = 0.5 \times 10^{-6} \text{ METERS}$$

$$R = 3.6 \times 10^7 \text{ METERS} = 22,300 \text{ MILES}$$

$$W_R = \frac{1 \times 1 \times (.707)^2 \times (0.5)^4}{2 \pi (20 \times 10^{-6})^2 \times (0.5 \times 10^{-6})^2 (3.6 \times 10^7)^4} = 3 \times 10^{-11} \text{ WATTS}$$

FIGURE 8. SAMPLE CALCULATION FOR MIROS IN SYNCHRONOUS ORBIT

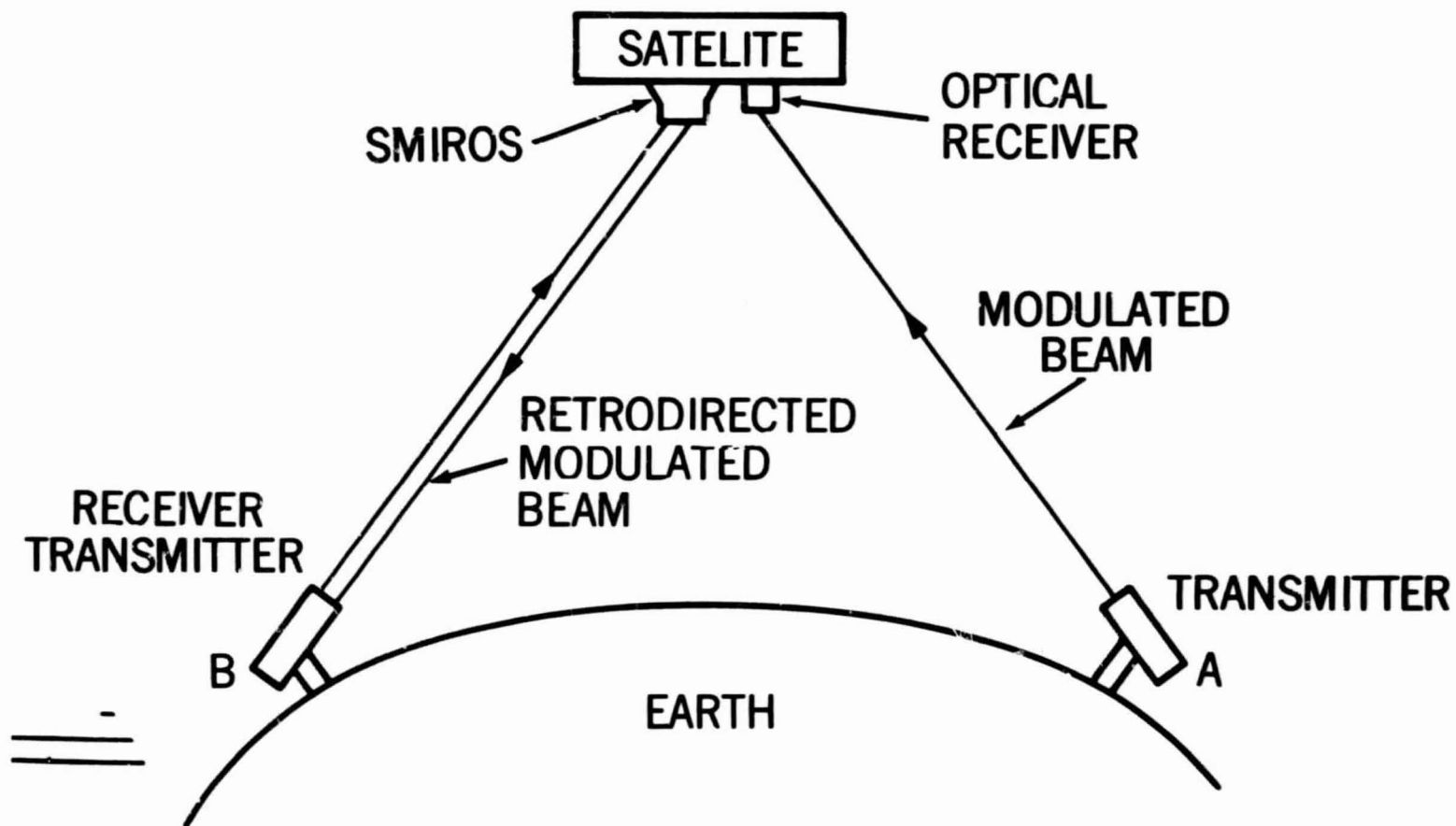


FIGURE 9. COMMUNICATIONS LINK GROUND TO GROUND

PRECEDING PAGE BLANK NOT FILMED

THE OPTICAL IMAGING SYSTEMS FOR RANGER, MARINER, AND SURVEYOR TELEVISION

E. P. Martz, Jr.
Jet Propulsion Laboratory
California Institute of Technology

N 68-31764

To date, NASA and JPL have had two fly-by programs for television photography of the moon and Mars: Ranger and Mariner. A third one is coming up soon for a soft landing and direct surface photography of the moon: Surveyor. This is an attempt to present a summary of some of the optical imaging hardware characteristics of these three projects.

Rangers 3, 4, and 5, the first three attempts, did not get photographs of the moon, but it was not the fault of the television cameras or optics. Figure 1 shows the 1-m focal length T/6.3 Cassegrainian telescope that was to resolve perhaps a Volkswagen on the moon from an altitude of 59 km.

Figure 2 depicts the telescope with fused quartz primary and secondary mirrors and the new and exotic design feature of a 20-cm-dia fused quartz tube, which, under spring pressure, was the basic mechanical structure separating the primary and secondary mirrors. This was employed in preference to Invar or other metals to reduce the probability of misalignment of the mirrors and de-focusing, by the heat of the sun on one side and the deep cold of space on the opposite side. The lens cap to protect the mirrors from damage by micro-meteorites on the 65-hour trip to the moon shows on the front.

The telescope broken down, showing the primary and secondary quartz mirrors, the quartz separator tube, the vidicon tube, and the TV camera electronic package, is shown in Figure 3.

Figure 4 is a view of the mount supporting the secondary mirror showing the off axis supporting spiders in two parallel pairs to form a double couple. This gives much greater torsional rigidity than conventional reflecting telescope design employing four radially symmetrical spider supports. This is essential to prevent radial displacement and de-focusing of the telescope during the severe vibration and shake of launch rocket take-off.

Rangers 7, 8, and 9 had a considerably better lunar photographic outcome than Rangers 3, 4, and 5. The TV cameras on Ranger 6 went out of

commission, but Rangers 7, 8, and 9 were classically successful all down the line. Here the camera aperture, which pointed toward the moon, is near the top of the nose cone (Fig. 5).

In Figure 6, the six television cameras, with overlapping fields of view, are shown as someone on the moon would see them. One of these cameras had a wide angle 25-mm f/0.95 French Angenieux lens, covering a field of view 25° square on the lunar surface over the 11-mm square vidicon photoconductor. Another had a 76-mm f/2 Bausch and Lomb Super Baltar lens covering a field of view 8.4° square. The other four cameras all had the vidicon aperture reduced to 2.8 mm square for faster scan and data transmittal rates as the spacecraft approached the moon to get pictures at the lowest possible altitude before impact. Two of these cameras had 25-mm f/0.95 lenses, and two had 76-mm f/2 lenses, with fields of view one quarter as large as the first two cameras. These lenses were both chosen after very extensive laboratory testing of over thirty high-speed, short focal length lenses from manufacturers all over the world. The resolving power as a function of contrast, optical modulation transfer function, distortion, and veiling glare were measured in the laboratory among other optical characteristics. The choice was a good one, as demonstrated by the results of Rangers 7, 8, and 9.

Figure 7 shows one of the wide-angle cameras, with the lens on the left, the vidicon tube fixture on the right, and the focal plane shutter, of the TIROS type, in the middle.

The next successful mission, Mariner C, demonstrated by its television photographs of the surface of Mars that Mars, like the moon, is covered by impact craters. Figure 8 shows the Mariner spacecraft with the television telescope pointing out of the bottom at the center.

The close-up view of Figure 9 shows the 300-mm focal length T/8 Cassegrainian telescope for the TV system, again with off axis supporting spiders for greater torsional rigidity of the secondary. Also shown here is the Canopus sensor that pointed the spacecraft and the extensive brilliant thermal shielding.

Figure 10 presents views of the telescope showing the gold plating applied to it, as was also done for Rangers 3, 4, and 5, for better thermal emissivity and temperature control. In this telescope we went to beryllium metal mirrors coated with an amorphous metal film of Kanogen, nickel-nickel-phosphorous, on which the optical surface was polished. On this was evaporated conventional aluminum reflecting films and silicon monoxide for protection. Beryllium was

used for the mirror base, in preference to fused quartz, because of its high thermal conductivity and better maintenance of focus in the space temperature environment. For applications on earth, such as severely heated solar telescopes, this appears to be very satisfactory. However, we are becoming somewhat concerned that in a long time in the vacuum of deep space, such as the 8-month trip to Mars, the Kanogen may have blistered and damaged the aluminum reflecting film. This would have introduced serious scattered light and veiling glare into our vidicon image. The Mariner Mars photographs were very sharp and detailed, but the contrast appears low and veiling glare from the telescope is suspected. In coating the Kanogen on the beryllium, monotomic hydrogen is formed, which is heavily absorbed by the beryllium. If this hydrogen has not all been driven off by proper heating before launch it can be expected to bubble out in the deep-space vacuum and through the Kanogen and aluminum films.

Figure 11 is a cross section of the telescope and TV system. The mechanical elements that hold the telescope mirrors and aperture stops in place are constructed of beryllium-copper metal, which has a close match to the thermal expansion coefficient of the beryllium mirrors. A Cassegrainian telescope system, if made completely of materials having the same coefficient of thermal expansion, and if not allowed to develop temperature gradients within itself, will merely scale itself optically and mechanically with changes in temperature. With a deep-space camera temperature of -12°C , as on the Mariner mission, the focus should not have changed more than 0.1 mm from the best focal position established in the laboratory room temperature. This focal excursion is five times smaller than the 0.5-mm depth of focus of the 300-mm f/7 telescope. The sharpness of the Mariner Mars photographs has justified this design.

Because the Surveyor spacecraft is very complex with many experimental functions, we can only touch on the television photography systems. Figure 12 shows the two survey television cameras. With the help of flat mirrors over their lenses panning in azimuth and elevation like a heliostat, these will photograph the lunar surface from a few meters away to the horizon. These are separated by 1.4 m and are capable of scanning the same lunar areas so that stereoscopic measurements of the distances and sizes of rocks and other lunar structures out to 28 m or more from the spacecraft can be made from the TV photographs. In addition to these cameras an approach camera of 100-mm focal length at f/11 will photograph the lunar surface as the spacecraft descends to help in identifying its landing place. This camera will only have a resolution of 35 m from the last probable usable photograph at 130-km altitude, where the retrorockets go on. However, there is no attempt to compete here with Ranger in resolution or purpose.

Figure 13 shows one of the survey TV cameras. The flat scanning mirror; also of Kanogen on beryllium, is at the top with the protective hood behind it which keeps out any lunar dust stirred up by the retrorockets and landing maneuvers. Below it is the variable focal length zoom lens, the shutter, and the vidicon tube and TV electronics.

The zoom lens varies its focal length from 25 mm to 100 mm at $f/11$ and its focus on objects at different distances automatically or on radio command from earth (Fig. 14). Its resolving power on objects 4 m distant should be 0.4 cm at 25-mm focal length and 0.1 cm at 100-mm focal length. This lens is necessarily very complex, as are all zoom lenses. It has 12 glass elements, all of which are uncemented to prevent damage that might occur with Canada balsam or even methyl methacrylate lens cements under the temperature extremes of the lunar surface in a deep vacuum. Therefore, there are 24 glass-air surfaces, and, although these are low reflection coated with magnesium fluoride, a great deal of scattered light in the camera image might be expected. In fact, if the lenses were uncoated, we could expect at least 50 percent veiling glare light. Rather surprisingly, initial laboratory tests indicate that the amount of veiling glare is not excessive, compared to other photographic lenses. There are problems with multiple reflections and ghost images when the bright sun is at certain positions relative to the camera axis. These can, in general, be eliminated by properly designed internal and external stops, though vignetting must be watched for with these. At the middle of the photo on the left is the beam splitter, which diverts a portion of the incoming image forming light to photoelectric system for automatic correction of the iris diaphragm opening to adapt to changing conditions of solar illumination on the lunar surface being photographed. In addition to recording the bright lunar surface during midday and twilight, this lens and TV camera have the capability to record the lunar surface during the full dark of the moon by extended 3-minute time exposures employing the reflected light of the earth and will be able to record 5th or 6th magnitude known stars for a check of the exact location and attitude of the Surveyor spacecraft on the moon.

Figure 15 is of the Surveyor camera filter wheel, which provides alternate pictures of the same areas in red, green, and blue light, or with no filter at all. It is mounted in front of the lens and is operable on radio command. The color filters have been carefully chosen by the CIE and other color standards. Extensive photometric and colorimetric surveys of the lunar surface are planned from these television cameras to aid in identifying lunar rocks and surface materials by comparison with known earth materials studied under identical goniophotometric and heterochromatic conditions.

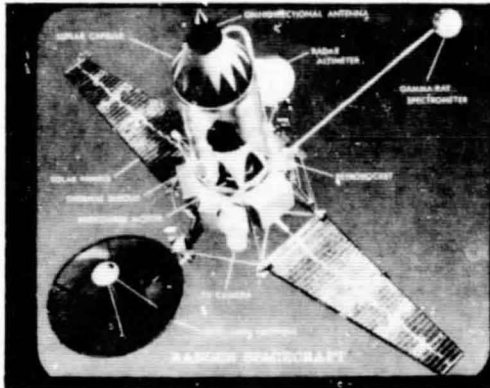


FIGURE 1. RANGER 3,4,5
SPACECRAFT

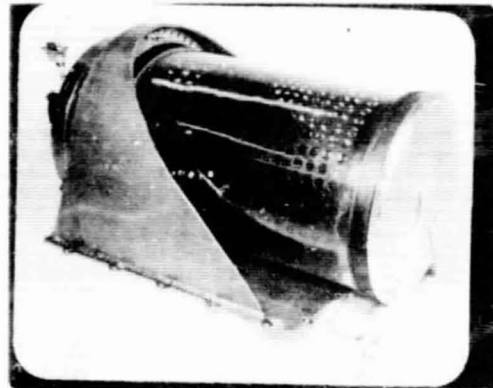


FIGURE 2. RANGER 3,4,5
VIDICON TELESCOPE



FIGURE 3. RANGER TELESCOPE
DISASSEMBLED

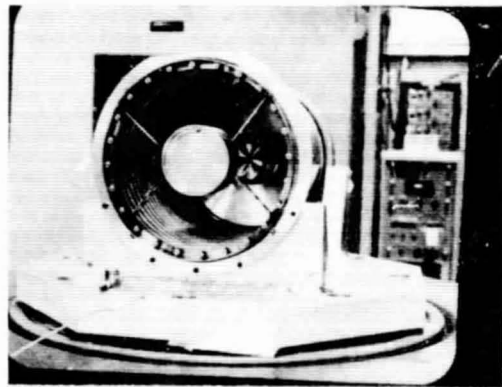


FIGURE 4. FRONT OF RANGER
TELESCOPE

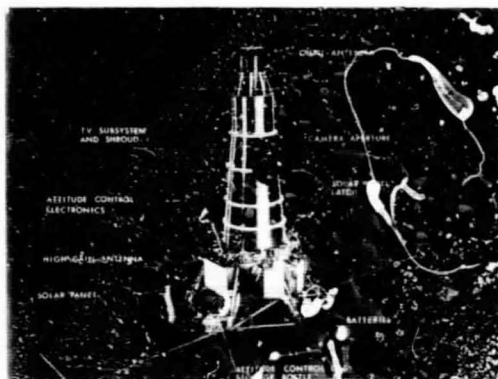


FIGURE 5. RANGER 6,7,8,9
SPACECRAFT

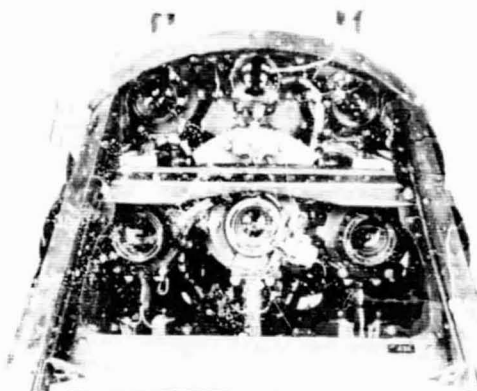


FIGURE 6. RANGER 6,7,8,9
VIDICON CAMERAS

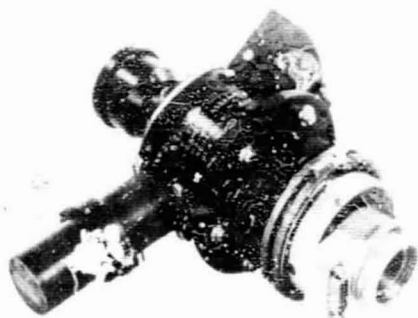


FIGURE 7. RANGER 6,7,8,9
F CAMERA

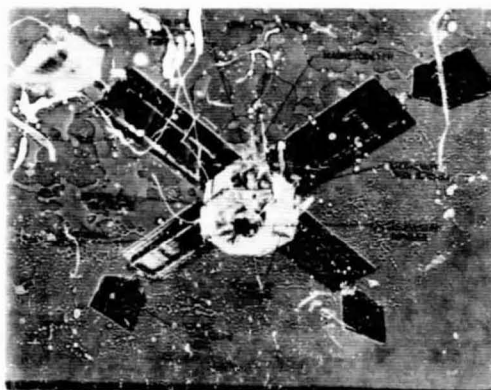


FIGURE 8. MARINER IV
SPACECRAFT

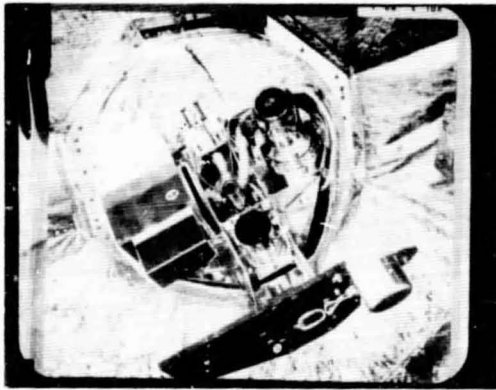


FIGURE 9. MARINER IV TV CAMERA TELESCOPE

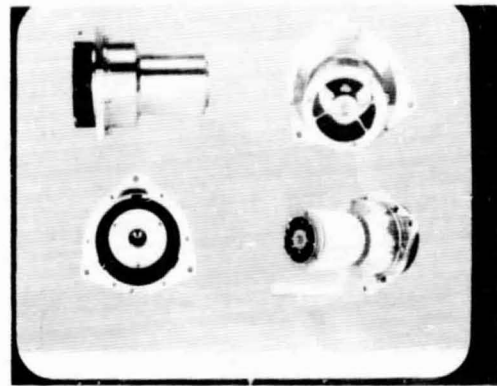


FIGURE 10. MARINER IV TV CAMERA TELESCOPE



FIGURE 11. CROSS SECTION-MARINER TELESCOPE

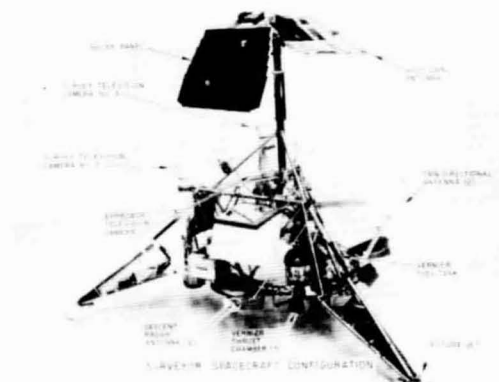


FIGURE 12. SURVEYOR SPACECRAFT

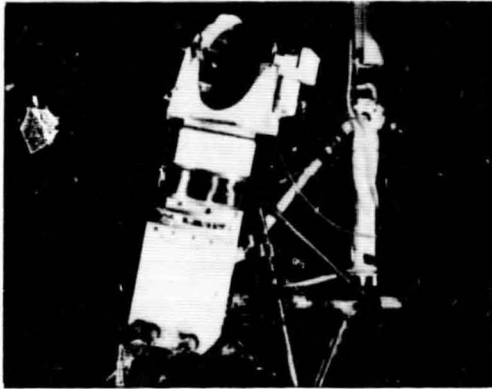


FIGURE 13. SURVEYOR TV
CAMERA HEAD

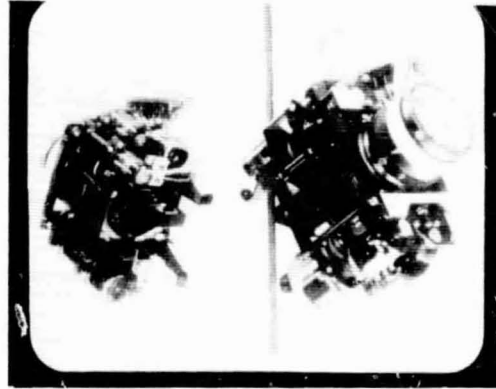


FIGURE 14. SURVEYOR TV
CAMERA ZOOM LENS

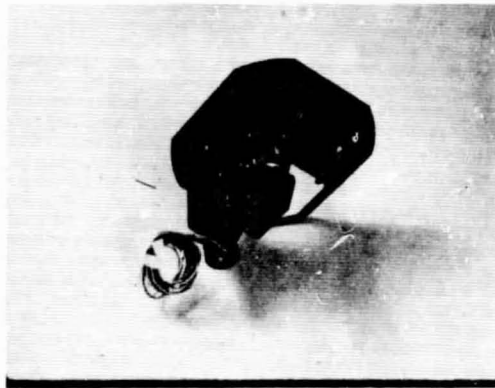


FIGURE 15. SURVEYOR TV CAMERA
FILTER WHEEL

ADVANCED COMPUTER DESIGN TECHNIQUES FOR OPTICAL SYSTEMS

John M. McLauchlan
Jet Propulsion Laboratory

N 68-31765

The Jet Propulsion Laboratory has been using and designing a program for the automatic design of optical systems since January 1964. Although the original program was developed by the Los Alamos Scientific Laboratory, extensive modifications have been made by JPL.

The original program has been supplied by Los Alamos to approximately 30 organizations. In addition, similar programs for use on large computers have been developed at Eastman Kodak, Lincoln Lab, University of Rochester, and elsewhere.

This paper describes experience at JPL with the present program, including the basic techniques used by the program, the capabilities of the program, and the results JPL has obtained on some of its design efforts.

The program does not make use of the classical aberration theories. The design function is accomplished by first tracing a set of rays through the optical system. Additional sets of rays for different object locations and indices of refraction are also traced. A figure of merit is calculated for these sets of rays from the sum of the rms spot sizes of the spot diagrams on a specified image surface. Additional criteria such as the correction of distortion can also enter into the determination of the figure of merit. Next, one of the parameters of the optical system that is to be determined is allowed to change by a small increment. The sets of rays are then retraced, and a new figure of merit is calculated. This process is again repeated one at a time for all the other parameters that are to be determined in the design. Next, the amount that these parameters are to be simultaneously changed in order to minimize the figure of merit is computed by a least squares method. This represents one design cycle. Using the new values of the parameters the design cycle is repeated. Further iterations continue until no significant improvement is being made in the figure of merit. This process requires many computations, and it is only the recent advent of the large computing machines that have made its use practical.

To design an optical system an initial configuration must first be given. In the extreme it may consist of only flat plates of glass. The following parameters may be held fixed or allowed to vary with their value to be determined in the design process.

1. All geometrical properties of spherical, conic section, aspheric polynomial, and cylindrical surfaces that are refracting or reflecting and are axially symmetrical, displaced, or tilted with respect to the optical axis.

2. The location of a plane or curved image surface.

The design may be performed under the following conditions:

1. Minimum and maximum values may be placed upon the parameters that are allowed to vary.

2. As many as 100 skew rays from a single object point can be used.

3. Up to 50 surfaces can be used.

4. Up to 7 different object locations can be used.

5. Up to 6 different indices can be used.

6. Stops utilizing circular or rectangular shapes can be used.

7. In the computation of the figure of merit different weights can be assigned to such factors as: the x and y rms values of the spot size, the relative importance of different colors, and the amount of distortion correction desired.

Upon completion of the design the program can provide the following information:

1. The complete geometrical description of the design including the maximum required clear aperture of all elements of the optical system.

2. The performance of the design as determined by:

- (a) The rms image surface spot sizes as determined from sets of rays from object points

- (b) The average x and y values of each set of rays in the image surface
- (c) The individual x and y coordinates of each ray with respect to the average x and y value for the set
- (d) The focal length
- (e) The back focal distance
- (f) A spot diagram for visual interpretation of each set of rays in the image plane.

The following examples demonstrate JPL's experience with this program. A sun simulator of the solar radiance precisely collimated is being used to test sun sensors.

The sun is an approximate 6000° black body source. Because an optical system cannot increase the apparent radiance of a source it is necessary to use the hottest point in an arc to provide the necessary radiance. A 5000-W high pressure Xenon arc lamp is being used for the source. A condenser lens images the hottest point in the arc onto a quartz scrambler rod. The uniformly distributed flux emitting from the other end of the rod is collimated and gives a good approximation to the solar radiance. The condenser is located 7.62 cm (3 in.) from the 5000-W lamp, and an immediate problem was the continual breaking of the elements of the condenser due to thermally induced stresses. Preheating of the condenser did not eliminate the breaking.

The optical designer had originally advised that quartz could not be used for the first element as the required color correction could not be achieved. Nevertheless, a design using a quartz element was attempted. Figure 1 shows the design sequence. The upper system represents the initial prescription with an arbitrary amount of positive power given the first two quartz elements. The middle system is an interim solution, and the lower elements represent the final design. Although Figure 1 does not appear to show spherical surfaces, all of the surfaces were constrained to be spherical for ease of manufacture. The final spot size is an improvement of almost a factor of 10 over the image quality of the original design done by an optical designer using the classical methods. JPL has fabricated this condenser lens, and subsequent testing has verified the image quality predicted by the program. In addition, no breakage has occurred in using the condenser in the sun simulator.

Another example of JPL's experience with the program is the design of a lens for a star tracker application. The image plane of this optical system is constrained to be a spherical surface of fixed radius convex to the optical elements. This is necessary because the image surface is the photocathode of an image dissector tube, and the electron optics require this curvature of the photocathode.

Several years ago, an optics company was asked to design an optical system for this application. They were unable to successfully meet the requirements, and we subsequently incorporated fiber optics into the image dissector. Another optical design company provided a catadioptric optical system to work with the plano front surface of the fiber optics. The image dissector is a complex and costly component, and it is desirable to eliminate the fiber optics, if possible. A design attempt using the program was initiated; Figure 2 shows this design sequence.

The initial prescription was chosen to use several glasses so that proper color correction could be obtained. The three colors used in this design were n_d (0.5993), n_f (0.4861), and n_h (0.4047). The first element was chosen to be quartz for radiation protection of the other elements. Again, all the surfaces are spherical. The intermediate design shows a point in the design where the results were examined, and it appeared that two of the elements had become very thin and might not be necessary. These two thin elements were eliminated, and the design was continued. The final design shows an rms spot radius of 0.00381 cm (0.0015 in.). This sequence is interesting because it appears that the computer has told that the initial configuration selected could be reduced to a simpler configuration.

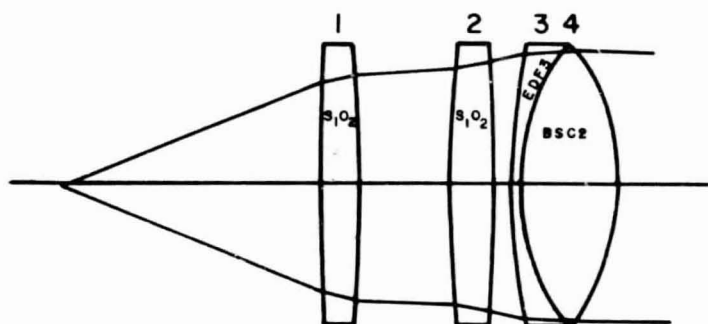
This optical system has not been fabricated because it was subsequently decided that since the star tracker is a single axis sensor we would like to smear the star image somewhat in one direction. A system in which two of the surfaces are cylindrical elements is now being designed. Weighting factors used in the computation of the figure of merit are given different values for the rms x and rms y spot size.

On other optical designs accomplished, the results are similar to those described. In a recent article in the Journal of the Optical Society of America, Joseph Meiron has noted that the superiority of the automatic program over the traditional methods can no longer be disputed. In addition, he noted that under proper guidance the machine invariably attains a higher degree of correction than can be achieved by even the most experienced designer in the past, and in only a fraction of the time required by conventional methods. Experience to date has certainly borne this out, and we are now at a point where we can also add at a fraction of the cost.

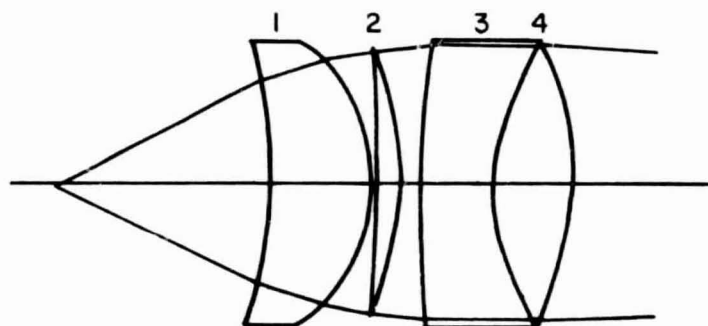
It cannot be said just how much these designs described here have cost in computer time, as a considerable amount of experience has been gained in learning to use the program and in incorporating improvements to the program mixed up with the design time. However, to give some sort of quantitative feel for the cost involved, JPL pays approximately 3.5 dollars a minute for 7094 computer time. With our present proficiency, it is estimated that the design described could be performed for less than 400 dollars each. Ways to modify the least squares method to improve the convergence rate are being studied currently. This will result in less computer time for a given design and will further reduce costs.

This program is available to any of the other NASA centers if they are interested. The program in its present form is only usable on the 7090 or 7094 machines. By the middle of next year, it is expected that the program will be converted completely to Fortran language, and it can then be used on any large computer. Any potential user of the program should plan on a considerable period of time for learning to design with the program before useful results can be obtained. It is most efficient to have a single individual who is devoting a reasonable amount of his time to continuous usage of the program and is available to assist infrequent users with setting up the specifications and input data and interpreting the results. A background in optical design would certainly be most helpful.

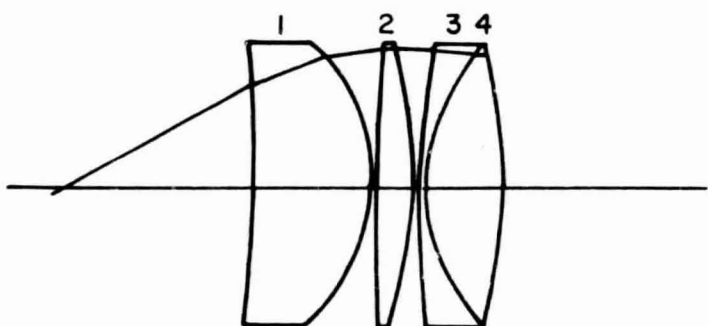
A distribution list for a report JPL is publishing, which describes the details of using the program, is available through the author, John McLauchlan, at Jet Propulsion Laboratory.



INITIAL PRESCRIPTION
 1.605 cm (0.632 in.) rms
 SPOT SIZE RADIUS

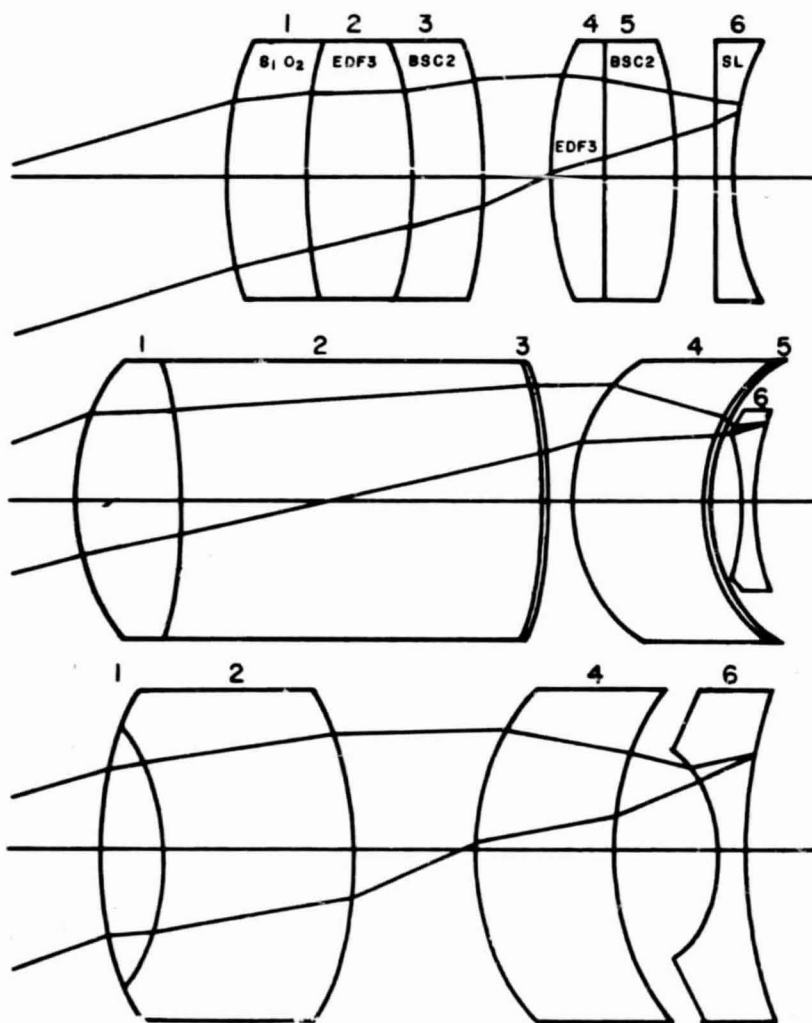


INTERIM DESIGN
 0.058 cm (0.023 in.) rms
 SPOT SIZE RADIUS



FINAL DESIGN
 0.0150 cm (0.0059 in.) rms
 SPOT SIZE RADIUS

**FIGURE 1. CONDENSOR LENS, SUN SIMULATOR; OBJECT DISTANCE
 7.6 CM (3.0 IN.), IMAGE DISTANCE 41.9 CM (16.5 IN.)**



INITIAL PRESCRIPTION
 0.089 cm (0.035 in.) rms
 SPOT SIZE RADIUS

INTERIM DESIGN
 0.0069 cm (0.0027 in.) rms
 RADIUS ELEMENTS
 3 AND 5 ELIMINATED

FINAL DESIGN
 0.0038 cm (0.0015 in.) rms
 SPOT SIZE RADIUS

**FIGURE 2. STAR TRACKER LENS; 32° ANGULAR DIA FIELD OF VIEW,
 2.49 CM (0.98 IN.) FOCAL LENGTH, f/2.0**

PRECEDING PAGE BLANK NOT FILMED

FEASIBILITY STUDIES OF OPTICAL SPACE COMMUNICATIONS AND TRACKING, AND OTHER ACTIVITIES OF THE JPL QUANTUM ELECTRONICS GROUP*

Willard H. Wells**
Jet Propulsion Laboratory

N 68-31766

Continued feasibility studies of optical communications and tracking indicate that the new N_2-CO_2 laser at 10.6μ has significant advantages over other lasers for this purpose. Two difficulties need to be overcome: (1) some loss of coherence in the turbulent atmosphere even at this long wavelength when received at the best observatory sites and (2) inability to tune the laser enough to compensate Doppler shifts. The assumptions behind the wavelength choice include an economic constraint that results from the experience of the Jet Propulsion Laboratory (JPL) operating a world-wide tracking network; viz., we do not consider numerous redundant tracking stations as a solution to the cloud problem. Optical systems are considered only in flexible situations when interruptions are tolerable.

Other activities of the JPL Quantum Electronics Group include building a molecular beam device to attempt maser action at 81μ . We are also considering procurement of a study directed toward large aperture telescopes of unconventional design.

The optical communications portion of the JPL Quantum Electronics Program is guided by a continuing feasibility study of optical communications and tracking in deep space. The only published results of this study are now obsolete in technical detail. In the process of publishing more recent results, we find that inventions of more lasers, detectors, and improved efficiencies change the

* This paper (for the Optical Space Technology Conference, Huntsville, Alabama, Nov. 2, 1965) presents the results of one phase of research carried out at the Jet Propulsion Laboratory, California Institute of Technology, under Contract No. NAS 7-100, sponsored by the National Aeronautics and Space Administration.

** Group Supervisor, Quantum Electronics Group, JPL Communications Elements Research Section, Pasadena, California.

detailed conclusions with a time constant less than that of the publishing process. In particular, it now appears that the recently invented $\text{N}_2\text{-CO}_2$ gas laser [1,2,3], which oscillates at 10.6μ , has sufficient advantage over other existing types to be the primary candidate for a meaningful consideration of the application of very short wavelengths in deep-space communications and tracking.

Our studies of optical communications at JPL differ from many others in two important respects. First, we are unwilling to accept the concept of large numbers of redundant optical tracking stations as a potentially practical way to maintain continuous tracking in spite of clouds. Second, we are unwilling to accept as potentially practical the extremely narrow beamwidth, i.e., 9.1 sec of arc, which is necessary to show a significant advantage at the popular, visible laser wavelengths. The first constraint results from JPL experience with the long-term operations of a network that includes a number of overseas tracking stations. When operational, they contain a great deal more than just an antenna and receiver. Their initial cost and "half-life" operating costs greatly exceed that of the antenna and receiver alone. If optical stations were situated far enough apart for the cloud cover to be statistically independent, then it is doubtful if any facilities could be shared by two or more. Moreover, the geography and politics of our planet could force stations into unpleasant, insecure, and costly locations. Hence, we conclude that spacecraft will always use one weather-independent communication frequency (microwave region). Parenthetically, we also believe that a means of providing an ultra-high reliability command and scientific/engineering data link (two-way) via a spacecraft omni-directional radiator must always be a part of a deep-space communications system; this link requires the use of radio frequencies. Optical or other exotic high frequencies may be used only for flexible functions such as to dump backlogged video data from the spacecraft storage system during favorable weather.

The second constraint, i.e., no pointing accuracies exceeding a few arc seconds, does not have a rigorous basis. It results from professional judgments of those who are experienced with spacecraft systems and the problems encountered when integrating one system with all the others on board. Nevertheless, narrow beam systems have been considered by a number of students of optical communications, so we shall include this type presently when counting decibels to study the relative merits of different frequencies.

We have selected five wavelengths for comparison (Fig. 1). The first is 13 cm (s-band), to be used with the 64-m (210-ft) -D antenna which is nearing completion at the Deep Space Instrumentation Facility (DSIF) Goldstone site. The second is 10.6μ , which is generated by a particularly efficient gas laser and is probably a long enough wave to use a coherent type receiver (optical

detector not the first component). The limitation on coherent reception is caused by atmospheric turbulence, which at $10.6\ \mu$ disturbs the phase significantly and limits reception to the very best observatory sites. The third wavelength is $3.5\ \mu$, which represents a nearly noise-free band between scattered sunlight (blue daytime sky) and planetary albedo at short wavelengths, and atmospheric and planetary thermal emissions at longer wavelengths. Efficient lasers and incoherent detectors (quantum counters) are missing at $3.5\ \mu$, so we shall merely guess future possibilities to see if this band deserves watching for later developments. The fourth choice is $0.84\ \mu$, generated by the particularly efficient and compact GaAs injection laser. The fifth is $0.63\text{-}\mu$, red light generated by the popular helium-neon laser, which would require extreme pointing accuracy to reach a performance level even close to the other four.

The table of decibels (Fig. 1) compares the relative possibilities of these wavelengths. It compares only those factors in the communications range equation that differ from one wavelength to another. The decibel count is not normalized to any particular mission data requirements, or available spacecraft power, because laser communication is too far into the future to associate with any mission presently being planned. When it becomes necessary to assume something for the problem of pointing an optical beam to a particular part of the earth's disc, we have taken the range to be 2 AU, i.e., 300 Gm.

Many items in the decibel table need explanation. For example, the high upper limits in the first and fifth items of the $0.84\text{-}\mu$ column allow for further improvements in laser and detector efficiencies, areas that have been developing rapidly. However, for the purpose of this brief paper, let us confine detailed explanations to the 13-cm and $10.6\text{-}\mu$ columns. The other columns could be in error nearly 10 dB without altering the conclusions significantly.

The decibels in the 13-cm column are all operational or near operational values except for the large 3.35 to 6.4-m (11 to 21-ft) spacecraft antenna. This large size was assumed because surface accuracy requirements are greatly relaxed by comparison to optics, and because plans for JPL spacecraft design now include microwave systems to insure both all-weather communication and omniconmunication, whether or not provision is made for another data rate channel. Therefore to some extent we are comparing the difficulty of a complete optical system to that of merely enlarging the capacity of an existing microwave system. However, such qualitative considerations become complex, because one can argue in rebuttal that a coherent infrared system pays its own way aboard a spacecraft in terms of unique tracking data, accurate angles and high Doppler shifts, and the scientific results, celestial mechanics, relativity, etc., that such data may yield. Also entering this argument is the inherent simplicity of some optical components

compared to their microwave counterparts. We cannot take the comparison of $10.6\ \mu$ and 13 cm as seriously as we can the comparisons among the optical systems. To conclude the s-band column, we note that there is doubt about 50° or 25° for the system temperature. The latter has been achieved with a 25.9-m (85-ft) antenna in an operational planetary radar; the former is the performance obtained with the operational DSIF used to support the Mariner IV (Mars) mission.

In the $10.6\text{-}\mu$ column, the first item is 1-4 percent power conversion. One percent is typical of present $\text{N}_2\text{-CO}_2$ lasers when sealed off, as a spacecraft gas tube would be. Four percent is now attained in flowing gas systems and perhaps future sealed ones. The next entry, spacecraft antenna gain, involves the problem of laser beam pointing from a spacecraft. Fortunately this problem involves great precision only in small angular displacements, not measurement of large angles to high accuracy from reference directions. The transmitting telescope would be simultaneously an earth-viewing telescope with the same angular resolution as the transmitted beamwidth. We assumed a 0.64-cm (2.1-ft) telescope because it seems reasonable to position the resulting 4-sec beam on a 10-sec earth-disc, using fairly conventional means. For example, the earth's visible disc or crescent as imaged in the spacecraft telescope could be divided into quadrants and positioned for equal light power in opposite quadrants. The transmitted beam could be offset from the quadrant center by command, and the offset could be updated every hour or two as required.

In the third item, earth-based receiving antenna area, which is proportional to antenna gain, we chose 121.9 cm (48 in.) because data on atmospheric effects in the very best sites, e. g., the northern Andes, suggest that this large an aperture can be used before large-scale atmospheric irregularities seriously limit effective antenna gain. Of course these effects are weather dependent, so we included an allowance of 37 percent down-time due to weather in the sixth item. Obviously such a system needs a flexible spacecraft data rate. However, the real limitation in ground hardware is economic. As far as installation costs go, the 64-m (210-ft) antenna costs $\$12 \times 10^6$, while a 121.9-cm (48-in.) optical antenna is estimated at only $\$38 \times 10^4$. For the cost of the 64-m (210-ft) antenna, we can afford many 121.9-cm (48-in.) telescopes and still have a few million dollars left for the problem of phasing together an adaptive array and thereby providing a dynamic correction for the changing atmosphere.

The fifth item, i. e., the reciprocal of the spectral density of noise, is derived from the theoretical noise limit of an optical heterodyne receiver or of a maser preamplifier when $hf \gg kT$. We allowed 3 dB excess noise for imperfect quantum efficiency of an optical heterodyne receiver or for imperfect population

inversion in a laser amplifier. The remaining items are self-explanatory. The totals strongly suggest 10.6μ as the wavelength for further research. We cannot be fully confident of this conclusion until we know more about the effects of atmospheric turbulence on this wavelength. We especially need to know the rms deviation of a nominally plane wavefront in the daytime at the world's best observatory sites. Observational conditions in these places have been studied mainly at night because the persons interested are astronomers.

There is another and rather curious difficulty with the N_2 - CO_2 laser, but it affects only the receiver and can probably be circumvented. The Zeeman and Stark effects practically vanish in CO_2 , so that there is no apparent way to tune the laser in the receiver through 500 MHz or so to compensate for Doppler in the incoming signal. It may be necessary to use an optical heterodyne receiver in which the local oscillator is modulated, and the appropriate side band is filtered out for mixing with the signal.

Those who have not yet seen a high-power N_2 - CO_2 laser have a treat in store for them. The gas discharge tube consuming only a few hundred watts looks quite innocent, but its invisible output will quickly char wooden objects, clothing, or skin. An ordinary sheet of asbestos makes an effective image converter to view the mode structure of the output. Those fibers in the most intense parts of the beam quickly reach incandescent heat and are visible in a lighted room.

This paper purposely has not covered another principal activity of the JPL Quantum Electronics Group because the N_2 - CO_2 laser seems to be such a significant and timely development. The majority of the in-house group is currently attempting to build a molecular beam maser (laser?) oscillator at 81.25μ , i.e., a wavelength in the pure rotational spectrum of hf. The population inversion is expected to result from resonant cooling of the terminal state by weak interactions with cold rarefied HC1 gas [4]. We are also considering a procurement action for a study of unconventional telescopes of large effective aperture for communications.

REFERENCES

1. Patel, C. K. N.: CW High-Power N_2 - CO_2 Laser. Appl.Phys. Lett. , American Institute of Physics, vol. 7, July 1, 1965, p. 15.
2. Patel, C. K. N.: Continuous-Wave Laser Action on Vibrational-Rotational Transitions of CO_2 . Phys.Rev., American Institute of Physics, vol. 137, Nov. 30, 1964, p. A1187.
3. Patel, C. K. N.: Selection Excitation Through Vibrational Energy Transfer and Optical Maser Action in N_2 - CO_2 . Phys.Rev.Lett., American Institute of Physics, vol. 13, Nov. 23, 1964, p. 617.
4. Wells, W. H.: Proposed Gas Maser Pumping Scheme for the Far Infrared. Jour.Appl.Phys., American Institute of Physics, vol. 36, Sept. 1965, p. 2838.

Wavelength	13 cm		10.6 μ		3.5 μ		0.84 μ		0.63	
S/C transmitter power conversion efficiency	Operational	-7 dB	1 - 4% N ₂ -CO ₂ laser (.63 cm (2.1 ft) 4 sec	-17 \pm 3 dB	Guess for future	(-25 dB)	2.5% GaAs laser, 63% pulse source	-18 ⁺⁸ db	He-Ne laser	-30 dB
S/C antenna gain 0.65 ($\pi D_t/\lambda$) ² ; at 2 AU; earth subtends 10 sec	3.35-6.3 cm (11-21 ft)	39 \pm 3 db		104 dB	Upper limit for simple pointing	105 dB	17.78-cm (7-in.) aperture, 1 x 10 sec beam	106 dB	0.63 cm (2.1 ft) 0.2 sec	128 dB
Ground receiver antenna area (20 log D _r , ft)	63 cm (210 ft) at \$12 x 10 ⁶	46.4 dB	1.22 m (4 ft) at reduced eff., -2 dB, at \$380 000	10 \pm 2 dB	9.75 m (32 ft)	30 dB	482.6-762 cm (190-300 in.), \$12 x 10 ⁶ at 4.7 in. ² /K\$	26 \pm 2 dB	same as for 0.84 μ remarks	26 \pm 2 dB
Number of ground antennas	1	---	7-10, eff. loss, adaptive array	8 \pm 1 dB	1	---	1	---	1	---
[Spectral density] ⁻¹ of noise	(K 50%) ⁻¹ 25%?	211.6 ⁺³ ₋₀ dB	50% $\frac{10.6 \mu}{2 \text{ hc}}$	197 dB	0.9% $\frac{3.5 \mu}{2 \text{ hc}}$	(169 dB)	1/4% $\frac{0.84 \mu}{2 \text{ hc}}$ SI photosurface	157 ⁺¹⁶ ₋₀ dB	5% $\frac{0.63 \mu}{2 \text{ hc}}$	169 dB
Down-time { weather, effective horizon	---	---	---	---	-1 -1	-2	-1 -1	-2	-1 -1	-2
Absorption { atmosphere, filters, optics	---	---	-1 0 0	-1	-1 -1 0	-2	-1 -7 \pm 1 -2 \pm 1	-10 \pm 2	-2 -7 \pm 1 -2 \pm 1	-11 \pm 2
Excessive background	---	---	---	---	---	---	---	-1	---	-2
Total decibels (relative)		290 ⁺⁶ ₋₃		298 \pm 6		(275)		258 ⁺²⁸ ₋₄		278 \pm 4
	(287 - 296)		(292 - 304)		(Unknown)		(254 - 286)		(274 - 282)	
Qualitative considerations	All weather, S/C omni mode nearly opera- tional		Unique tracking data		---		Compact solid-state trans- mitter with only 17.78-cm (7-in.) telescope		Extreme pointing problem	
	Phase of carrier wave under control									
	No large dish to erect on spacecraft, and no high voltage microwave problems such as multipactor and gas discharge; basic simplicity of optical components									

FIGURE 1. COMPARISON OF FIVE SELECTED WAVELENGTHS

PRECEDING PAGE BLANK NOT FILMED.

TECHNOLOGY FOR A MANNED ORBITING TELESCOPE

W. E. Howell
Langley Research Center

N 68-31767

Approximately two years ago, Langley Research Center began a study of the requirements for large orbiting telescopes. The objectives of the efforts are to determine the requirements of large diffraction-limited astronomical telescopes in space and to develop the technology necessary for their design. This paper is intended to describe the work that is being done. However, some introductory remarks as to the size of the telescope and the role of man are in order.

During the in-house phase of the studies, consideration was given to telescopes as large as 1016 cm (400 in.); however, it was immediately obvious that such a large telescope was beyond the range of foreseeable technology and available boosters. This latter restraint limits the physical size of the primary to something less than 381 cm (150 in.) without major modifications to the upper stages. Figure 1 illustrates some of the reasons for choosing a 304.8-cm (120-in.)-dia. mirror. Here the telescope resolution in arc seconds versus the aperture in inches has been plotted. The straight line represents the theoretical maximum resolution for any given aperture. As is shown by the horizontal line in the figure, the factor that determines the resolution for telescopes on the earth is not the aperture; it is the atmosphere. Hence, the Palomar 508-cm (200-in.) telescope has no better resolution than a high-quality 38.1-cm (15-in.) instrument, but it does have considerably more light gathering ability. By placing diffraction-limited telescopes in orbit, great advances in resolving power can be made. Presently designed telescopes for use in space have resolution capabilities in the order of 0.1 second of arc, while the 304.8-cm (120-in.) system that is under consideration has a resolution of about 0.03 second of arc. This 304.8-cm (120-in.) size would provide about a factor of 3 improvement in resolution and 10 in light gathering ability over present space systems.

One point should be made regarding collecting power of large optics. Although the collecting power of the 508-cm (200-in.) telescope is theoretically about three times greater than a 304.8-cm (120-in.) telescope, such is not actually the case if the 304.8-cm (120-in.) telescope is outside the atmosphere and the 508-cm (200-in.) remains on earth. This is because the background noise is less and image spread and attenuation are reduced. Because of this,

the (304.8-cm) (120-in.) system will "reach" from 1 to 2 magnitude fainter stars than can presently be seen. The overall improvement in both resolution and collection power is 3 to 5, which represents a significant advance in the state of the art.

As can be inferred from the title of this paper, man is considered to be a part of the system. One of the initial areas of consideration was the contribution man could make if he were physically associated with the telescope. From the most elementary analysis two facts concerning man became clear. The setup, alignment, and checkout of the instrument would be virtually impossible without man, primarily because of our inability to get a system of this complexity and precision through the launch environment in a completely operational condition. Also, past experience with orbiting vehicles has taught us that despite our best efforts and the use of redundant systems, mechanical and electrical components will fail, requiring experiments to be compromised if not dropped entirely. The result of these considerations was the conception of a vehicle that would allow man to perform the task of initial setup, alignment, and checkout and periodic maintenance of the vehicle, and to provide for his removal at all other times. An additional benefit of man being associated with the telescope is that he can retrieve data such as photographic film directly from the vehicle and return it to earth without the degradation normally encountered when these data are transmitted via telemetry. He may also install new experimental equipment that was not available or considered in time to be included in the original launch.

Study has shown that man cannot be physically located within the instrument during periods when it must be controlled to the ultimate precision because his normal movements would degrade the operation. The most convenient way to accomplish satisfactory operation is to connect the Manned Orbiting Telescope (MOT) to an orbiting space station.

Figure 2 shows an artist's conception of a configuration considered during studies by the Boeing Company. The MOT is shown here being coupled to a space station by a man working in the lower left-hand side. This type of operation, with the MOT coupled to the space station, was one of the two modes recommended by Boeing as being the most reasonable. The other was a completely separate operation providing crew transfer when necessary by a shuttle. In the attached mode, the telescope would weigh about 11 794 kg (26 000 lbm) at launch and 9979 kg (22 000 lbm) at orbit. It is about 19 m (61 ft) long and 4 m (14 ft) in diameter. With a suitable space station, the entire structure would be over 31 m (100 ft) long and weigh in excess of 27 216 kg (60 000 lbm). In the detached mode, the telescope alone would be about 18 m (60 ft) long and weigh about 11 700 kg (28 000 lbm) at launch and 10 886 kg (24 000 lbm) in orbit.

Three studies covering various areas of the instrument have been made and are shown in Figure 3. The first was a mission objectives study performed by the University of Virginia, the goal of which was to determine examples of experiments. This study was not intended to define specific experiments to be carried out with the telescope, but to determine classes of experiments that would tax the various capabilities of the telescope such as its resolution and light gathering ability.

From the requirements set forth by the above, an optical system study was made by American Optical Company. The goal of this study was to investigate the optical design and to consider the problems inherent in obtaining the required optics. The recommended optical design was a classical Cassegrain with interchangeable secondaries to provide various f-numbers for the different experiments.

Using these studies as a foundation, a third study entitled "Systems Study of a Manned Orbiting Telescope" was made by the Boeing Company. This is the latest and most detailed work that has been done and is discussed in detail in another paper in these proceedings. The four major goals are shown in Figure 3 and were to investigate the modes of operation; the guidance, control, and stabilization system; structural configuration; and the effects of the thermal environment. From an operational standpoint, it is desirable to have the telescope physically attached to the space station to provide easy access for the crew to perform their duties. However, such coupling places restraints on the space station and greatly decreases the required response time of the control and stabilization system that is required to point the telescope to within the desired accuracy of 0.01 second of arc. If the response time of the control system is made sufficiently fast to overcome the high disturbances of the station, it can excite structural modes that are unacceptable. With due consideration of these factors and others, a soft gimbal mode (coupled to the space station through a spring suspension as shown in Figure 2) and a separate mode were selected as the most desirable. Some of the modes that were considered, but discarded, were a rigidly attached mode, tethered mode, and a gimbaled mode without shock isolation.

As a result of these studies, certain areas requiring further research were identified and are shown in Figure 4. The mission modes study would further investigate in depth the two competing concepts recommended by our previous studies to determine which of these is indeed better suited for the task. The specific material from which the large primary should be constructed and the exact technique to be used should be the subject of extensive studies and development to insure the achievement of the desired performance. Figuring

and testing the mirror and supporting it during launch will require construction and test of reasonably sized blanks as a stepping stone to the development of the MOT mirror. The control of the telescope is of prime importance as it is required to be stabilized to about 0.01 second of arc to realize the full potential of the telescope. Also, the thermal protection of the primary mirror requires considerable attention because small thermal gradients across the surface will greatly distort the figure. Development is also required in the area of detectors to cover spectral regions that have previously been unavailable because of the earth's atmosphere.

To give a better appreciation of the magnitude of some of the problems and what might be done in certain areas to overcome the difficulties, these basic areas are discussed further.

Because the major problem involves obtaining the large primary mirror, the optics are considered first. Some of the aspects of this problem are shown in Figure 5. The prime candidates for mirror materials are beryllium, fused silica, and a class of partially recrystalline glasses known under various trade names such as Cer-Vit.

The chief advantages of beryllium are that it is lightweight, rigid, and has a high thermal conductivity that allows it to equalize temperature quickly and hence reduce the effects of thermal gradients on the blank. The main disadvantages are that it tends to show hysteresis due to thermal cycling and vibration, it has a high coefficient of thermal expansion, and it may not exhibit the required stability over extended periods of time as required by this application.

As for fused silica, more is probably known about this material than the others. Desirable characteristics of fused silica include its ability to accept a good figure and its low coefficient of expansion; however, it is heavier than beryllium and its low thermal conductivity is likely to result in thermal gradients producing figure distortions in spite of the low coefficient of expansion.

Material such as Cer-Vit has about the same properties as fused silica except for its thermal expansion; this has been reported up to 10 times less than fused silica. Insufficient data are available on this material, and further effort is needed to determine if it has the required stability and is indeed as attractive as it appears.

Once a material has been chosen, it must be figured to $\lambda/50$ (at 5000 \AA) to obtain the required performance. For a mirror of this size and accuracy, new

facilities and extremely refined and carefully planned test procedures are required. The problem is further complicated by the fact that the mirror must be figured and tested in a 1-G environment and still have the correct figure under zero-G conditions. Another matter of concern is the manner in which the mirror is supported during launch. At present, the use of pneumatic bladders beneath the mirror during the period of launch is being considered as one possible approach.

From a review of these optics considerations, it is apparent that the majority of the problems are due to the size of the mirror being contemplated. Smaller elements have been figured to the required accuracy, for example, the 91.24-cm (36-in.) Stratoscope mirror. Rather than try to build a single piece mirror, another approach to the problem is to build the mirror in segments and control each segment in tilt and longitudinal displacement relative to a reference element to the required $1/50$ wavelength. It should be pointed out that such an approach merely trades optical figuring and testing problems of large mirrors for precise control problems and is but one possible solution. This approach is the subject of a contract with Perkin-Elmer Corporation in which they are attempting to demonstrate the feasibility of this concept (see Figure 3). The basic concept is shown in Figure 6. On the right is a segmented primary with a figure sensor located at its center of curvature behind the standard secondary. The figure sensor scans each element and detects tilt and longitudinal displacement relative to the reference element. The error signals are used to control actuators behind the mirror which correct these errors. The present contract is aimed at demonstrating the feasibility of this concept on a 50.8-cm (20-in.) spherical mirror to an accuracy of $\lambda/20$.

The next item to be dealt with is the thermal problem, the details of which are outlined in Figure 7. The primary sources of heat are the sun, earth, and equipment aboard the telescope, the radiation from which has several effects upon the telescope. Of major concern are thermal gradients across the mirror itself. Calculations have indicated that thermal gradients of as little as 0.067 Kelvin degree (0.12 Fahrenheit degree) between the center and edge of a 304.8-cm (120-in.) beryllium mirror can create as much as a $\lambda/20$ error (rms) between the actual figure and the best fit parabola. Because of this extreme sensitivity to temperature gradients, the telescope mirror must not view the earth; and to prevent this, doors must be provided which will be closed whenever radiation from the earth impinges on the primary mirror. In recognition of the problems created by temperature gradients, in-house investigations are being made of various thermal control techniques. For example, the thermal behavior of the instrument when placed in a spherical shell with a highly reflecting interior is being studied. These investigations are being carried out on a 50.8-cm (20-in.) model.

Because of the size of the instrument, 9.14 m (30 ft) from primary to secondary, it is not considered feasible to expect the telescope to maintain collimation and focus without active control. The allowable tolerances and the techniques presently under evaluation for sensing misalignment are shown in Figure 8. The optical control requirements for an f/4 primary are: tilt of the secondary about the optical axis of 0.1 second of arc, lateral displacement of secondary to 0.01016 cm (0.004 in.) and focus control to 0.000762 cm (0.0003 in.). Four of the many possible techniques that might be used for sensing these misalignments are shown in Figure 8. Tilt error might be sensed by autocollimation devices. Possible techniques for determining lateral displacement include sensing image degradation, the use of artificial stars, and triangulation methods.

Image degradation involves scanning a star image and comparing its shape with what it should be for its particular location within the field of view. From this, an error signal is generated that indicates the direction the secondary is off. The prime problems involve difficulty in mechanizing the concept and the availability of suitable stars. The second technique, artificial stars, involves directing collimated light beams of approximately 15.24 cm (6 in.) in diameter at the primary. These rays are brought to focus at the focal plane, and any motion of the secondary will cause a motion of the images. Triangulation involves making three measurements of the distance from the primary to the secondary and, by geometry, determining the location of the secondary relative to the primary. Because the distance involved is about 9 m (30 ft) and the tolerances are so small (parts in 10^6), the only technique that appears suitable involves the use of laser interferometers. For this purpose, an automatic interferometer has been designed and is in the construction phase. All of these techniques will be under active laboratory evaluation at Langley within the immediate future.

After optical alignment, the next consideration is that of attitude control, which is outlined in Figure 9. The requirements are that the control system provide stabilization of one-tenth the diffraction pattern using guide stars of 10th magnitude or brighter for durations of up to 8 hours. The control system must have provisions for off-axis guidance and planet tracking. There are basically two techniques available. The first involves control of the entire vehicle to the desired accuracy such as was done on OAO and is the approach used by Boeing/GE in their systems study. A second method is to point the optical axis to the desired region within approximately 2 seconds of arc and obtain fine stabilization by moving suitable optical elements within the telescope, as is done in Stratoscope. This latter approach has certain advantages in that it reduces the response requirements of the high torque system or else allows a higher level of disturbance torque to be accepted by the instrument, which in turn permits a closer coupling of the telescope and space station. This approach

is being evaluated at Langley along with the development of one type of fine guidance sensor and the investigation of interactions between the fine and coarse control system. One technique of obtaining fine control by moving optical elements is presently under laboratory evaluation.

The last area to be covered is that of detector technology, some of the requirements of which are shown in Figure 10. The telescope being contemplated is reasonably efficient over that portion of the spectrum ranging from microwave to about 600 Å. In the microwave region, other types of systems are probably more suitable, and below approximately 600 Å the telescope is not reflective. Within this band only the visible portion of the spectrum can be classified as adequately covered; however, sensors do exist that will go up to about 39 μ and down slightly into the ultraviolet. While the ultraviolet region has sensors capable of detecting this radiation, they could stand considerable improvement. In addition, there exists a requirement for filters and calibration sources. In the infrared, there is a region starting around 39.5 μ and extending to the microwave band in which there are no suitable detectors. Langley's present efforts are in the infrared region and involve two items. The first is a contractual effort for improved thin-film thermistor bolometer detectors with the General Electric Company. The purpose here is to develop thin-film bolometers with positive temperature coefficients and to improve the responsivity and lower the contact noise. The principal advance to date is that GE has learned how to manufacture these thin films and make the necessary transfers from one substrate to another. The second effort is an in-house development of thin-film solid-state detectors in the 39.5- μ region. These use the semiconductor material photoconduction phenomena and thermoelectric cooling for maintaining optimum temperature. The techniques being employed here are well suited to the region between 39.5 μ and the visible.

Figure 11 summarizes Langley's program in the development of the necessary technology for large space telescopes. Research on optics and control will involve the items previously discussed, particularly materials and fabrication techniques for large optical systems. Studies are currently being pursued in-house regarding the use of Apollo flight systems as a step in the development of a Manned Orbiting Telescope. A 152.4-cm (60-in.) optical system is under consideration, and the key items for flight evaluation are as indicated in this final figure.

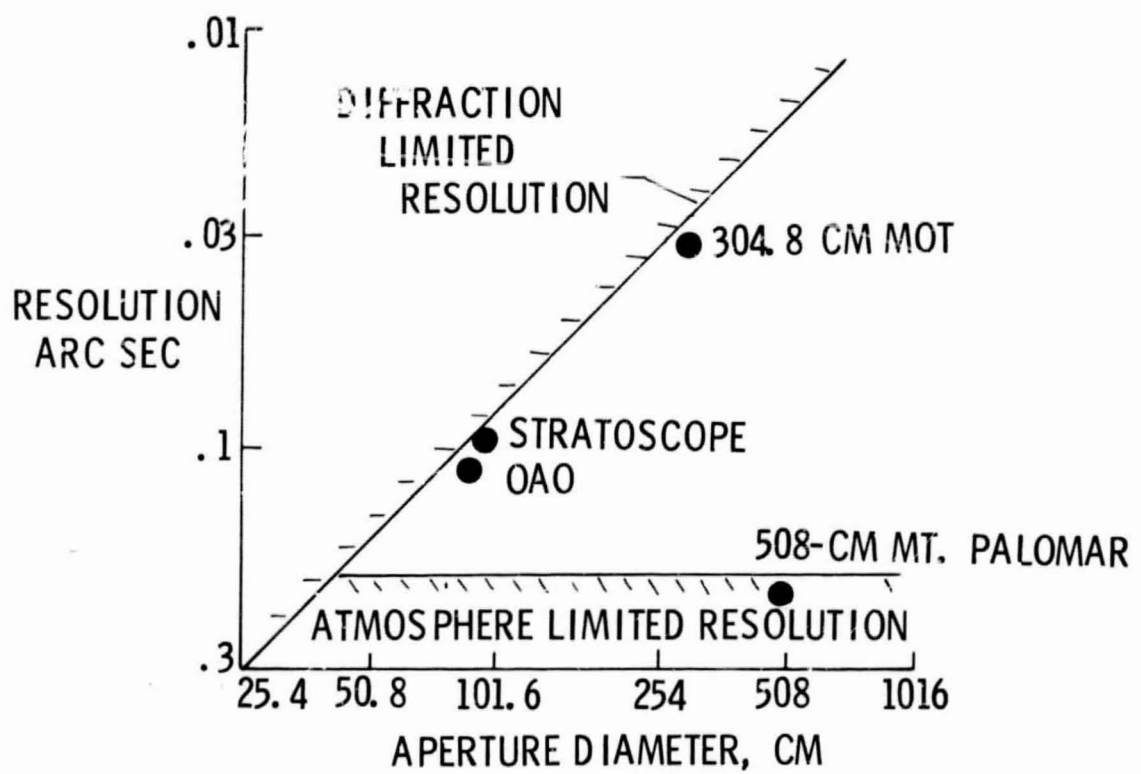


FIGURE 1. RESOLUTION VERSUS APERTURE

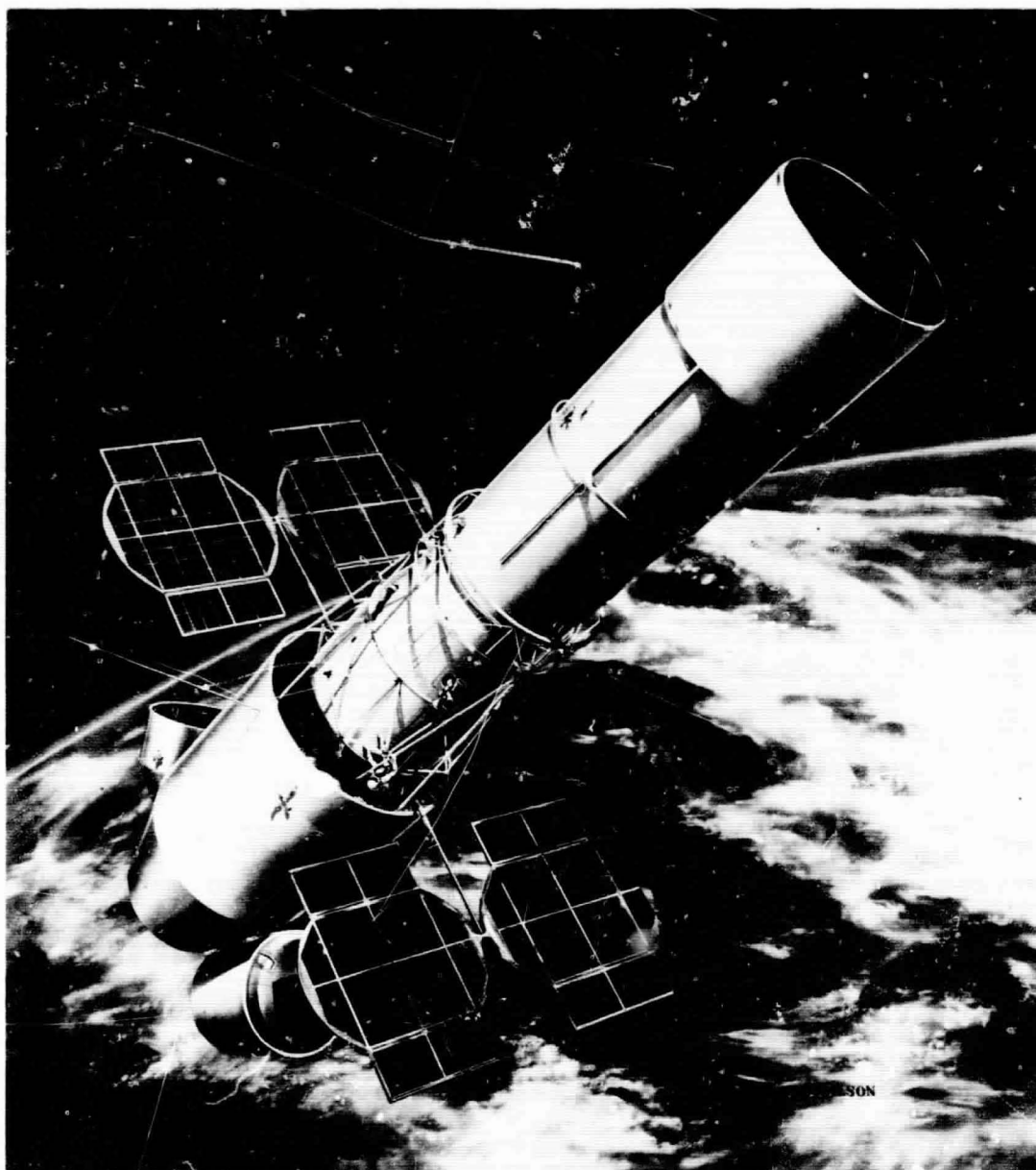


FIGURE 2. MOT AND SPACE STATION

- TYPICAL MISSION OBJECTIVES - UNIVERSITY OF VIRGINIA (NSG-480)

GOAL: TO OUTLINE TYPICAL EXPERIMENTS

- OPTICAL SYSTEM STUDY - AMERICAN OPTICAL COMPANY (NAS1-1305-18)

GOAL: TO INVESTIGATE OPTICAL DESIGN AND THE PROBLEMS
INHERENT IN OBTAINING THE REQUIRED OPTICS

- SYSTEMS STUDY OF A MANNED ORBITING TELESCOPE - BOEING COMPANY (NAS1-3968)

GOAL: TO INVESTIGATE
THE MODES OF OPERATION
GUIDANCE, CONTROL, AND STABILIZATION SYSTEM
STRUCTURAL CONFIGURATION
EFFECTS OF THERMAL ENVIRONMENT

ACTIVE OPTICS FOR SPACE APPLICATION - PERKIN ELMER (NAS1-5198)

GOAL: TO DEMONSTRATE THE FEASIBILITY OF OBTAINING
PRIMARY MIRRORS BY CONTROLLING SEGMENTS

FIGURE 3. STUDIES AND CONTRACTS

- MISSION MODE STUDIES
- MIRROR MATERIALS AND STRUCTURAL DESIGN
- FIGURING AND TESTING
- MIRROR SUPPORT DURING LAUNCH ENVIRONMENT
- THERMAL PROTECTION OF PRIMARY MIRROR
- CONTROL OF TELESCOPE
- DETECTORS

FIGURE 3. AREAS REQUIRING FURTHER RESEARCH AND DEVELOPMENT

- CHOICE OF MIRROR MATERIALS

BERYLLIUM

FUSED SILICA

OTHER MATERIALS

- FIGURING AND TESTING

$\lambda/50$ FIGURE CONTROL

FACILITIES REQUIREMENTS

TEST PROCEDURES

- MIRROR SUPPORT

DURING FIGURING AND TESTING

THROUGH LAUNCH ENVIRONMENT

FIGURE 5. OPTICS CONSIDERATIONS

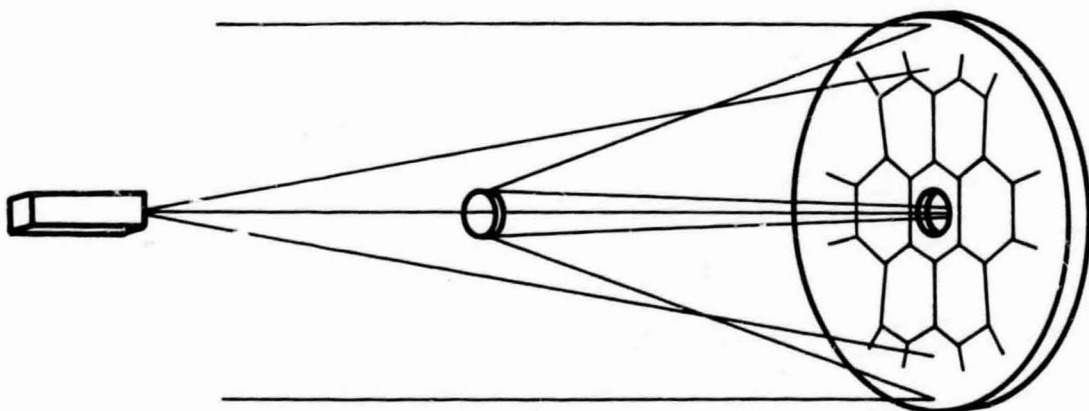


FIGURE 6. ACTIVE OPTICS CONCEPT

- SOURCES

SUN

EARTH

EQUIPMENT

- EFFECTS ON TELESCOPE

MIRROR FIGURE DEGRADATION

STRUCTURAL WARPING

MISALIGNS STAR TRACKERS

MISALIGNS INSTRUMENTATION

DESTROYS OPTICAL COLLIMATION AND FOCUS

FIGURE 7. THERMAL CONSIDERATIONS

- REQUIREMENTS (F/4 PRIMARY)

MAINTAIN PROPER FOCUS AND COLLIMATION

TILT OF SECONDARY - 0.1 SECOND

FOCUS CONTROL -0.000762 CM

LATERAL DISPLACEMENT OF SECONDARY -0.01016 CM

- TECHNIQUES

AUTOCOLLIMATION

IMAGE DEGRADATIONS

ARTIFICIAL STARS

TRIANGULATION METHODS

FIGURE 8. OPTICAL CONTROL

- REQUIREMENTS

STABILIZATION - 0.1 OF DIFFRACTION PATTERN

GUIDE STAR - 10TH MAGNITUDE OR LESS

DURATION - UP TO 8 HOURS

OFF AXIS GUIDANCE

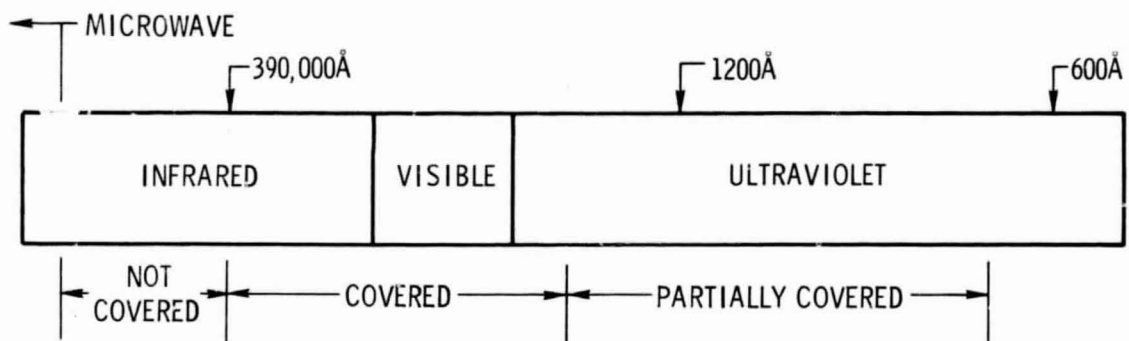
PLANET TRACKING

- TECHNIQUES

CONTROL ENTIRE VEHICLE TO DESIRED ACCURACY

FINE CONTROL BY OPTICS

FIGURE 9. ATTITUDE CONTROL



- LRC PRESENT PROGRAM

IMPROVED THERMISTOR BOLOMETER DETECTORS - GENERAL ELECTRIC

DEVELOPMENT OF THIN FILM, SOLID STATE DETECTORS - 39.5μ

FIGURE 10. DETECTOR TECHNOLOGY

- GROUND-BASED RESEARCH ON OPTICS AND CONTROL
- CURRENT STUDIES 15.24-CM DEVELOPMENT SYSTEMS ON AES
- FLIGHT EXPERIMENTS TO EVALUATE
 - EFFECTS OF LAUNCH ENVIRONMENT ON PRIMARY
 - EFFECTS OF ZERO G
 - THE ABILITY TO PROVIDE ADEQUATE THERMAL SHIELDS
 - EVALUATE MAN'S ABILITY TO PERFORM PRECISE
 - OPTICAL ALIGNMENT AND CONTROL

FIGURE 11. LRC PROGRAM

OPTICAL COMMUNICATIONS EXPERIMENTS ON GEMINI VII

D. S. Lilly
Manned Spacecraft Center

N 68-31768

MSC-4, an experiment in optical communications, will be given its initial in-flight testing during the flight of Gemini VII. The experiment will be a study in a pulse-frequency-modulation optical communications link and will make available a coherent optical radiator outside the earth's atmosphere. Atmospheric data such as transmission properties, background levels, scintillation, scattering, and index-of-refraction variations will be recorded. Further, the use of a laser in an optical communications system in a space environment will be evaluated.

Data obtained from the experiments will be useful in designing more sophisticated and reliable communications systems for manned space vehicles. Background levels, information bandwidths, and system performance may be investigated in a logical manner. Atmospheric data obtained will also be useful in developing a mathematical model of the atmosphere and in characterizing the effects of turbulence upon an optical transmission link. Thus, the capability of the communications system can be predicted more accurately.

A ground-based optical receiver and a flashing beacon are synchronized with the orbital-track radar. In this manner the receiver and the beacon are always directed toward the spacecraft, within the limits of radar accuracy. Three ground receiver sites -- White Sands, N.M.; the Ascension Islands; and Hawaii -- will be used. This will contrast atmospheres differing in humidity content, weather conditions, and elevations.

As the Gemini VII spacecraft comes above the horizon (Fig. 1), it is tracked by the radar. The crew will orient the spacecraft into the proper attitude for the initial sighting of the ground beacon. The pilot will sight through a telescope on the laser transmitter and initiate a spacecraft-roll action for fine adjustment of attitude. He will then transmit a laser signal to the receiver. This procedure will be followed under day, night, and twilight conditions as often as time allows.

The ground-based receiver will demodulate the spacecraft signal and record the data. Information can be extracted and displayed in a manner applicable to the particular measurement being made. A processor will vary

the flash rate of the visible beacon to give the spacecraft crew a real-time indication that the signal is being received. The effect of any optical bias in the system is thereby reduced.

The on-board laser transmitter will have two modes of operation, a constant 100 pulse-per-second train and an 8000 ± 500 pps train capable of conveying audio. The mode of operation will be established for each test point.

The basic device in the on-board transmitter is the gallium arsenide (GaAs) diode laser. The diode normally emits light energy in a rectangular pattern about 2° by 15° . The radiation wavelength is strongly dependent upon temperature; but, when operated at room temperature, it is centered at approximately 900 angstroms. The rectangular radiation pattern is fully utilized by employing four GaAs diodes and stacking the radiation patterns (Fig. 2). Each emitting diode has its own optics to focus the output into a rectangular pattern about one milliradian by four milliradians. The total flight hardware peak power output is about 20 W. The flight hardware is shown in Figure 3.

The electrical schematic and the output characteristics of the transmitter are shown in Figures 4A and 4B. The transmitter normally operates at 100 pps. The drive amplifier triggers a silicon control rectifier (SCR), applying a large current load to the diodes. A frequency modulator allows ± 500 pps deviation in the 8000 pps oscillator; the amount of deviation is determined by the audio input into the microphone.

The on-board transmitter is equipped with a 6-power telescope having a 2.54-cm (1-in.) aperture followed by a 400-angstrom-wide filter centered at 5000 angstroms.

An argon laser, mounted on the optical receiver, serves as the visible beacon. The laser has a 3-W output with a one-milliradian beamwidth. The receiver is in turn mounted on a modified Nike-Ajax tracking pedestal (Fig. 5). The pedestal is slaved to an RCA FPS-16 orbital-track radar. Tracking accuracy in the slaved mode is 0.4 milliradians.

The receiver has a Dall-Kirkham folded-mirror system with a 76.2-cm (30-in.) primary collector and a one-milliradian field-of-view. A cooled photomultiplier is employed as the detection unit. Wavelength rejection is accomplished with a 100-angstrom bandpass interference filter centered at 9060 angstroms.

The signal detected by the photomultiplier is amplified by a video pre-amplifier (Fig. 6). It is then fed through a coaxial cable to an electronics van for processing. At this point, one branch of the signal is separated for use in a study of atmospheric phenomena. The recording and the processing of this signal is described in another paper.

The other branch of the signal is fed simultaneously to the audio demodulator, the signal level detector, an oscilloscope, and a tape recorder. Each of these devices records or displays the signal. An automatic gain control (AGC) loop regulates the photomultiplier tube (PMT) supply voltage to maintain a constant noise level in the receiver. A record of the PMT voltage is thus a measure of the sky background (daytime operation) illumination. A sun sensor protects the PMT from direct rays of the sun by initiating a shutter action when the sky illumination exceeds the AGC capability to respond. Signal and background levels are recorded on a pen-recorder with a common time reference. The FPS-16 radar angle and range data are also recorded.

For a daytime pulsed optical communications system, the following signal-power-requirement equation is applicable. Daytime operation of the system requires peak power, about 9 W.

$$P_t = \frac{\Omega R^2 P_r}{A_r T_a T_t T_r} \quad \begin{array}{l} \text{for daytime} \\ \text{operation} \end{array}$$

where:

$$P_r = \sqrt{\frac{(S/N) \cdot h \nu b A_r \omega \Delta \lambda T_r}{N \tau}} \quad - \text{ required}$$

Power to Detector (input)

P_t required transmitter peak power

Ω transmitter beamwidth, $7 \cdot 10^{-6}$ steradians

T_t transmission of transmitter optics, including spacecraft window, 0.5

T_a transmission of atmosphere for elevation angles greater than 20° , 0.5

T_r	transmission of receiver optics, 0.2
b	background radiance, $10 \text{ W/m}^2\text{-sterad-}\mu$
ω	receiver field-of-view, 10^{-6} sterad
$\Delta\lambda$	interference filter bandpass, $10^{-6}\mu(100\text{\AA})$
A_r	area of receiver dish, 0.45 m^2
τ	receiver observation time, $0.7 \cdot 10^{-7} \text{ s}$
N	detector quantum efficiency, $4 \cdot 10^{-3} \text{ A/W}$
$h\nu$	energy/photon, $2.2 \cdot 10^{-19} \text{ J}$
S/N	desired signal-to-noise ratio, 10
R	range, assume 1000 n. mi., $1.85 \cdot 10^6 \text{ m}$

In tests conducted at White Sands, N. M., sky background measurements were made on a clear day with scattered cumulus clouds near the horizon. Near the zenith the background varied smoothly between 1.5 and 2.5 $\text{W/m}^2\text{-sterad-}\mu$. At 24° elevation, a minimum of 3 $\text{W/m}^2\text{-sterad-}\mu$ was recorded, rising to approximately 10 $\text{W/m}^2\text{-sterad-}\mu$ as the azimuth angle approached west. Local time was 3:00 pm.

Signal-level measurements were made with the transmitter mounted on a tripod. At an elevation angle of 1.2° , 3 to 4 percent atmospheric transmission was recorded, with short-term peak variations as great as 15 percent occurring in 1/5 second. Large drops in the received signal occurred about every two seconds when the transmitter was freely held.

OPTICAL RECEIVER AND
BORESIGHT BEACON
SLAVED TO WSMR
FPS-16 RADAR

SPACECRAFT



FPS-16 RADAR



TRANSMITTER

AUDIO



CABLES



VAN

RECEIVER AND
BORESIGHT BEACON

NIKE-AJAX

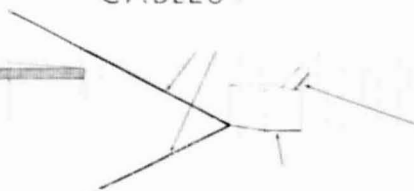


FIGURE 1. GEMINI LASER EXPERIMENT AT WHITE SANDS MISSILE RANGE

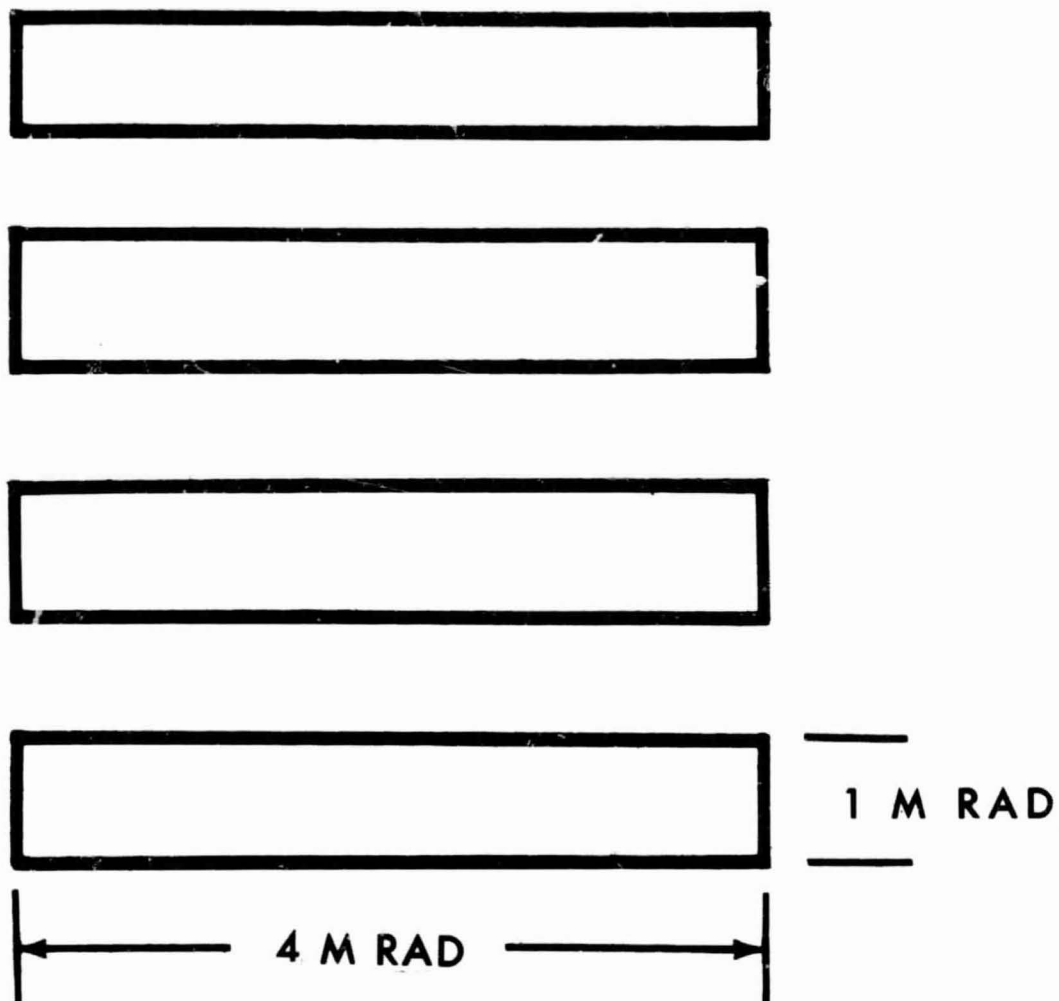


FIGURE 2. STACKED RADIATION PATTERNS

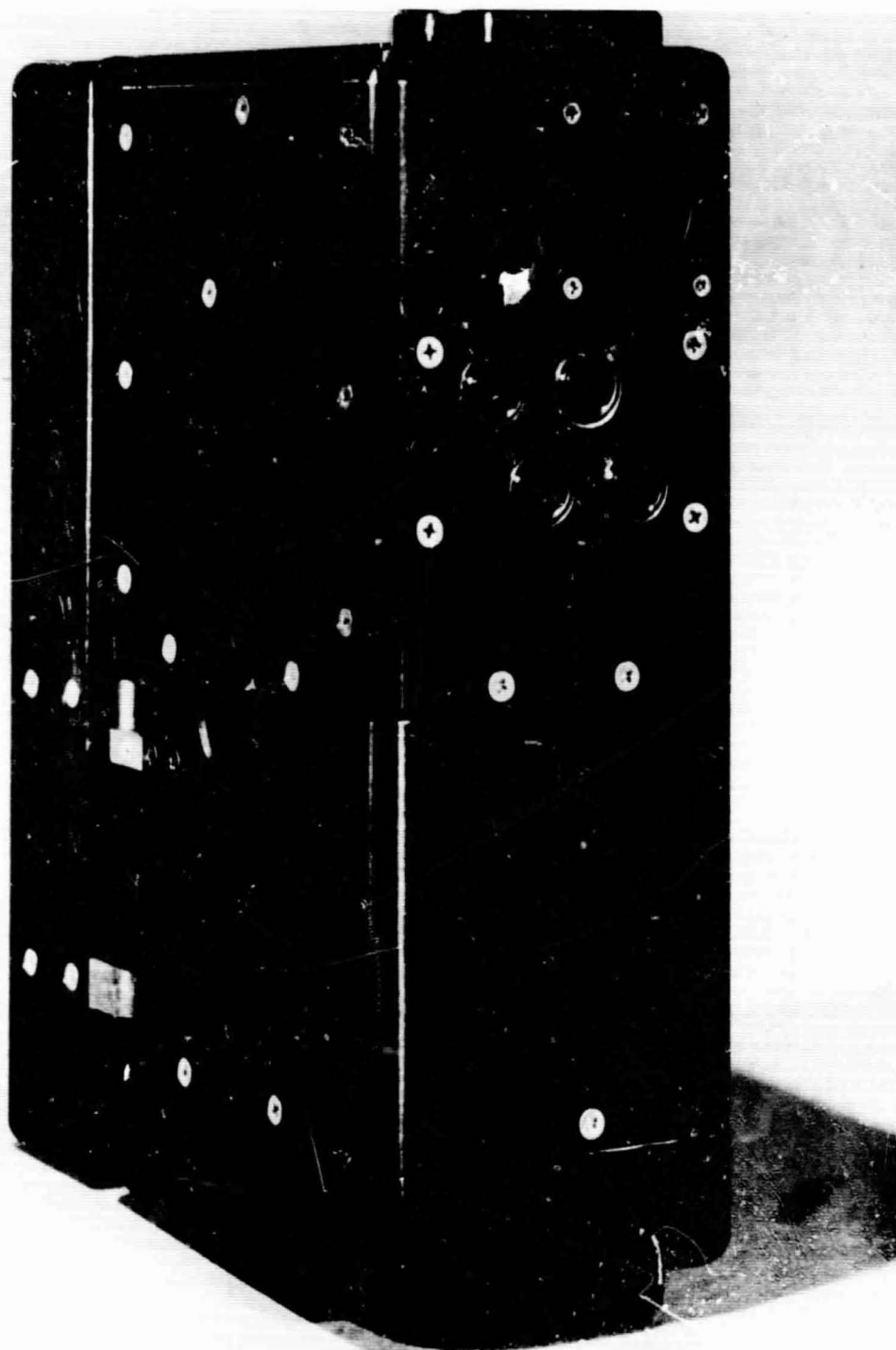


FIGURE 3. GT-7 GEMINI LASER COMMUNICATION TRANSMITTER

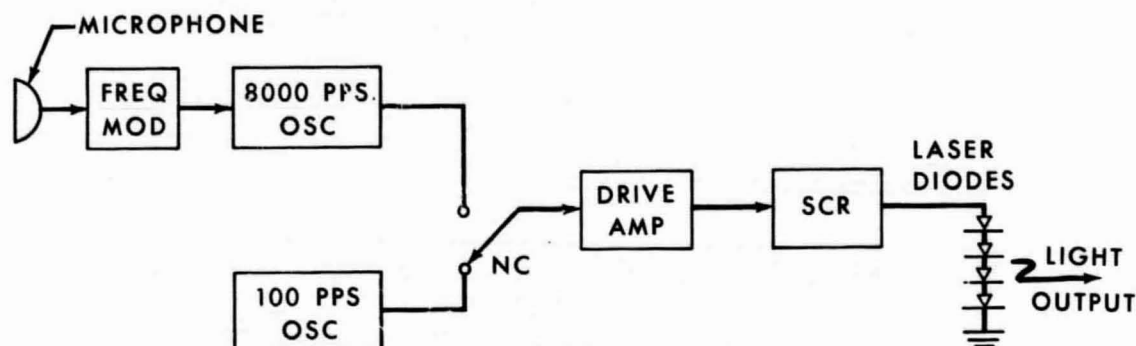


FIGURE 4A. LASER TRANSMITTER BLOCK DIAGRAM

PEAK OUTPUT POWER	20 WATTS
BANDWIDTH	4 MILLIRADIANS
WAVELENGTH	9060 Å
SPECTRAL WIDTH	40 Å
PULSE DURATION	.75 NS
AVERAGE PULSE REPETITION RATE	8 KHZ OR 100HZ
PULSE FREQUENCY DEVIATION	± 500 HZ
INFORMATION BANDWIDTH	3 KHZ
MODULATION METHOD	PFM
WEIGHT (INCLUDING BATTERY PACK)	2.36 KG
SIZE	12.7 x 7.6 x 20.3 CM
TELESCOPE POWER	6X
TELESCOPE FIELD OF VIEW	.6°

FIGURE 4B. LASER TRANSMITTER CHARACTERISTICS

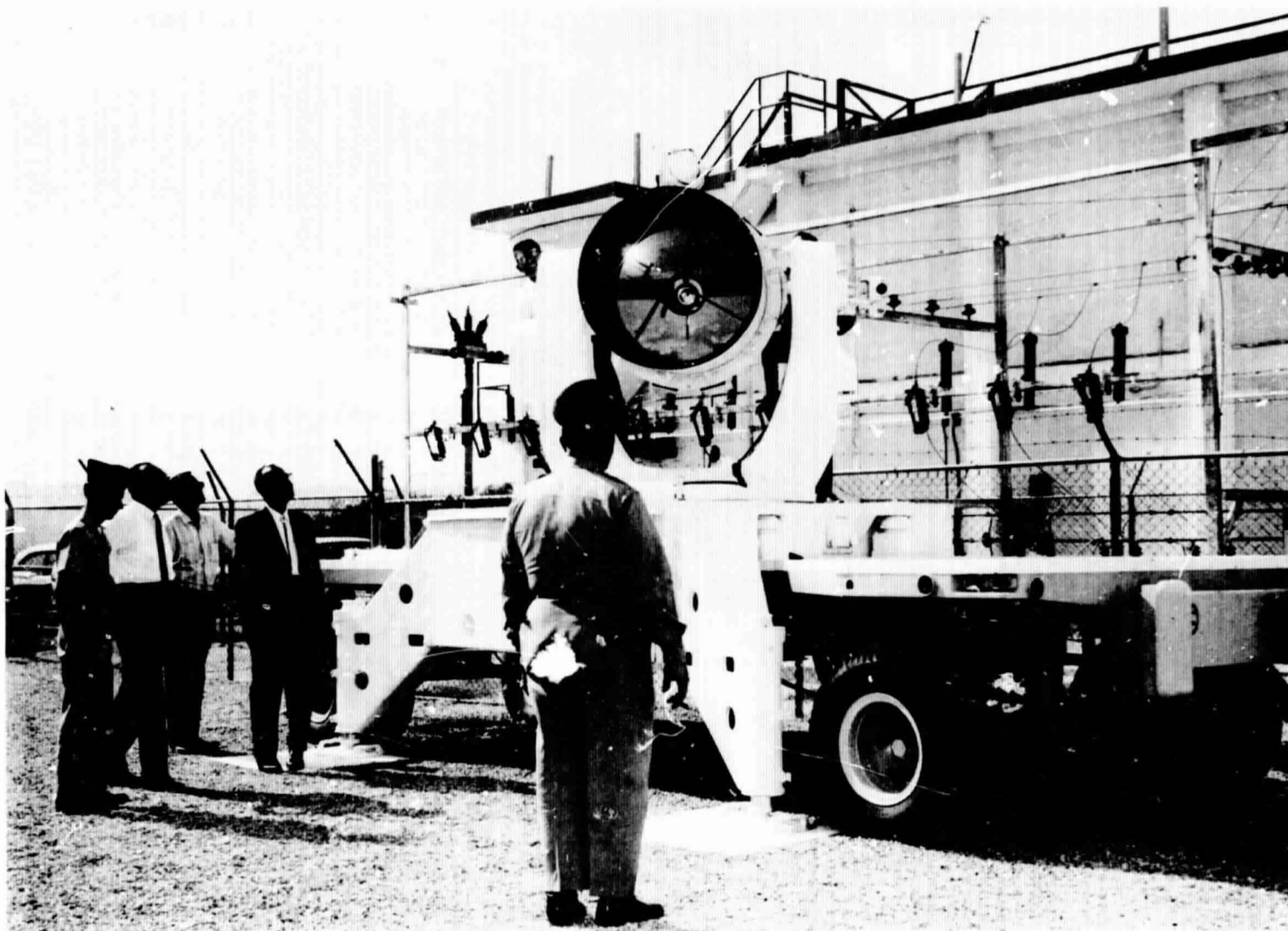


FIGURE 5. OPTICAL RECEIVER AND NIKE-AJAX TRACKING PEDESTAL

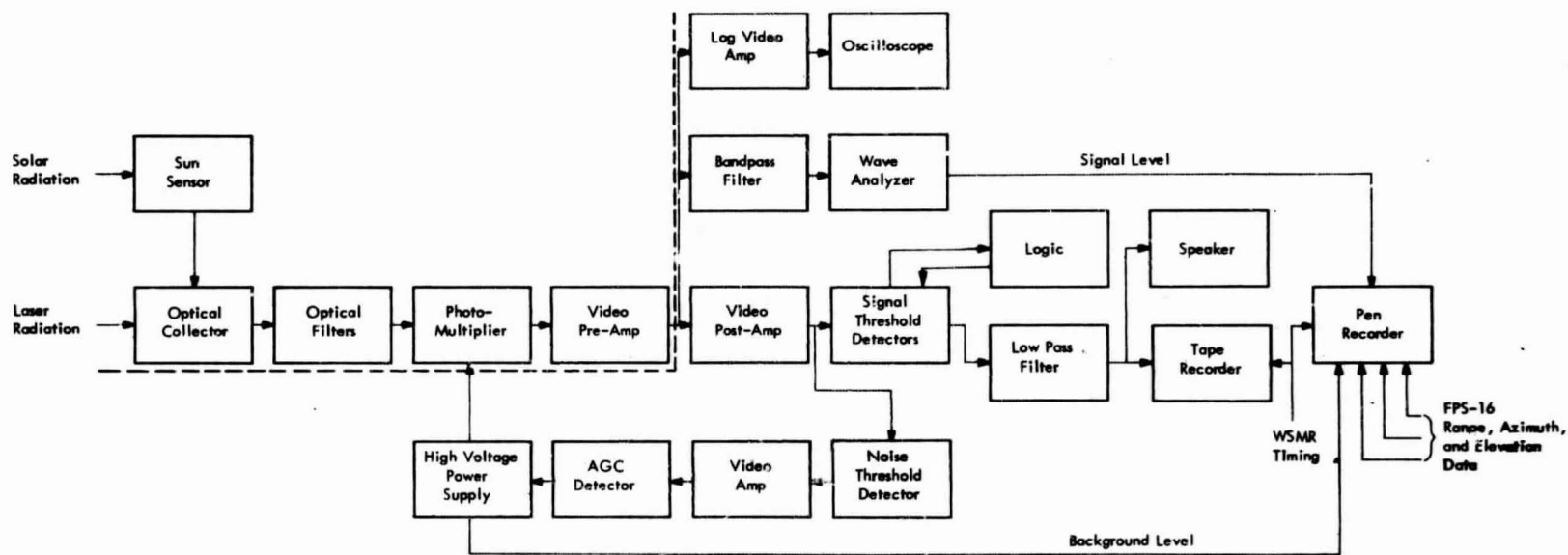


FIGURE 6. RECEIVER SIGNAL FLOW

MANNED SPACECRAFT CENTER LASER PROGRAMS AND PLANS

W. L. Thompson
Manned Spacecraft Center

N 68-31769

The Manned Spacecraft Center (MSC) is currently conducting work in two areas of laser systems: Optical communications as applied to future manned deep-space missions, and laser radar intended as a backup system for the x-band LEM radar.

The MSC investigations on deep-space optical communications were initiated in late 1962 with a feasibility study. This study indicated the advantages of laser communications as compared with projected microwave systems. The more difficult subsystems areas of development were also pinpointed. It was shown that the major emphasis should be placed in these areas so that the predicted laser communication model could be produced for deep-space missions. Four of the major problem areas were defined: (1) acquisition and tracking of the very narrow beams, (2) prime power requirement for the relatively inefficient laser transmitter, (3) choice of optical modulator material and design to take full advantage of available bandwidths, and (4) atmospheric effects on a coherent beam. This atmospheric problem is based on the consideration that an earth station would be used as the terminal for deep-space subsystems.

The work being conducted by MSC to resolve the problems in these four areas has led to the development of several special subsystems.

The acquisition and tracking problem in its simplest terms amounts to knowing where to point and how to point. But this involves the knowledge of a reference system, the aberrations of transmitting equipment, the calculation of lead angles, and several lesser corrections.

To define the problem in detail and to propose solutions, a six-month study was conducted for MSC by the Northrop Space Laboratories. This study included investigations of the sky foreground radiation, the types and number of terminals required for a manned deep-space mission, the numbers of switchovers needed per mission, the stabilization and location of equipment on assumed manned deep-space vehicles, the reliability of the system, the cost per earth terminal, and finally the total system cost. Detailed surveys were carried out to determine the present state-of-the-art component level. As a prelude to a complete system design, studies projected the advances in lasers, detectors,

space optics, and pointing stabilization. To accomplish the task, two manned deep-space missions were assumed. The trajectories for missions to Mars and Venus were plotted. The capability of the deep-space instrumentation facility in the year 1969 was assessed. The instrumentation facility communicates to an earth satellite acting as an earth terminal in a deep-space link. A satellite relay in polar orbit, at an altitude of 14 816 km (8000 n. mi.) or greater, was picked for the earth terminal. Fewer switchovers are required, and a maximum reliability of communication is effected. A laser transmitter weight-versus-efficiency analysis resulted in a dual choice of laser devices with the final choice dependent on state-of-the-art advances over the next few years. A 10-joule, un-q-spoiled ruby laser emitting one pulse per second was found to be adequate. However, the high efficiency of the semiconductor lasers was found to be very attractive, in spite of the heavy collimating optics required. Block diagrams and specifications for a complete system were evolved. The next phase of this program will be the experimental demonstration of the most critical parameters for the equipment involved. In particular, the resolution of an image-tube cathode and optics must be shown, and the electronics to accommodate that detector resolution must be developed. Gimbal accuracy must be demonstrated. This will allow communication with narrow beamwidths to be successfully employed.

Three prime energy sources to supply the power for a deep-space laser-communication system were considered. These are shown, along with the paths necessary for conversion to communicator energy, in Figure 1. Of course the design of a power system for a deep-space mission must be based on the overall spacecraft requirements, of which communications is only one item. Prime power would be available from this source, at least on an emergency basis. Since direct sunlight conversion to laser communication power appears feasible and inherently more efficient, this technique has been pursued. A contract with the Radio Corporation of America was initiated late in 1964 to demonstrate the performance of a solar-pumped solid laser. During this contract, two crystals — yag and $\text{CaF}_2 : \text{Dy}^{2+}$ — have been successfully sun-pumped. The yag material appears to be superior in performance; also, it may be operated at room temperature while the $\text{CaF}_2 : \text{Dy}^{2+}$ must be pumped at cryogenic temperatures. Two primary problems are apparent in the approach, the dissipation of the unconverted incident solar energy and the coupling of the modulator and beam-directing devices to the light energy being pumped from the crystal. Figure 2 shows in simple form the rooftop assembly of equipment used to pump the yag crystal, producing approximately 100 mW continuous output. It was estimated that the laser was pumped at about 40 percent above threshold in this configuration. A series of prisms was installed and aligned to extract the laser beam. This output has been modulated at MHz with both KTN and GaAs modulators as a second portion of the contract. Future work on this

system will be concerned mainly with the design of better optical couplers, more efficient heat dissipation, and better sun-tracking techniques.

A program was undertaken approximately ten months ago to produce a complete 30 mega-bit pulse-code communicator. The initiation of this study was to demonstrate the feasibility of wideband laser-communication systems and to advance the development of wideband optical modulators. The system is intended both to transmit and to receive a PCM polarized video signal at commercial rates, a quality voice channel, and one telemetry channel. Such a division of information will probably never be used during a space mission. However, once the high information rate can be demonstrated, it can then be subdivided into a greater number of narrow bandwidth channels. By using commercial video as the determining yardstick, available video test equipment may be used to judge information fidelity. The block diagram shown in Figure 3 outlines the major subsystems and components within the equipment. Without question the most critical component is the electro-optical modulator. The contractor for this development, Hughes Aircraft Company, has chosen a special configuration of KDP material for this application; it is a multi-element device separated by flat-ring electrodes. The KDP material was picked primarily because of the availability of unstrained crystals in large sizes, lower power requirements in this configuration on the modulator driver, and past experience in use of the material. The system uses time-division multiplexing with no data compression. The receiver uses the polarized pulses to separate the binary information into PCM video. The voice, telemetry, and sync signals are separated from this output. An argon laser with a one-watt continuous output will be used as the power oscillator. Another important facet of this equipment development is the need to design high-rate encoders and decoders to handle the great information content. Because this system is a straight PCM system using no data compression, its performance will be used as the yardstick for systems using various data compression techniques. For example, it is now planned to compare the output of systems based on delta modulation and its derivatives, pulse-position modulations and FM, with the relative standard pulse-code unit.

The first laser communication study conducted by MSC indicated that before a complete systems analysis could be obtained for an earth laser terminal, the atmospheric effects on a coherent beam would have to be measured. Further, a complete path through the atmosphere obviously was needed. This was one of the major purposes for implementing the MSC-4 optical communication experiment, to be tested during the flight of GT-7. The description of this experiment will be detailed in several papers to be presented at this conference. The data obtained from this work will either confirm the statistical model of the transmission path assumed in our initial study or alter the resulting choice of modulation techniques.

The emphasis on the second laser study program, that of developing a laser radar for use during rendezvous and docking of the LEM vehicle, is currently undergoing a change. Emphasis is no longer on the use of semi-conductor sources but rather on the use of solid-laser sources. This change is necessary because of the lack of sufficient power in the semi-conductor laser diodes, as well as the disappointing rate of improvements in this feature. The reliability of the solid-laser system has been much improved with the new pumping tubes and lower threshold crystals. An optical rendezvous system not employing a laser is presently being developed for use on the LEM. This system employs a mercury-flash lamp on the Command/Service Module. This lamp is tracked by a telescope on the LEM during its ascent from the lunar surface. The angles read out from the telescope are fed to the LEM on-board computer where range and range rate are computed. The system is simple and light, but it is handicapped by high background-level interference. As an addition to the present tracker, the use of the solid laser to obtain range and range rate is being considered. To support this work, an optical tunnel 80 m long is nearing completion at MSC. An artist's conception of the completed tunnel is shown in Figure 4. The tunnel, 4 m in diameter, is enclosed inside an insulated, air-conditioned tunnel so that its ambient temperature can be regulated to within $\pm 2^\circ \text{F}$ over the entire length. It can be evacuated to 10^{-3} torr. For this testing, a hard vacuum is neither needed nor available; instead, a controlled atmosphere is obtained. An optical track runs the full length of the tube and provides a varying range for the test articles carried on a small cart. Two axis pedestals, accurate to within 10 arc seconds, are placed at the ends of the tunnel to support the test radar. Some of the planned tests to be conducted with this facility are as follows:

1. Reflectivity measurements on materials irradiated by the radar
2. Absorption, scattering, and dispersion measurements in various gases
3. Angular and linear resolution measurements
4. System evaluation in the presence of background radiation including solar, lunar, and earth.

In conclusion, the laser communication work at MSC may be described as that of solving major problem areas by demonstrating the feasibility of special subsystems. Complete spacecraft communication systems are not yet being assembled, but the technology for this final task is being developed concurrent with the spacecraft-communication components. The deep-space vehicle and its mission must be better defined before the final system design can be implemented.

Current effort on the rendezvous radar is changing emphasis from semiconductor to solid sources to obtain greater output powers.

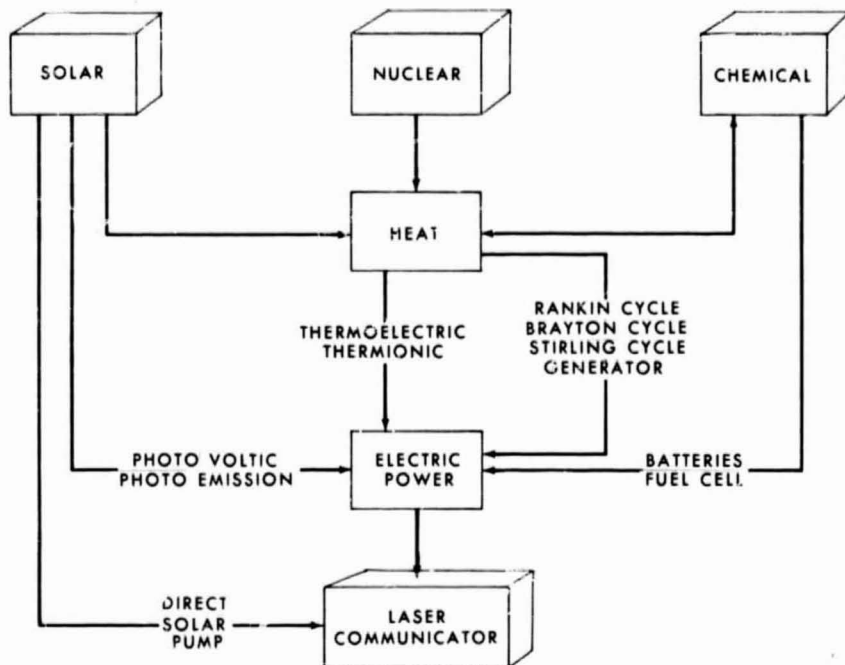


FIGURE 1. LASER COMMUNICATOR POWER

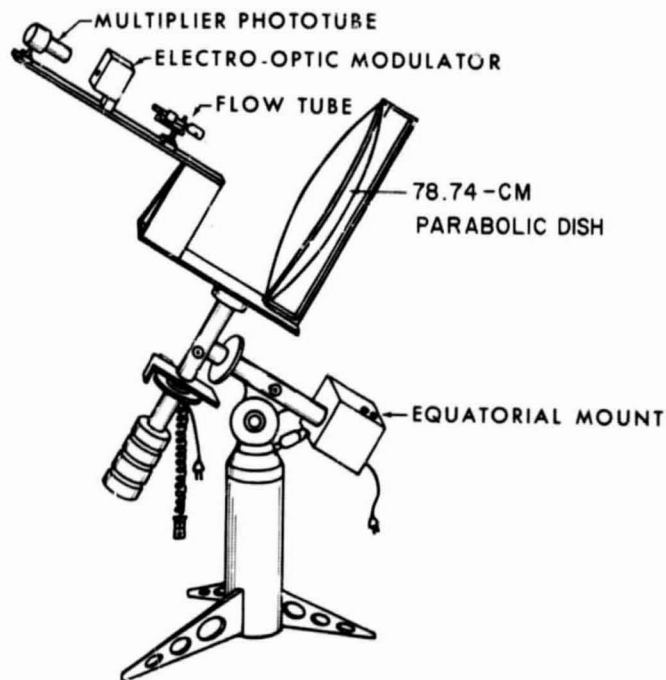


FIGURE 2. SOLAR-PUMPED LASER MODEL

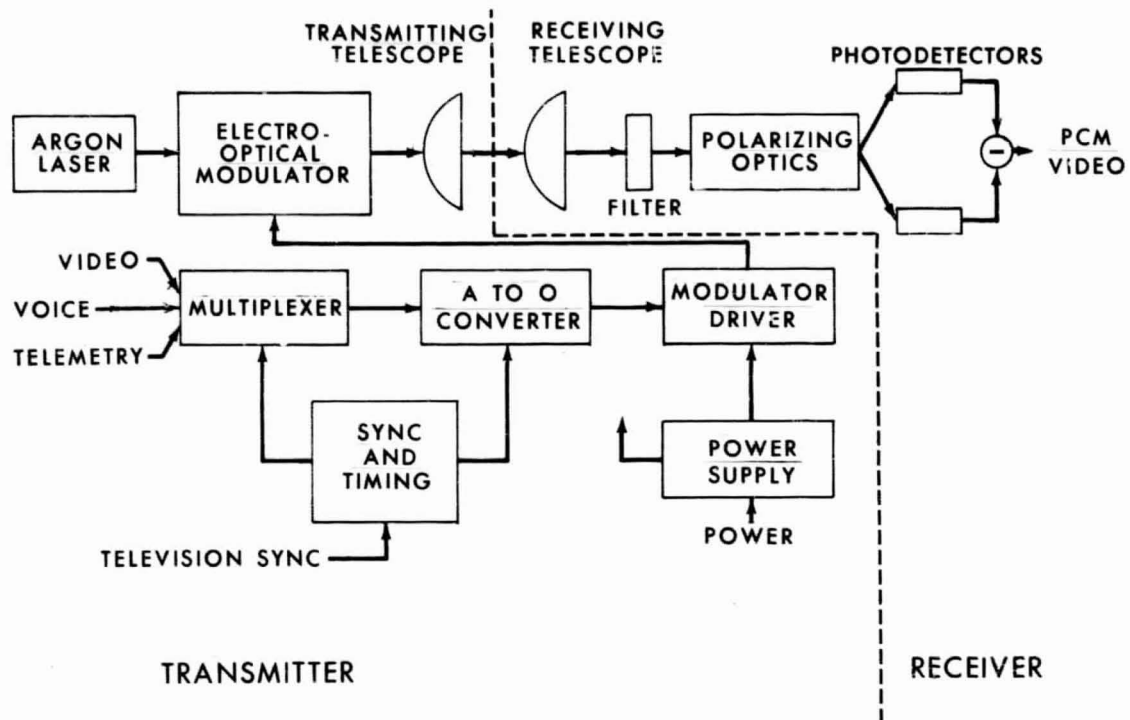


FIGURE 3. HIGH DATA RATE EQUIPMENT

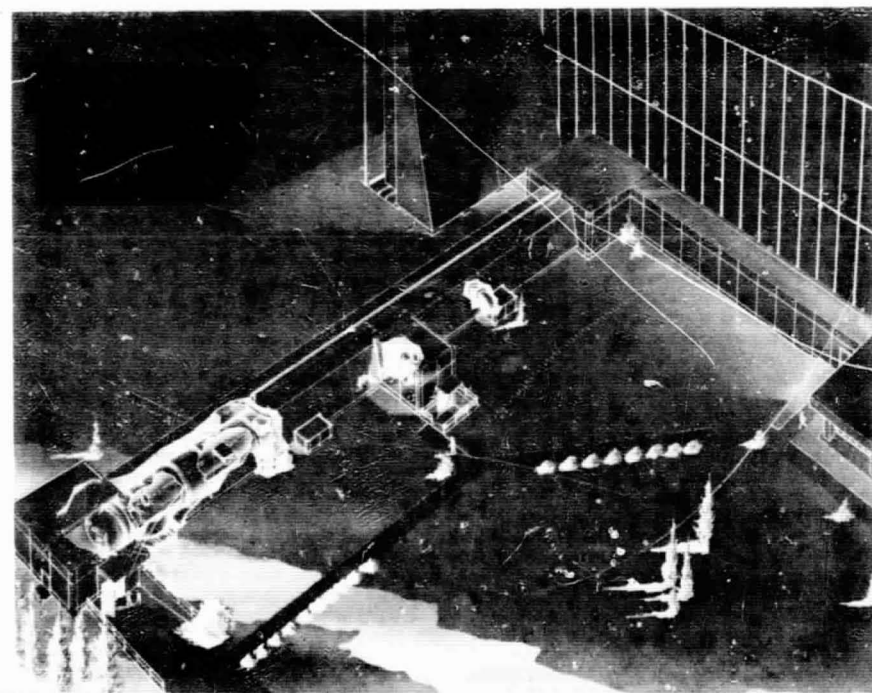


FIGURE 4. OPTICAL FREQUENCY RANGE

WHITE SANDS MISSILE RANGE STATION FOR MSC-4

By R. W. Ward
Manned Spacecraft Center N 68-31770

The initial planning for MSC-4 outlined the testing of an optical communications system. Later, it was decided to test the system during the flight of Gemini VII. The flight plan for the mission had already been arranged, thereby placing a constraint on the quantity of atmospheric data that could be obtained.

The data received will be used to verify existing models of the atmosphere and to develop a more detailed model.

When a statistical analysis of a phenomenon is made, two of the most important parameters are the variance and the autocorrelation function. These parameters are defined in Figure 1. The variance can be interpreted as a measure of the fluctuation of the value of a function from its mean. The square root of the variance is the generally accepted standard deviation. The autocorrelation function is a measure of the dependence between any two values in a nonfluctuating process, $V(t)$ and $V(t + \gamma)$, where γ is an arbitrary time delay.

$R(\gamma)$ as shown in Figure 1 is referred to as the long-term autocorrelation function, since the values of γ are long when compared with the time between pulses. In Figure 2 the short-term autocorrelation function is shown. Here, a dependence is investigated over values of γ which are compatible with the duration of each individual pulse. This function provides a measure of pulse degradation and pulse stretching caused by dispersive effects of the atmosphere.

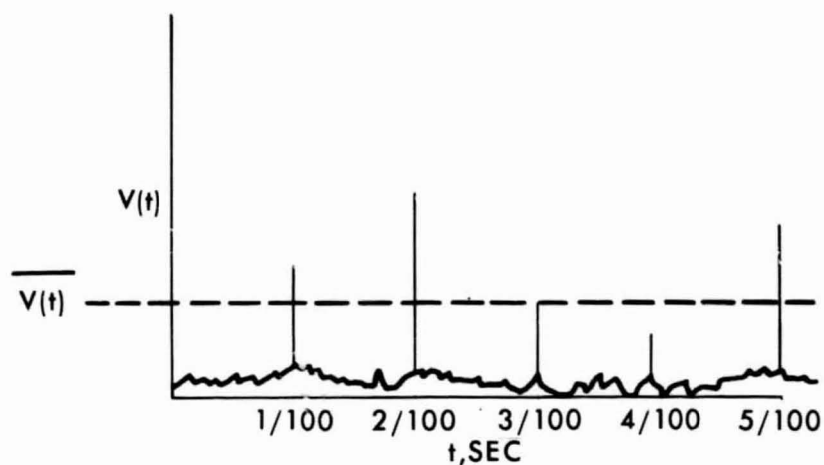
A block diagram of the correlation equipment used at the White Sands Receiving Station is shown in Figure 3. The signal, after being collected by the optics and detected by the photomultiplier tube, is preamplified and sent to the data collection and analysis complex. A wide-bandpass amplifier is used to multiply a part of the signal, which is then recorded on an RCA model TR-5 video tape recorder.

From this video tape, most of the data will be analyzed and reduced in the laboratory. However, on-site data processing is used to obtain real-time analysis and to improve resolution in the measurement of the short-term autocorrelation function. This is possible since the bandwidth of the circuit is wider than that of the video tape recorder.

A time reference that can be related to the spatial position of spacecraft in orbit will be provided for the audio channel of the video recorder and for one channel of a 7-channel FM tape recorder. A part of the signal is sent through a pulse stretching network and is recorded on a second channel of the FM recorder. To insure that the analysis is made on transmitted pulses and not on random noise pulses, a periodicity extraction network is used to control a gate. This allows only signals with a period of 100 cycles, plus or minus a small increment, to be passed into the autocorrelator. The autocorrelator consists of a delay line with five outlets, corresponding to five values of γ . The output signals from the autocorrelator are multiplied electronically by the original signal, and the results integrated. The sums are then stored in channels 3 through 7 of the FM recorder.

One model of the atmosphere can be constructed of small patches having index-of-refraction values which vary randomly about some average. If the mean size of these patches is ρ , then a solution of the wave equation leads to relations shown in Figure 4. These relations state that the signal variance depends reciprocally on wavelength. Further, the signal variance depends directly on range and the product of average patch size and atmospheric index-of-refraction variance. It has also been shown that for signal propagation in a randomly varying medium, the autocorrelation function for the signal is equal to the autocorrelation function for the medium.

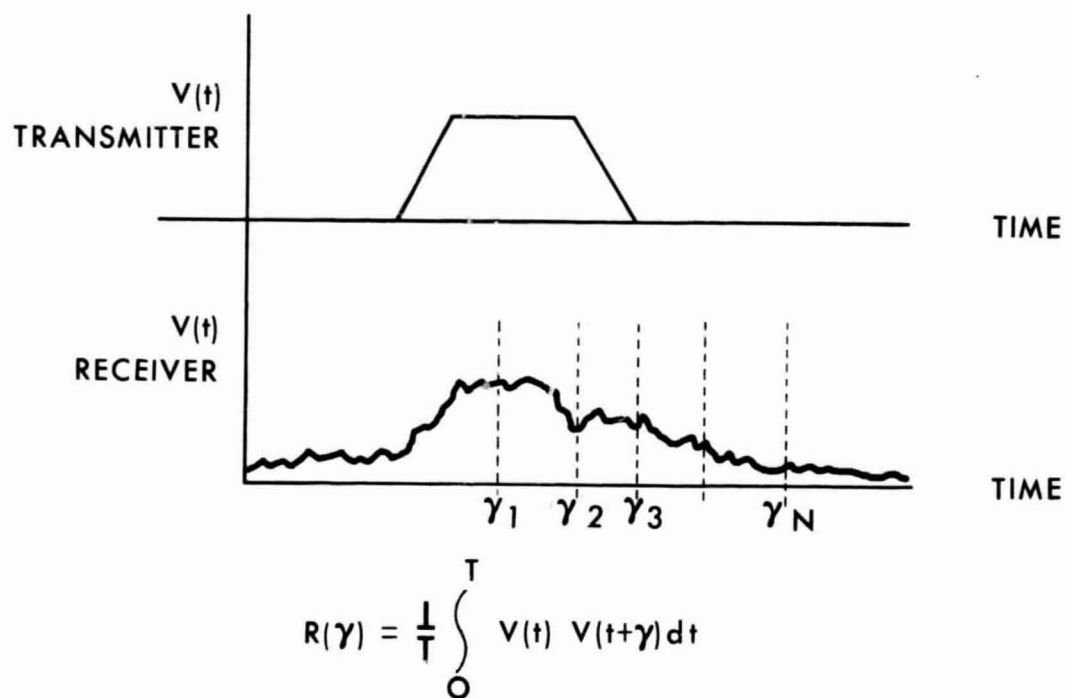
The types of data to be collected at the White Sands Receiving Site and the interpretation of the data in relation to the statistical properties of the atmosphere have been discussed. The facility will be set up and operated by Melpar, Inc., under contract to the Manned Spacecraft Center.



$$\text{VARIANCE} = \sigma^2 = \overline{(V(t) - \overline{V(t)})^2}$$

$$\text{AUTO CORRELATION FUNCTION} = R(\gamma) = \lim_{T \rightarrow \infty} \frac{1}{T} \int_0^T V(t) V(t+\gamma) dt$$

FIGURE 1. VARIANCE AND AUTOCORRELATION DEFINITION



$$R(\gamma) = \frac{1}{T} \int_0^T V(t) V(t+\gamma) dt$$

FIGURE 2. SHORT TERM AUTOCORRELATION FUNCTION

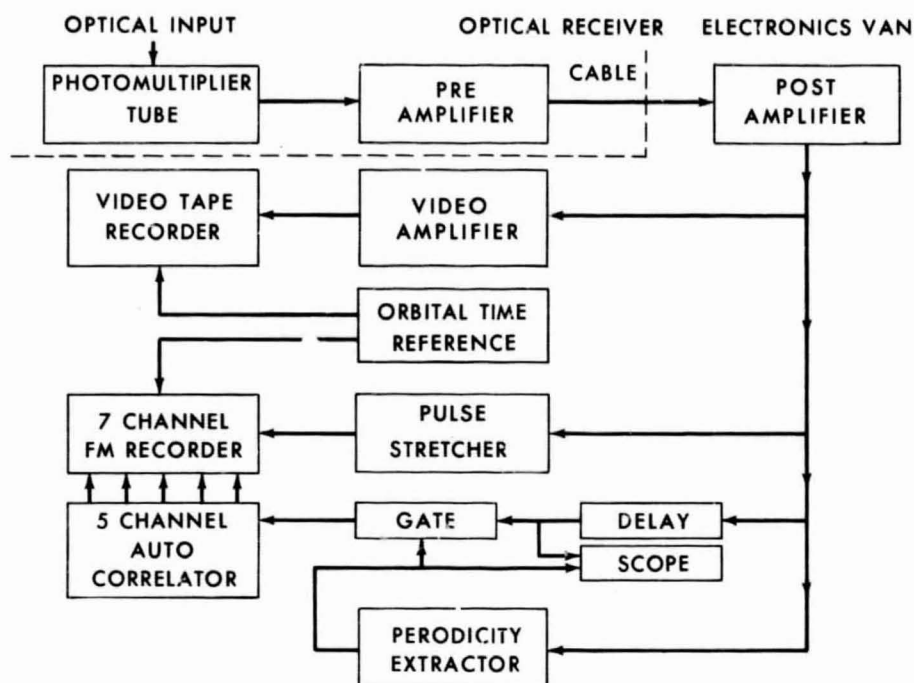


FIGURE 3. BLOCK DIAGRAM OF SYSTEM

$$\sigma_v^2 \sim \frac{1}{\lambda^2} \rho \sigma_A^2 \gamma$$

$$R(T) = A(T)$$

σ_v^2 → SIGNAL VARIANCE

σ_A^2 → ATMOSPHERE VARIANCE

λ → WAVE LENGTH

ρ → MEAN INHOMOGENOUS PATCH SIZE

γ → RANGE

$R(T)$ → AUTOCORRELATION FOR SIGNAL FLUCTUATIONS

$A(T)$ → AUTOCORRELATION FOR ATMOSPHERE FLUCTUATIONS

FIGURE 4. RELATIONS APPLIED TO ATMOSPHERIC PROPERTIES

THE OPTICAL GUIDANCE SYSTEM FOR RENDEZVOUS

Charles L. Wyman
George C. Marshall Space Flight Center

N 68-31771

Many important space missions of the future, including the moon landing, require rendezvous and docking. A list of such missions includes orbital refueling, supply shuttles to large manned space stations, assembly of large complexes in orbit, and space rescue operations. Furthermore, many of these missions will require completely automatic operation of the guidance and docking equipment.

Clearly, with rendezvous being so important an operation in space, the guidance equipment of the future must use the most efficacious techniques available. The guidance package should be characterized by simplicity and reliability. It should be small, lightweight, and of low power consumption.

A developmental program during the past four years, investigating laser and optical techniques for rendezvous and docking, has established that a laser radar and tracker will provide such a package. The program has progressed from a feasibility study, through a breadboard development and evaluation, to a test prototype development that is nearly complete. The breadboard development and evaluation has established feasibility and practicality. The prototype development is a first attempt at packaging the system in a possible spaceflight configuration and has already provided a clear-cut indication of the size, weight, and power advantages of a laser system over more conventional approaches.

Plans now being formulated include testing the prototype on a rendezvous simulator and in aircraft; a thorough reevaluation of various rendezvous requirements; a continuing study of newer optical techniques; and finally, design, fabrication, and integration of an experimental system to be flown and tested operationally on an earth orbit mission.

The prototype optical guidance system uses both pulsed and cw radar techniques. A laser beacon is used on the target vehicle for acquisition. Image dissectors generate angular information for acquisition and tracking. Figure 1 is a block diagram of the system.

The acquisition system uses a wide-angle laser beacon on the target vehicle and a wide-angle telescope and image dissector on the chaser. The image

dissector is a photomultiplier in which a small internal aperture is used to limit the active area of the photocathode. By electrostatic focusing and magnetic deflection of the electrons emitted from the cathode, the active area can be made to scan across the face of the tube. Thus, by a quadrature magnetic field, a small instantaneous field of view may be scanned over a larger field of view to generate angular information for acquisition and tracking purposes.

Acquisition is performed as indicated in Figures 2 and 3. The chaser system image dissector is raster scanned to locate the target beacon. Once the beacon comes into the field of view, acquisition occurs. The image dissector then goes into a cross scan mode and generates angular information causing the chaser to align to the beacon. When alignment occurs the target will be illuminated by the gallium arsenide laser transmitter on the chaser. The target contains a similar angle detector that allows alignment to the chaser. Once both vehicles are aligned, acquisition is completed. The system goes into the tracking mode and is prepared for the rendezvous maneuver.

When the two vehicles are aligned the target falls within the field of view of the tracking telescope. This telescope is coaxial with the acquisition telescope and uses the same image dissector to generate tracking information. At the completion of the acquisition phase the target beacon is turned off. Corner reflectors on the target return a portion of the chaser transmitter signal back to the chaser. Tracking alignment is maintained by imaging the return beam on the tracking detector.

The gallium arsenide laser transmitter on the chaser performs a dual purpose in that it provides the signal for tracking and also generates range information to an accuracy of 30 m. Range is determined by measuring the time delay between the transmission of a laser pulse and the return of the pulse from the target. The time delay measurement is achieved with a digital counter system using a 4.88-MHz clock. The laser pulse starts the clock, and the return pulse stops it. The accumulated count is transferred to a storage register for read-out and data processing purposes.

The short-range system is activated at a range of 3 km and operates until docking is complete. An incoherent gallium arsenide diode continuously modulated at 4.88 MHz is used for this transmitter. The purpose of the system is to supplement the long-range system by generating vernier range information to an accuracy of 10 cm. Figure 4 is a block diagram of the short-range system. The output of the short-range register is added to the output of the long-range register to produce an unambiguous range reading.

A phase locked voltage controlled oscillator is used as a tracking filter to suppress noise. Heterodyne techniques are used to permit phase measurements between transmitted and return signals at a low frequency by a digital measurement of time delay.

Figure 5 is a photograph of the breadboard chaser vehicle system. The breadboard is presently in-house and is being prepared for use in making experimental acquisition measurements. The photograph shows the chaser optical head which contains both transmitters, the tracking and acquisition telescopes, and the tracking and ranging detectors. The electronics package contains the following: the upper two racks are the tracking and acquisition electronics, the next rack is readout and display equipment, the fourth and fifth racks are for signal conditioning, and the bottom rack contains the ranging circuitry.

The prototype consists of a miniaturized optical head mounted on a tracking pedestal to simulate spacecraft angular motion. Microelectronics have been used in all the electronics. Figure 6 is a diagram of the prototype chaser optical head. The refractive optical elements with the hole through the center comprise the acquisition telescope. The larger reflective telescope is for tracking and ranging. A miniaturized image dissector mounted coaxially with the optics is used for acquisition and tracking. A beam splitter diverts part of the incoming signal to the phototube for range detection.

The short-range transmitter is shown in front of the main telescope secondary. The small package mounted on the outer shell of the telescope is the laser transmitter. The target vehicle tracker is identical to the acquisition telescope shown here, except without the hole.

Figure 7 depicts the chaser prototype mounted on the tracking pedestal. Figure 8 is a closeup of the optical head and the microminiaturized tracking and acquisition electronics; Figure 9 shows the electronic package. The same type circuitry will be used for ranging and signal conditioning.

The prototype development is a first attempt to build a reasonable package and is in no way limited by the state of the art. Figure 10 indicates the physical characteristics and capabilities of the package; Figure 11 compares the prototype with two state-of-the-art rendezvous radars, using microwaves. Clearly, the laser system is already more than competitive.

Plans are now being formulated that will lead to experimental flight testing of a laser rendezvous radar in earth orbit. A test program is now being prepared for the prototype system. The major tests will be docking maneuvers

on a rendezvous simulator and acquisition, tracking, and ranging tests in aircraft. The results of the test program coupled with a review of requirements for various rendezvous missions will aid in determining the characteristics of the flight version of the optical guidance system.

During the next year a complete flight test plan will be determined. The flight model of the optical guidance system will undergo preliminary design. The design will incorporate the positive results of investigations into more advanced techniques. Any advanced techniques considered will be breadboarded and proven before incorporation into the flight model.

One possible configuration using more advanced techniques is shown in Figure 12. This concept uses laser beam steerers on the chaser vehicle. The use of these devices would allow freedom from either spacecraft attitude control or a gimballed tracking head as is necessary in the prototype. The use of beam steerers is now under investigation in house. Also, note the use of cw injection lasers in the concept of Figure 12. The development of cw room temperature injection lasers is expected in the near future. Their use would allow multiple frequency or swept frequency radar techniques for range determination and would result in the elimination of one transmitter on the chaser. Furthermore, these techniques coupled with the use of higher frequency image dissectors now available would allow ranging, tracking, and acquisition all with a single detector. With the development of better and more powerful lasers a system as depicted in Figure 12 might ultimately weigh less than half the present version and in addition provide all the implied advantages that go with freedom from attitude control or gimbal requirements.

The two developmental models are serving to demonstrate the practicality of optical and laser techniques for space guidance problems. Future models will use similar ranging and tracking techniques, but will become smaller and more versatile as better sources become available. Furthermore, use of some of the advanced optical techniques, such as laser beam steerers, will result in very advantageous system configurations for which there are no microwave counterparts.

Present schedules call for preliminary design of a spaceworthy optical guidance system within a year. Any new techniques that are incorporated will be proven in breadboard demonstrations. The first flight tests are possible within two and one-half years.

BIBLIOGRAPHY

1. Optical Guidance Feasibility Study - Quarterly Reports (8) and Summary Report. Contract NAS8-2661, Request No. TP-2-83-1469-S1, Data Corp., Mar. 1965.
2. Wyman, Charles: Laser Systems Research at MSFC. Research Projects Review Report, NASA TMX - 53364, Huntsville, Ala.
3. Advanced Spaceborne Detection, Tracking, and Navigation Systems Study and Analysis. Compilation Reports, Westinghouse Defense and Space Center Aerospace Div.
4. Danner, R. V. and Dorochen, W. L. Jr.: Martin Co., Request No. M-64-113, July 1965.
5. Quigley, William W.: Gemini Rendezvous Radar. Westinghouse Electric Corp., Air Arm. Div., Request No. 63-350 Aug. 1963.

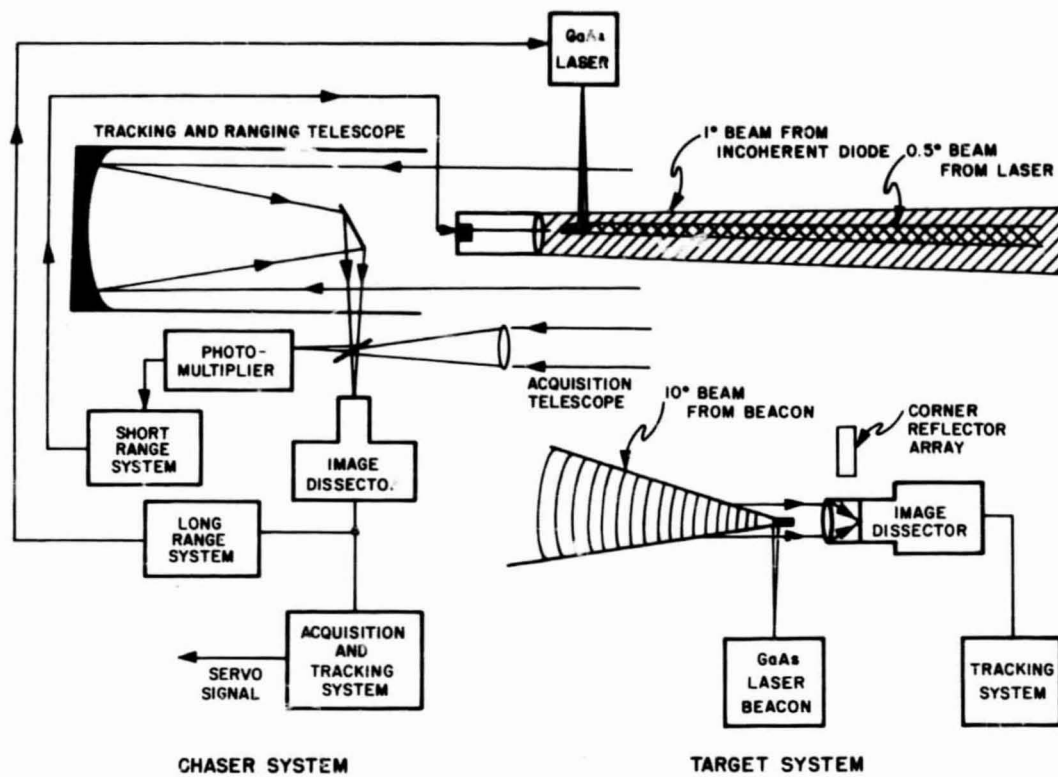


FIGURE 1. OPTICAL GUIDANCE SYSTEM

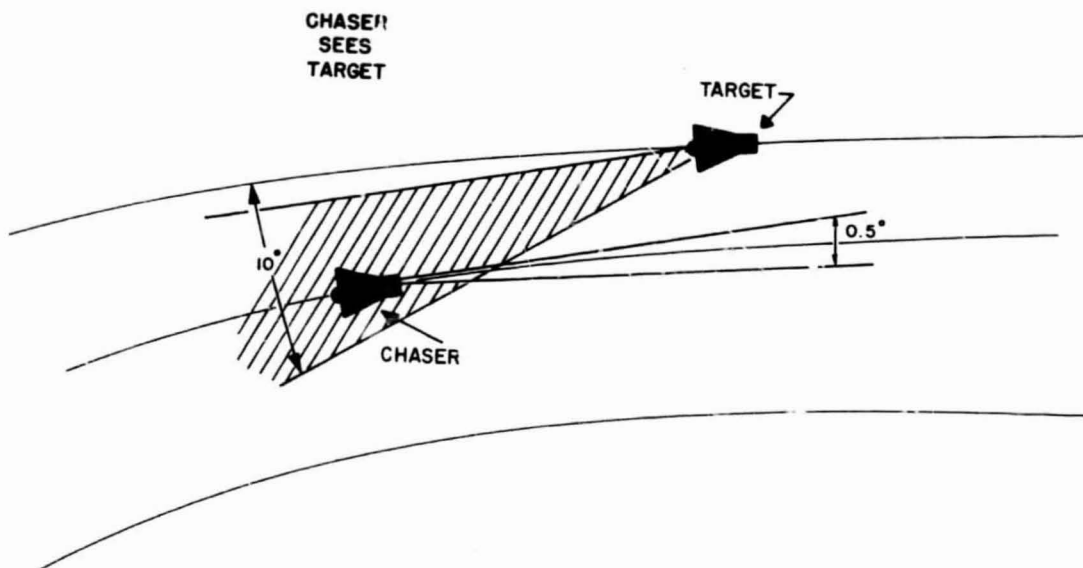


FIGURE 2. ACQUISITION PHASE I

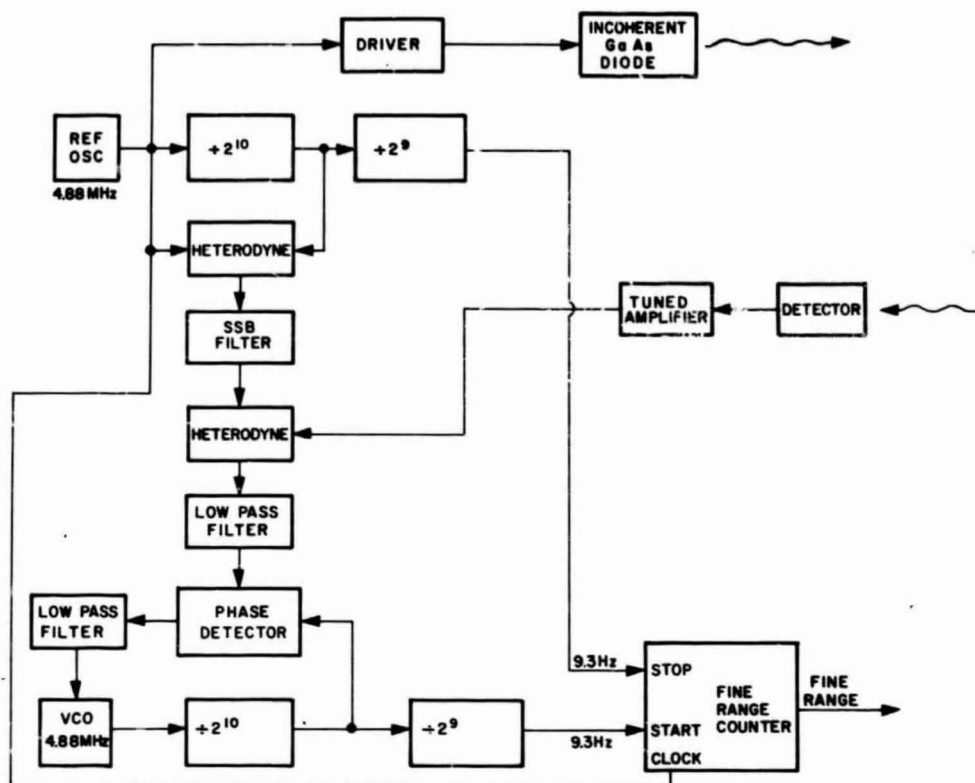


FIGURE 3. PHASES II AND III OF ACQUISITION

CHASER POINTS
TOWARD TARGET
& TARGET SEES
CHASER

TARGET POINTS AT CHASER
& TURNS OFF BEACON
CHASER TRACKS REFLECTED
BEAM

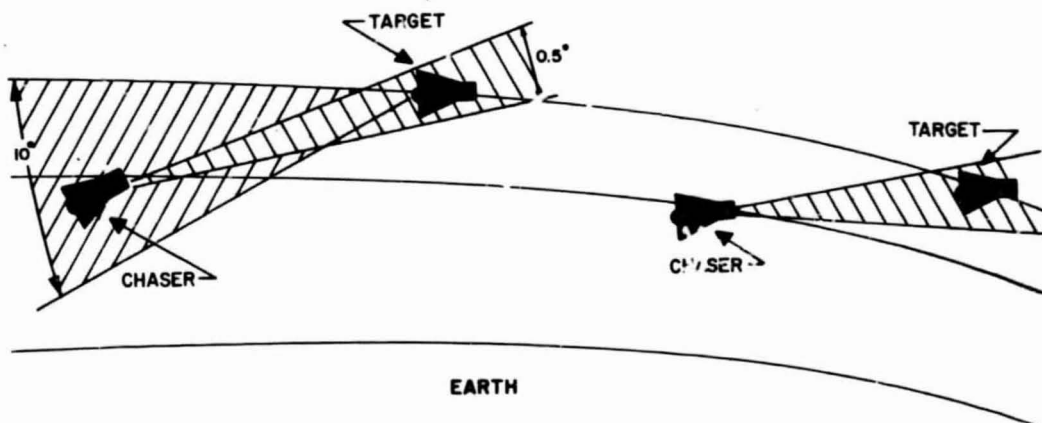


FIGURE 4. SHORT-RANGE SYSTEM

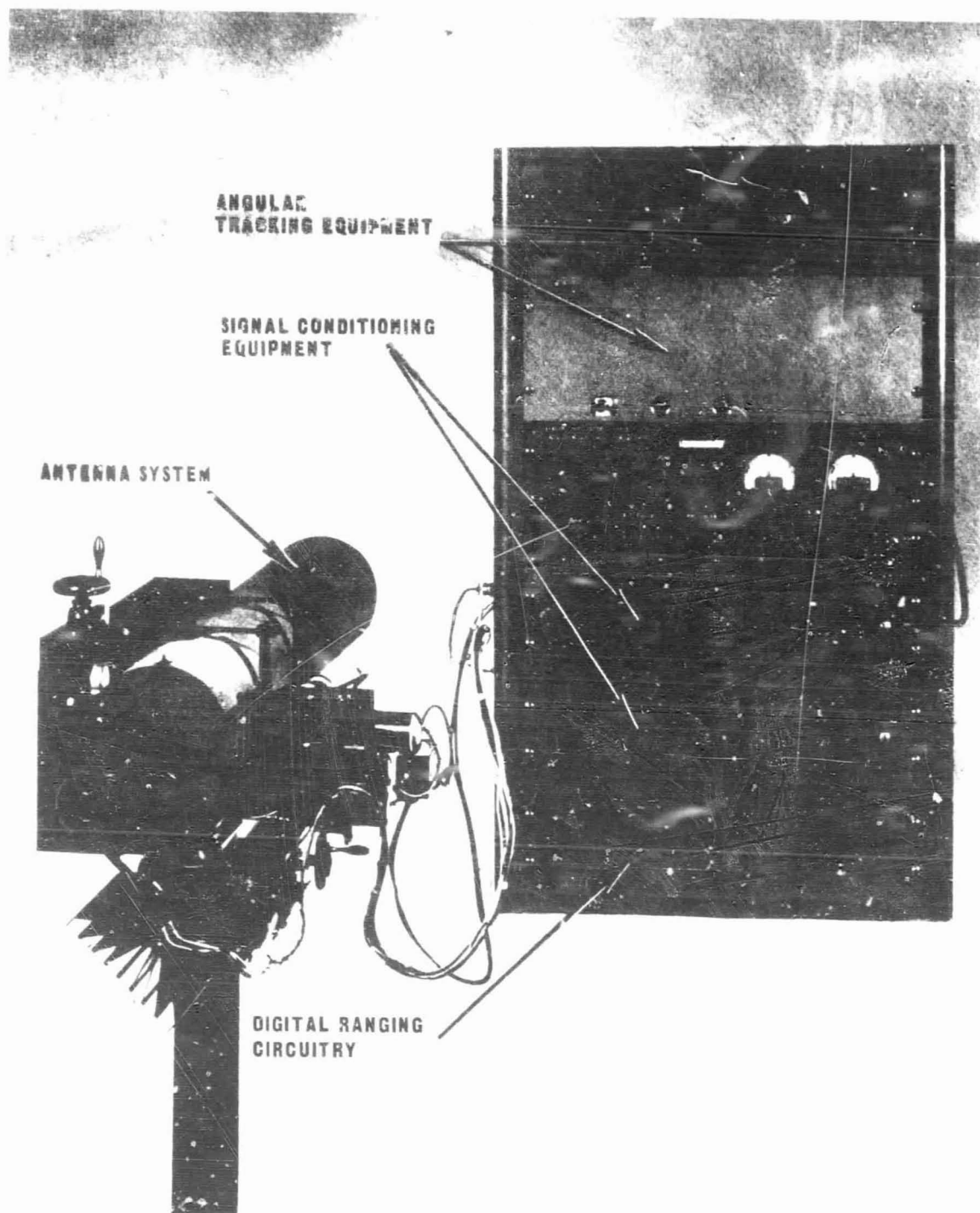


FIGURE 5. BREADBOARD MODEL OF CHASER VEHICLE SYSTEM

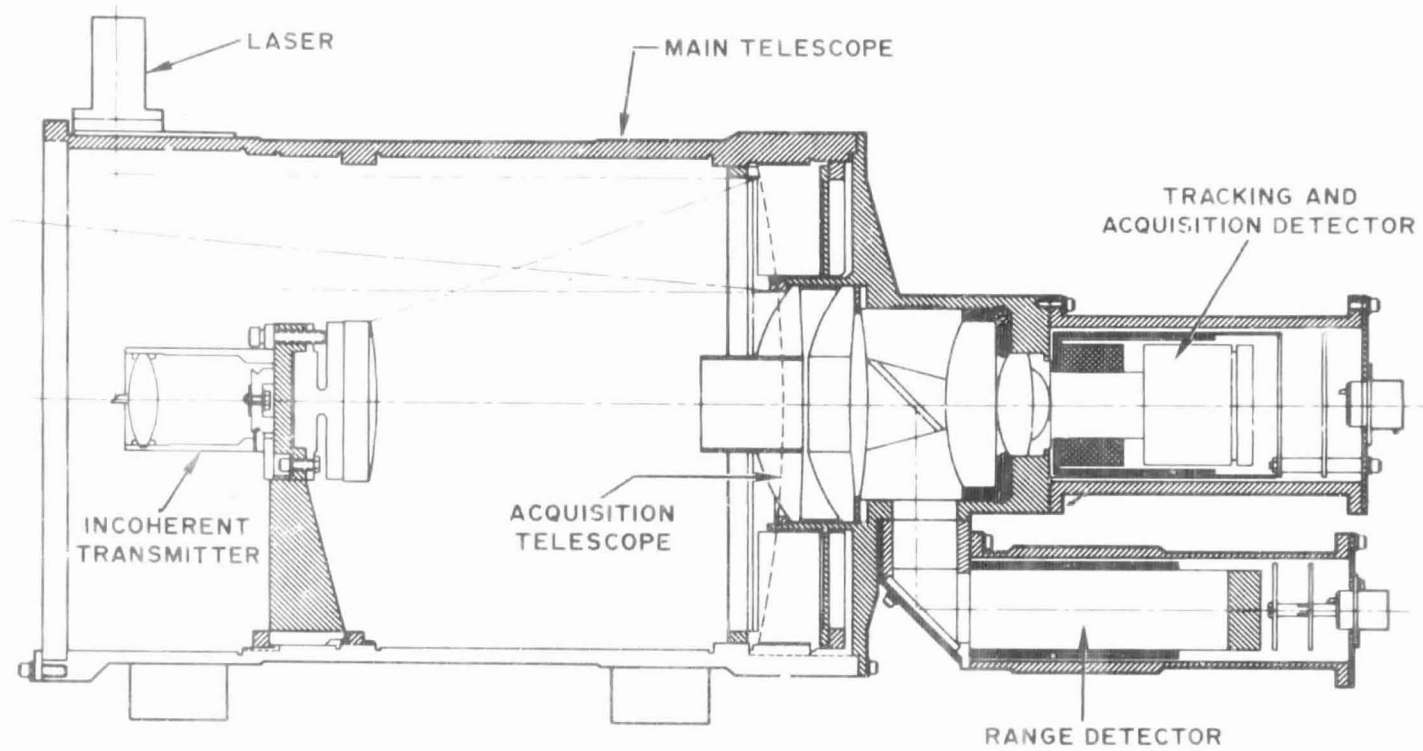


FIGURE 6. TELESCOPE, PROTOTYPE OPTICAL GUIDANCE SYSTEM

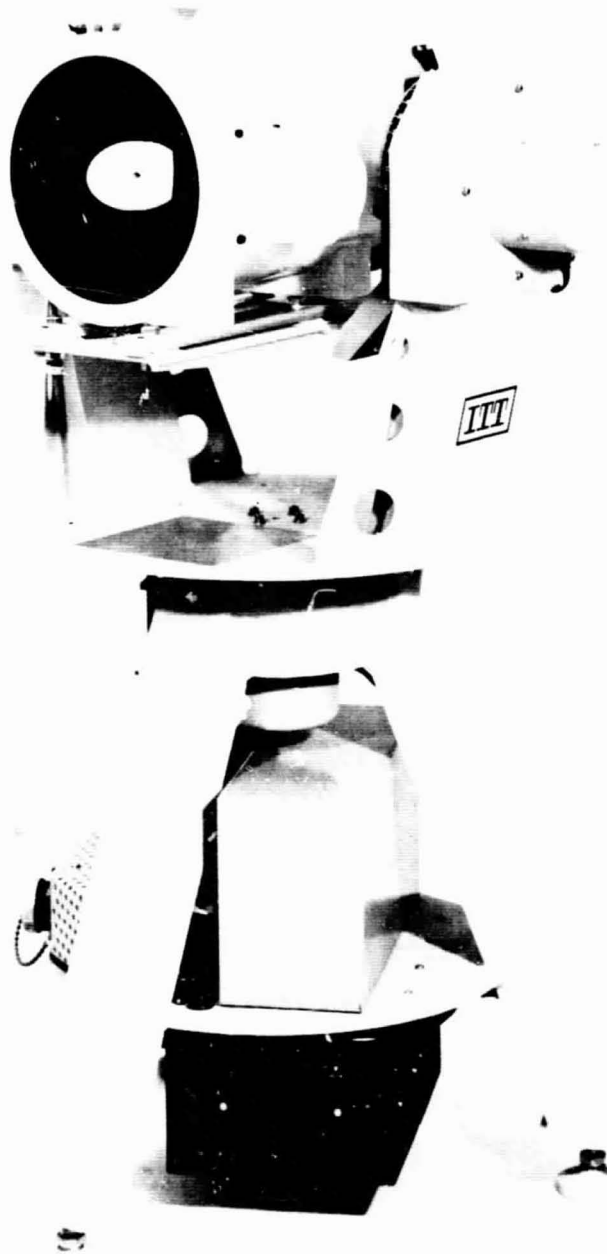


FIGURE 7. CHASER PROTOTYPE ON TRACKING PEDESTAL



FIGURE 8. OPTICAL HEAD AND MICROMINIATURIZED TRACKING AND ACQUISITION ELECTRONICS

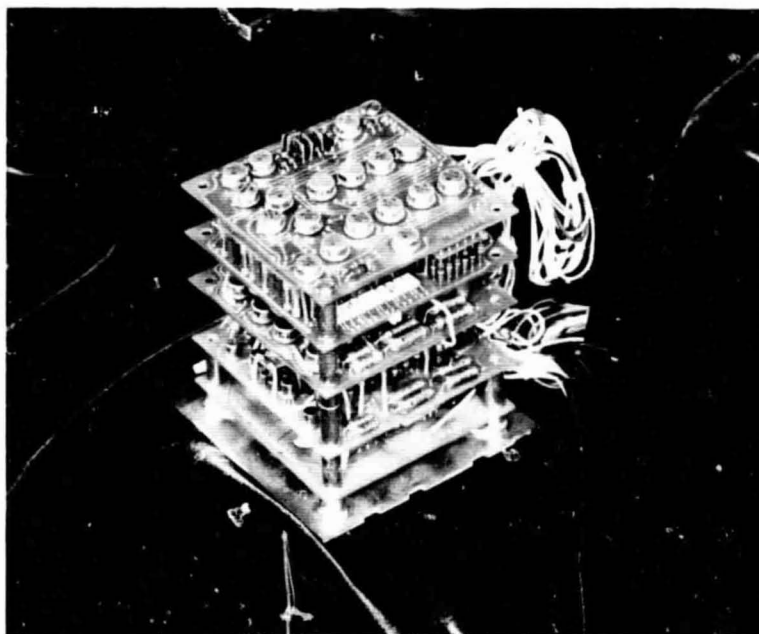


FIGURE 9. ELECTRONIC PACKAGE, PROTOTYPE SYSTEM

MEASURES RANGE: RANGE RATE, X AND Y
ANGLES, AND ANGLE RATE

- WILL RANGE AND TRACK TO 120 KILOMETERS
- RANGE ACCURACY 1/2% FROM 120km TO 3km
10cm FROM 3km TO DOCKING
- ANGLE ACCURACY 10 ARC SECONDS
- SIZE 0.025 CUBIC METER (1CU. FOOT)
- WEIGHT 15.9 KILOGRAMS
- POWER 15 WATTS

FIGURE 10. RENDEZVOUS GUIDANCE SYSTEM

	Optical Guidance System		Gemini Radar (Westinghouse)		Raytheon Locking Radar	
	Radar	Transponder	Radar	Transponder	Radar	Transponder
Weight Kilograms	16.88	1.54 Estimated	22.66	15.29	16.83 + Antenna Gimbal	2.72
Power Watts	15	10 Estimated	90		140	55
Short Range Accuracy	10.16 cm (4 in.)		15.24 m (50 ft.)		15.24 cm (6 in.)	
Angle Accuracy	0.05 mrad (0.0029°)		10 mrad (0.57°)		1.5 mrad (0.085°)	

FIGURE 11. RENDEZVOUS RADAR COMPARISON

OPTICAL TECHNOLOGY EXPERIMENTS FOR APOLLO APPLICATIONS PROGRAM

E. J. Reinbolt
J. L. Randall
Marshall Space Flight Center

N 68-31772

Present day capability of placing large experimental packages in space, along with the rapid development of lasers and associated optical components, would seem to make the exploitation of the optical spectrum for space applications inevitable. Judicious choice of flight experiments to be performed in the relatively near future can be invaluable in the implementation of optical communication, tracking, and guidance systems for future NASA programs. Because of the high degree of commonality of optical problems in space, proper selection of flight experiments will provide invaluable scientific and engineering data necessary for future design and use of large diffraction-limited optical systems for space astronomy.

The particular Optical Technology Apollo Applications Program that will be discussed has a past, a present, and a future. What is intended to be examined here is the technical and philosophical life of the program on the assumption that "the unexamined life is not worth living."

The premise of the program is that there are a number of experiments using the optical spectrum that need to be performed in space; and these experiments are so systematically related that their performance in a single integrated package represents appreciable advantages:

1. The various experiments can be performed with reasonably common elements.
2. The conditions required for the experiments are reasonably common, i.e., orbits, guidance and control, attitude stabilization.
3. The integrated experimental package itself can be considered as a single experiment giving needed design knowledge.

An examination of the literature reveals that there is a general agreement as to the potentialities of the optical spectrum for deep space. The utility of space-borne telescopes, manned or unmanned, has not been seriously questioned.

There have been, of course, many statements as to the difficulties of realizing that potential.

The principal advantage of the laser for communication lies in its ability to deliver a highly collimated (fractional arc-second), high-energy, high-frequency beam with relatively small apertures. High bandwidth is a consequence of these features. The greatest criticisms are generally based upon the difficulty of pointing such a beam and hence a limitation upon the degree of useful collimation. Other criticisms are based upon the problem of the atmosphere in the transmission link and the requirement for the use of diffraction-limited optics. Figure 1 shows the size of aperture required to achieve these diffraction-limited beams as a function of wavelength. For example, an HeNe laser operating at 0.6328μ would require approximately a 127-cm (50-in.) aperture to achieve a 0.1-arc sec beamwidth (half power); yttrium aluminum garnet, neodymium doped, at 1.06μ would require a 215.9-cm (85-in.) aperture for a 0.1-arc sec beam; and a CO₂ nitrogen laser at 10.6μ a 215-cm (85-in.) aperture for a 1-arc sec beam.

The principal advantage of the space-borne telescope for astronomical use lies in the elimination of the atmosphere as part of the "seeing" path. The space-borne telescope allows observation without the deleterious absorbing and scattering effects of the atmosphere; and it allows the resolution to be limited only by the aperture and optical imperfections rather than the approximate 1 arc second allowed by the atmosphere. Some of the problems associated with realizing the advantage of the astronomical telescope in space are: focus and alignment, pointing, stabilization and attitude control, attaining and maintenance of the mirror figure, and man's function in the system. Again, these are problems that are present in all space-borne optical systems.

Other papers herein have indicated the nature and degree of MSFC's involvement in optical technology, laser and laser components, and systems development. This program has been pursued in close cooperation with OART. In 1963, MSFC and OART believed that the state of laser and optical technology was at such a point that the planning for a major space experimental system was both warranted and needed to secure necessary experimental data and to provide an engineering demonstration of optical technology capabilities on a timely basis. To explore this belief further, a contract was let to the Perkin-Elmer Corporation by MSFC in June 1964. The contract was entitled "Determination of Optical Technology Experiments for a Satellite" and was completed in February 1965.

In an experimental effort of the nature we are discussing, the experiments and the spacecraft tend to become one. To avoid too great a generality and to provide a study framework for this initial effort, a Saturn IB-Centaur launch

capability was assumed. This assumption did not, and still does not, mean that there has been any sort of precommitment to this configuration. Perkin-Elmer was also directed to assume that part of the experimental package would be the incorporation of a primary reflector of sufficient size to uncover major problems involved in the operation and maintenance of large diffraction-limited surfaces in space, that one experiment would be the establishment of a two-way, 10-MHz bandwidth, laser communication and tracking link between the spacecraft and a ground station or stations, and that this link would be used to examine the problem of deep-space communications. These requirements were not particularly restrictive, but, rather, they tended to coalesce a great many optical technology requirements. To reiterate, some of the requirements of both deep-space communication systems and of space-borne telescopes are diffraction-limited performance of large apertures, fractional arc second guidance, isolation from vehicular disturbances, and ground controlled testing and adjustment.

In the execution of the study Perkin-Elmer noted that there was sufficient commonality in problems associated with the primary mirror and the requirements for a deep-space communication system to allow concentration on the communication aspect with no appreciable loss in generality. The selected experiments, or experimental areas, are listed. The communication experiments were chosen, where practical, to demonstrate communication requirements for ranges to 160×10^6 km (100×10^6 mi).

The selected list of optical technology experiments that resulted from this study are:

1. atmospheric scintillation effects on coherent beams,
2. atmospheric effects on plane and circularly polarized light,
3. remote manual optical alignment on earth by an eye-hand servoloop,
4. optical heterodyne detection on the satellite,
5. optical heterodyne detection at the ground station,
6. tracking to 0.1 arc second in the satellite,
7. point ahead experiment,
8. space-to-ground-to-space loop closure,

9. tracking in presence of spacecraft motion,
10. telescope suspension system comparison,
11. transfer of tracking from ground station A to ground station B,
12. earthshine effects on acquisition and tracking schemes,
13. communication system with a bandwidth of 10 MHz, and
14. on-board determination of the effects of space environment on the large diffraction-limited optics.

An examination of this preliminary list bears out our previous statement about the commonality of experimental conditions, components, and the overall systematic relationship. The Perkin-Elmer final report discusses these experiments in some detail. All we can do here is touch lightly upon a few of them for conceptual purposes.

The basic concept for the two-way experimental and communication link is for the ground station and the spacecraft each to have a laser beacon and a precise tracking system so that each can track the other. Figure 2 shows a possible configuration for the spacecraft, which would have two telescopes with which to perform the basic experiment of acquiring, tracking to 0.1 arc sec, and communicating with large information bandwidth to the ground station. No sophisticated experiments, such as point ahead, tracking transfer, etc., would be attempted with telescope 1; reliable performance would be the main goal. Telescope 2 is the same size, but it is equipped to perform such experiments as point ahead, tracking transfer, optical heterodyning, and use of different lasers and laser optical components.

A synchronous circular orbit with the orbit plane tilted from 30° to 60° to the equatorial plane seems well suited to the experiment requirements. A low-altitude orbit would require excessive angular tracking rates in view of 0.1-arc sec tracking accuracy and would not simulate the angular rates encountered in deep space. A synchronous circular orbit in the equatorial plane would give no angular motion. If the orbit plane is tilted to the equatorial plane, an observer on the equator would see the satellite perform a figure eight motion. For an orbit plane that is 60° to the equatorial plane, the maximum east-west and north-south angular rates as observed on the equator are very close to the earth rotation rate and expected space rates of 70μ radian/second. The angular rates would be modified for an observer situated away from the equator. It may be that an elliptical synchronous orbit would be more practical. This would depend on the launch vehicle, launch site, ground station location, and spacecraft weight and size.

The use of beamwidths of the order of a few tenths of an arc second requires that the beam be accurately pointed to a fraction of its beamwidth if it is to communicate with another station. A scheme for tracking to 0.1 arc second and then pointing a laser to a few tenths arc second in the proper direction is shown in Figure 3. Common optics are used rather than a tracking telescope and a transmitting telescope because of the size reduction and the difficulty of boresighting and maintaining the boresight of two large independent telescopes. Both the ground station and the spacecraft could have telescope systems similar to this.

The received light from the ground station will be reflected by the primary Newtonian flat and reflected to the coarse optical tracking sensor. The error signal is generated by a prism that splits the focused light into four detectors. This error signal is used to move the telescope so that the received light falls through a hole onto a secondary mirror and, through optics, to a fine tracking sensor of the same general type as the coarse sensor. The field of view through the hole is 2 arc minutes. Because the mass of the telescope is so large, the fine tracking is done with a transfer lens. As the image moves off the apex of the prism, the error signals generated are fed to a transfer lens to bring the image back to the apex of the prism. At the same time this motion of the transfer lens corrects the pointing of the transmitter laser (Fig. 3). This technique has been used in Stratoscope II to track to 0.1 arc second. The information is then transmitted by a laser and modulator that transmits back out the same optics. If point ahead is required, a transfer lens can be placed at the laser to give the desired lead angle.

The Gregorian telescope is shown only for the purpose of illustrating the concept. It has a disadvantage in that the secondary mirror is beyond the focus of the primary. This makes the telescope rather long if an 81.3-cm (32-in.) primary is desired. A Cassegrain form has the secondary in front of the focus of the primary and thus can be shorter. At this stage of design, a modified Cassegrain known as a Ritchey-Chretien form with an 81.3-cm (32-in.) f/3 primary held to 1/50 wavelength appears to be a good choice. It has good off-axis properties to $\pm 0.5^\circ$.

Another requirement for a deep-space optical communication link is the ability to point a laser back at a distant transmitter. This will almost always require a point ahead because of the transverse velocity of the two stations relative to each other. The lead angle for a two-way link is about 2 arc seconds per 1.6 km/sec (1 mi/sec) transverse velocity. The velocity of the earth in orbit around the sun is about 29 km/sec (18 mi/sec); therefore, for a station in deep space, lead angles up to 36 arc seconds may be required. The spacecraft may add transverse velocity that might increase or decrease this lead angle.

The proper lead angle can be computed on earth or in the spacecraft because the geometry of the two stations is known from tracking data. The transmitted beam from the spacecraft must then be pointed ahead at the proper angle. The accuracy of the lead angle, which is to be provided by the transfer lens mentioned earlier, must be less than the transmitted beamwidth to hit the ground beacon. A device that is 0.1 percent accurate would give an error that is less than anticipated beamwidths. It is believed that this can be done. However, the proper direction in which to point ahead must be determined. For a 0.1-arc sec beamwidth and a 36-arc sec point ahead, the accuracy with which this angle must be measured is 0.05° or 3 arc minutes. For smaller lead angles or larger beamwidths, the accuracy required is less severe.

Two methods are considered at the present to establish this reference angle. One is to polarize the light of the ground beacon to the proper lead angle. This could be detected at the spacecraft, and the spacecraft could be rolled about the telescope line of sight to the proper direction and the lead angle could be fed to the transfer lens. This technique could be fairly simply mechanized. An orbital spacecraft could use this method, but calculations show that this method has a serious drawback in the case of deep space because of low signal-to-noise ratio. This is true because of the fraction of total received power used for this polarization sensor. A second technique might use a star tracker to establish a given direction; the proper lead angle could then be computed.

A point ahead experiment is being considered. The experiment could use the polarization technique. To simulate a 36-arc second lead angle, a ground station could be located 5.8 km (3.6 mi) away (corresponding to 36 arc seconds at 32 200 km (20 000 mi) from the ground beacon. The satellite could then perform the point ahead angle experiment, and the beam would be received at that ground station. Evaluation of the ability to perform point ahead can be made from the experiments.

Because we consider the tracking and point ahead to be critical experiments, MSFC has instituted a contract with Perkin-Elmer to study theoretically and experimentally the following points:

1. boresight alignment,
2. focusing,
3. laser beam wander,
4. point ahead,

5. rotational line-of-sight measurements, and
6. laser beam transmitter-receiver interference.

Sample calculations on what can be done in the communication area are shown in Figures 4 and 5. The limiting assumptions are noted on the charts. The ability to transmit this data rate or better, of course, is dependent on how able we are to solve the laser tracking and point ahead problems that have been discussed.

Experiments are planned to determine the merits of optical heterodyne detection. The theoretical advantage of optical heterodyne detection is that of increased sensitivity in the presence of high background radiation. However, there are practical problems that will limit its use. One is the increased complexity because frequency-stable lasers that must have elaborate control and must account for large Doppler shifts are required. Second, the atmosphere will partially destroy the coherence of the wavefront at the collector and thus degrade the performance.

Coherent or heterodyne detection experiments could be performed. These results can then be compared to a communication link using predetection narrow band filtering and coherent detection.

A class of experiments that has considerable bearing on optical heterodyning and any other mode of optical communication is that dealing with atmospheric effects on optical transmission. Experiments to measure the effects of the atmosphere on coherent beams are:

1. Measurement must be made of the amplitude and frequency distribution of light after passing through the whole atmosphere.
2. Angle of arrival fluctuations should be measured. This would be useful in tracking system performance evaluation.
3. Since polarization might be used to determine the reference angle for point ahead and in a pulse code modulation/polarized light communication system, the effect of the atmosphere on plane polarized and circularly polarized light needs to be determined.

These experiments would be carried out for earth-to-spacecraft and spacecraft-to-earth paths as a function of collector aperture size, laser frequency, meteorological conditions, and slant angles.

We have mentioned before that a major advantage of the laser was its ability in conjunction with suitable optics to deliver a highly collimated beam of light from relatively small apertures. To do this it is required that the primary mirror in the telescope and the other optics be diffraction-limited. The monitoring of this performance as well as the possibility of making corrective adjustments is an experimental area of great importance.

One rather simple but effective monitoring method is to measure the pattern of the beam on earth and determine if the beam pattern corresponds to the theoretically calculated Airy disk. This test would not involve corrective procedures nor would it determine what part of the mirror has departed from its original shape.

To make a thorough analysis of the figure of the primary mirror, it would be necessary to place a measurement apparatus in the spacecraft. A phase measurement technique could be utilized to monitor the mirror. Because of the complexity of such a technique, a man might be necessary in the loop for this measurement. This would possibly require some sort of eye-hand servo-loop with the man making the necessary alignments with television. With such a technique, every section of the mirror could be examined and a procedure carried out to correct for slight changes in the shape of the mirror. The details for this experiment have not been determined at this time. However, such an experiment is worthwhile and further study will be made.

If we refer again to the list of experiments given earlier in this paper, it is obvious that we have taken only a superficial look at some of the experiments and have not even discussed others on the list. The intention has been only to give a feeling for the nature or general class of the experiments and to underscore the close interrelationship of the majority of them. It is not given as some inviolable list that is subject to no modification or rejection. However, we do feel strongly that this list and the study connected with it does justify the viewpoint that there are a substantial number of optical technology experiments that are closely related, use common elements, and share a common space environment requirement; and furthermore, that these experiments are feasible and can be performed with present or near present technology. It is interesting to note that essentially every experiment on this list is discussed in some depth by papers given at this conference, papers representative not only of MSFC interests but those of other NASA Centers.

So far we have discussed the past. Now we would like to discuss some of our present and future plans. Earlier, the statement was made that the Perkin-Elmer study was deliberately made somewhat restrictive to prevent too much

generalization. However, the results of that study have given us such a feeling of confidence in the desirability and feasibility of such an experimental package that an expanded study was deemed desirable. An examination of the 14 experiments suggests that we can make four broad and systematically related categories:

1. optical technology with emphasis on diffraction-limited performance, fractional arc-second guidance, and inflight testing and adjusting of optical systems,
2. optical communication and tracking with emphasis on deep-space aspects,
3. effects of the aerospace environment on the optical technology and communication problems with special emphasis on thermal problems, isolation from vehicle disturbance (man-made or otherwise), detection and correction of deterioration of optical quality, effects of background radiation and atmospheric effects on transmission, and
4. other experiments compatible with 1, 2, and 3, but that will not interfere with the basic purpose of 1, 2, and 3.

Of course, the consideration of these experimental categories must include a definite determination of man's possible function in the experiments and the maximum utilization of Apollo hardware.

In looking at the categories one might decide that they are so broad as to include anything. This is not intended. For example, we do not picture this as an astronomical package, in the sense of going through a routine of observation of celestial bodies. It is desired that the technology experiments generate data of use to those planning large space observatories. Again, for example, we do not intend that the experiments be devoted to earth observational sciences but we would hope that the technique and experimental data gained could be of great service in this area.

Two parallel study contracts were let in October 1965 by MSFC with OART's concurrence, one with the Chrysler Corporation and the other with the Perkin-Elmer Corporation. The experimental categories we have just been discussing are incorporated into the contract objectives. The reason for the two contracts is to obtain competent, independent, technical viewpoints. At the termination of the studies we intend to have enough information to intelligently choose between possible, and alternative, experimental systems and to have

established the feasibility of the program in enough detail to make possible an intelligent choice as to whether or not to proceed further. We will also have determined how the experimental systems can best make maximum use of NASA developed hardware and technology; in other words, how it can best fit into the Apollo Applications Program.

Previously it was mentioned that the experimental areas we are considering should be of considerable interest to other centers. While OART has selected MSFC to manage the study program, direct participation of interested NASA centers is both solicited and expected. To provide form and substance to that participation we have requested OART to assist us in setting up an Ad Hoc Working Group. The group would be composed of members from various interested centers and NASA Headquarters elements. This would be done to insure that the total technical input of NASA is considered rather than just that of MSFC. It would give all concerned an opportunity to evaluate the suggested experiments as the contractor proceeded. Such a working group could give material assistance in getting maximum value from the two contractual studies.

Rather than reiterate what we have said several times, I shall bring this paper to an end with a Shakespearian quotation, "There is a tide in the affairs of men which, taken at the flood, leads on to fortune; ---." We believe that space optical and laser technology is in such a flood tide; and that, by pursuing the Optical Technology Experiment System approach, a technical fortune is possible.

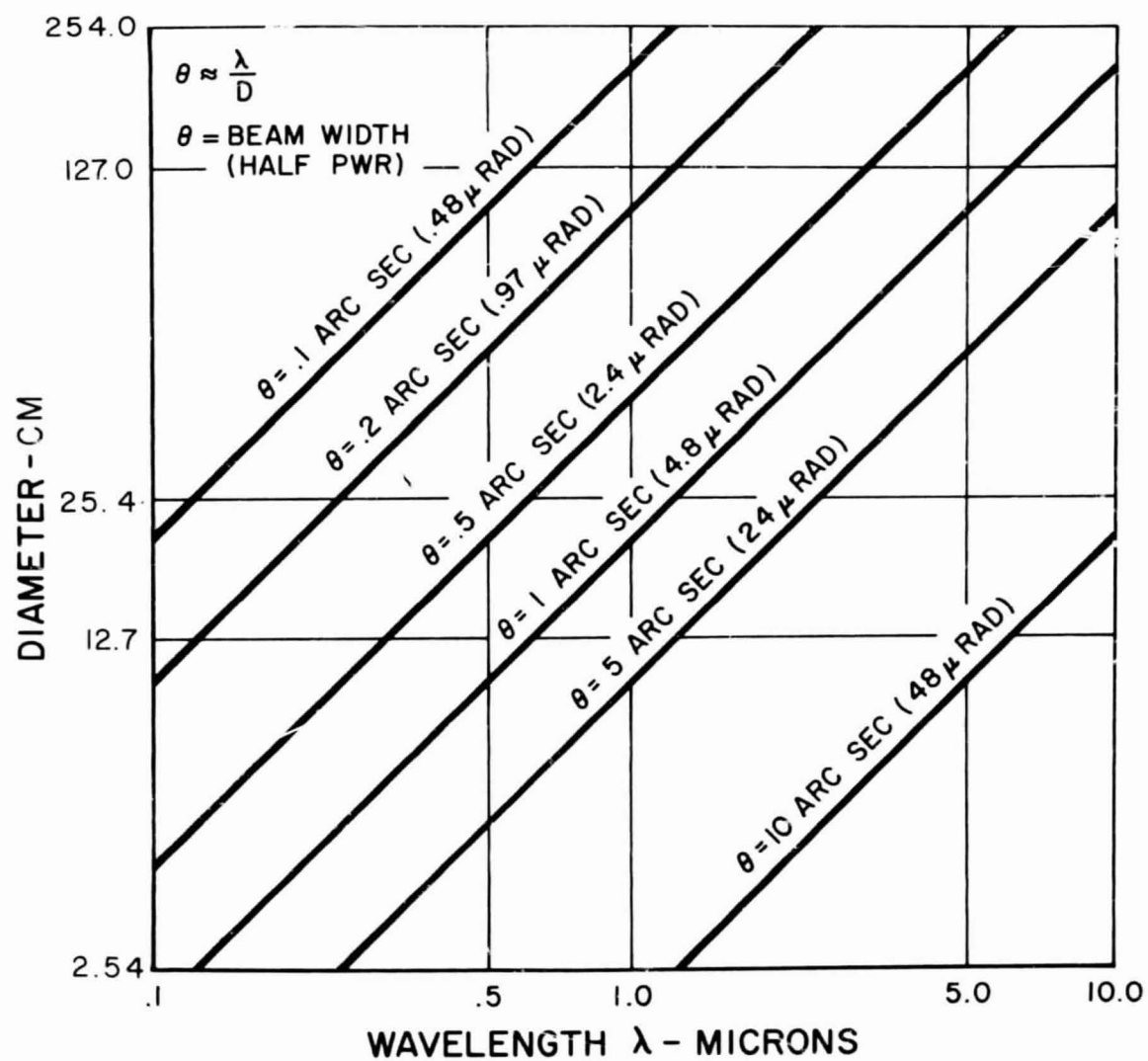


FIGURE 1. APERTURE VS WAVELENGTH FOR VARIOUS BEAMWIDTHS

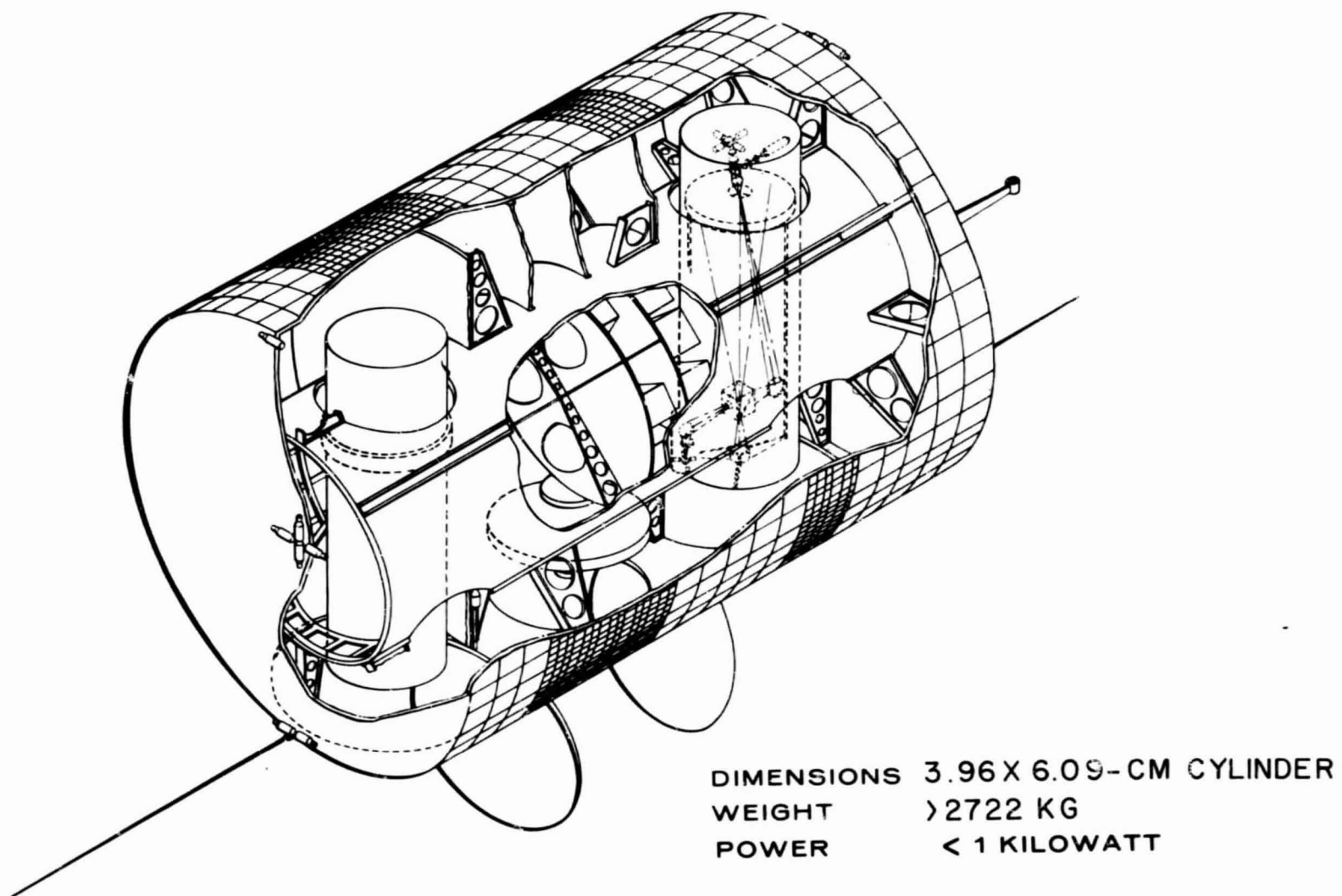


FIGURE 2. OPTICAL TECHNOLOGY EXPERIMENTAL SYSTEM

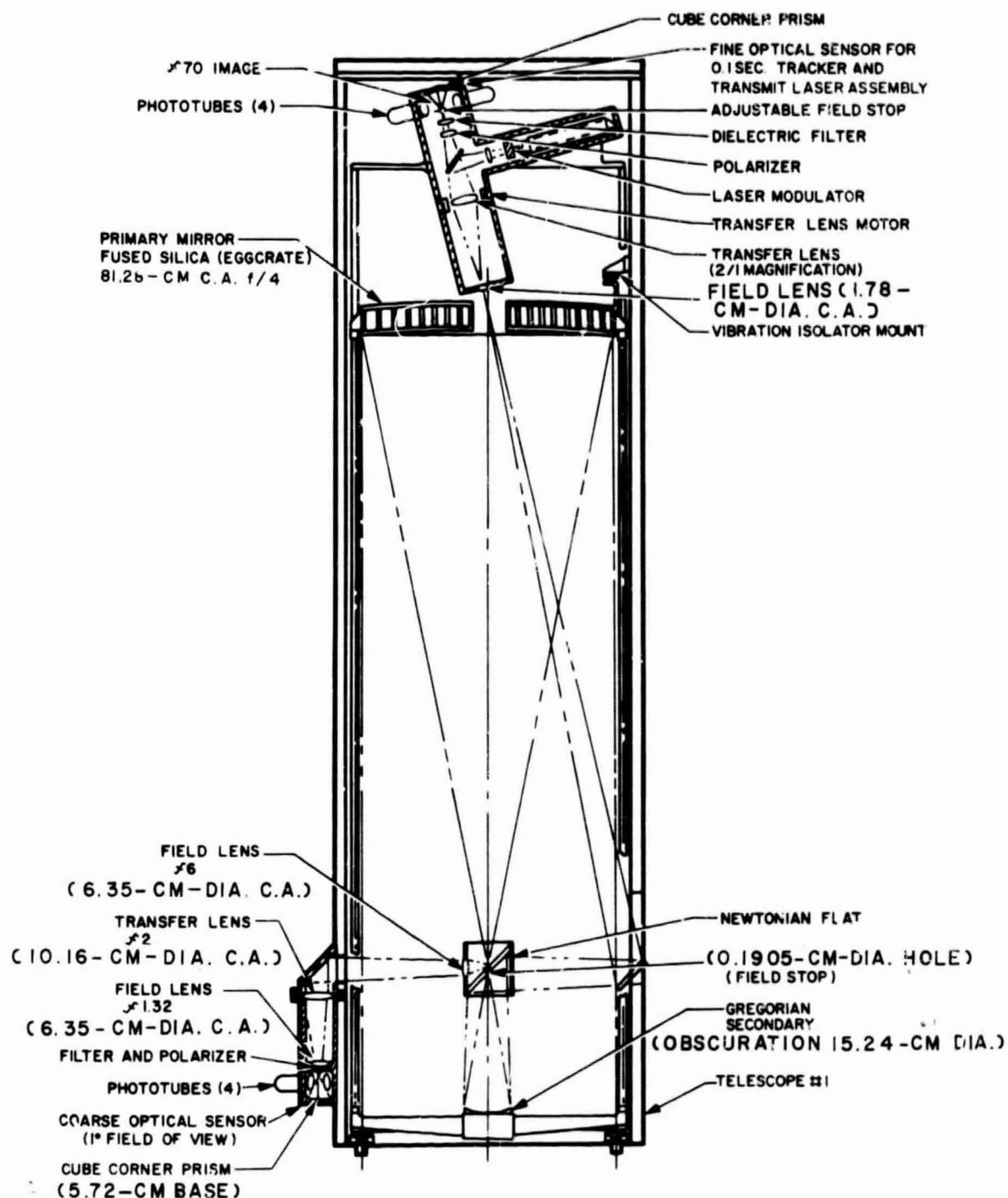


FIGURE 3. TELESCOPE ASSEMBLY

PARAMETER	RECEPTION ON EARTH FROM SATELLITE		RECEPTION IN SPACE FROM EARTH	
RANGE KILOMETERS	3.7×10^4		3.7×10^4	
WAVELENGTH	6328 \AA		8400 \AA	
TRANSMITTED POWER (WATTS)	0.01		0.5	
TRANSMITTED BEAM DIVERGENCE	0.16 ARC SEC		3 ARC SEC	
DIAMETER OF TRANSMITTING APERTURE	100 CM			
DIAMETER OF RECEIVING APERTURE	30 CM		100 CM	
RECEIVER FIELD OF VIEW	20 ARC SEC		3 ARC SEC	
OPTICAL TRANSMISSION (ATMOSPHERE)	70%		85%	
OPTICAL SYSTEM TRANSMISSION	50%		50%	
PREDETECTION FILTER TRANSMISSION	15%		50%	
PREDETECTION FILTER BANDWIDTH	0.5 \AA		5.0 \AA	
CAPACITY FOR PCM - PL 5-BIT CODE	DAY	NIGHT	DAY	NIGHT
MODULATION (BITS)	1×10^7	1×10^7	1×10^5	1×10^5
PROBABLE RATE OF ERROR PER BIT	$< 10^{-5}$		$< 10^{-5}$	

FIGURE 4. LASER COMMUNICATION BETWEEN SATELLITE IN SYNCHRONOUS ORBIT AND EARTH

PARAMETER	RECEPTION ON EARTH FROM SPACE-PROBE		RECEPTION IN SPACE FROM EARTH	
RANGE KILOMETERS	16^8		16^8	
WAVELENGTH RECEIVED	6328 A°		8400 A°	
TRANSMITTED POWER (WATTS)	0.1		200	
TRANSMITTED BEAM DIVERGENCE	0.16 ARC SEC		3 ARC SEC	
DIAMETER OF TRANSMITTING APERTURE	100 CM			
DIAMETER OF RECEIVING APERTURE	1000 CM		100 CM	
RECEIVER FIELD OF VIEW	20 ARC SEC		3 ARC SEC	
OPTICAL TRANSMISSION (ATMOSPHERE)	70%		85%	
OPTICAL SYSTEM TRANSMISSION	50%		50%	
PREDETECTION FILTER TRANSMISSION	15%		50%	
PREDETECTION FILTER BANDWIDTH	0.5 A°		1.0 A°	
CAPACITY FOR PCM - PL 5 BIT	DAY	NIGHT	DAY	NIGHT
CODE MODULATION (BITS)	3.2×10^6	9.9×10^6	1×10^5	1×10^5
PROBABLE RATE OF ERROR PER BIT	0.18	0.0012	4×10^{-5}	4×10^{-5}

FIGURE 5. LASER COMMUNICATION BETWEEN A DEEP-SPACE PROBE AND EARTH

PRECEDING PAGE BLANK NOT FILMED.

SOME ASTROPHYSICAL INSTRUMENTATION CONSIDERATIONS RELATED TO SPACE OPTICAL TECHNOLOGY

N 68-31773

G. A. Vacca
NASA Headquarters

Instrumentation is fundamental to the success of all NASA missions. Manned earth orbital flights; landings on the moon; unmanned scientific flights to Mars, Venus, or other celestial bodies; all require sensors and instruments on the ground and in spacecraft for success.

In the context of space exploration, astrophysical instrumentation describes those devices needed to study the phenomena encountered in the earth's atmosphere and in interplanetary and interstellar space and to measure the characteristic physical properties of celestial bodies and their environments. Typical phenomena to be measured are gravitational and electromagnetic fields; the radiation and composition of planetary atmospheres; interplanetary charged particle fields; and the spectra of stellar radiation. Since the penetration of the earth's atmosphere has now become almost routine, the previously limited observable spectrum has given way to the complete spectrum from cosmic and γ rays to the far infrared and radio waves.

Complementary to the astrophysical category of instrumentation, other instruments are required to test the behavior of launch vehicles, spacecraft materials, and models in simulator facilities and to measure spacecraft integrity and performance during prelaunch and launching and in transit.

In addition, for manned space flight, another category of instrumentation is required for the measurement of physical, physiological, and biological factors. To illustrate the wide variety of instrumentation required for space exploration, Figure 1 shows a variety of instrumentation that might be required, for example, by a space station such as one might use for a Manned Orbiting Telescope.

The third column of the chart headed "Scientific Observation" lists those instruments that would be required primarily to obtain scientific data. The first two columns list those instruments required to monitor the spacecraft and men, and the fourth column lists items required to support and insure accuracy of measurements.

The relationship between astrophysical instrumentation and optical technology is a dual one. One is to support the advancement of optical technology, and the second is to exploit it to obtain better scientific data.

A few examples of the wide variety of instrumentation problems will be considered.

Although many types of ionization gages for measuring ultra-high vacuum have been developed in the last decade both here and abroad, none of these can properly measure the vacuum found in space. Shown in Figure 2 are a number of these gages, and their ranges, and estimates of the vacuum pressure in space. At ultra-high vacuum, the common concept of "pressure" is no longer valid. For example, at atmospheric pressure, there are approximately 10^{19} particles per cubic centimeter in random motion. This large number permits the use of statistical averaging of the random gas particle motion to measure "pressure." At the pressure estimated to exist at lunar and interplanetary distances (10^{15} torr), there are only 10 particles present in 1 cubic centimeter of gas, and statistical averaging cannot be used. The level to which low pressure can be measured is still orders of magnitude from the desired level. Absolute measuring methods do not exist for very low pressure and are urgently needed. The development of mass spectrometer techniques for measuring gas compositions has progressed to a point where the use of intense ion sources and more advanced electronic counting systems should make it possible to increase the sensitivity of these analytic devices by several orders of magnitude. Knowledge of the qualitative and quantitative composition of gas residues in evacuated chambers can then be used to analyze possible sources of system limitation and thus to investigate new techniques for measuring very low pressures.

Here the advent of the laser makes it possible to change from purely passive remote sensing into an active/passive investigation, similar to radar. A strong laser source will not only serve for communication and tracking, but it would be an investigating source for actively determining characteristics of planetary atmospheres and their density by pulse interrogation.

For example, to obtain accurate data on density in the upper atmosphere, systems are being developed using the principle of backscatter of electromagnetic radiation as shown in Figure 3. Such measurements are of primary importance in connection with possible exploration of Mars' atmosphere and landings on its surface. Backscatter of laser energy is one technique being studied.

Another illustration of an application of optical technology to instrument advancement is the development of fiber optics shown in Figure 4. Fiber optics have already been used for remote viewing and photographing of events such as stage separation, where environmental conditions and difficult access prevent direct installation of cameras or TV equipment. Their improvement toward wider spectral passbands and reduced absorption is desired.

Astrophysical instrumentation and measurements are intimately related to opto-electric and opto-electronic principles. The telescope, one of the main instruments, has seen many improvements since Galileo first used it for astronomical observations. Better lens design and more powerful mirrors have helped to penetrate the universe. The original sensor, the human eye, has been greatly helped by improved image sensors, photodetectors, and photomultipliers. Considerable progress in astronomy was made when these devices, together with physical-optical concepts and methods, were applied to widen the field of astronomy into the broader one of astrophysics.

Electro-optical sensors are being developed to attain higher resolution and sensitivity and wider spectral response for TV-imaging application in meteorological satellites and planetary probes. New methods of imaging, such as a photo-transistor solid-state image converter matrix as shown in Figure 5, are being developed. A photon-limited imaging system is being developed to achieve high gain for ultraviolet photometric studies of distant nebulae.

Radiation such as that measured in the emission and absorption spectra from celestial bodies covers the whole range of the electromagnetic spectrum. From the radio frequency end where we measure hydrogen line intensities to the short-wave ultraviolet, the spectral intensity distribution, intensity fluctuations, Doppler phenomena, fine line structure, and other spectral observations have contributed to the picture that we have formed of the universe. Observations from the ground have been limited all through the centuries because atmospheric absorption permits us to look at only a portion of the overall spectrum, a band extending roughly from 3000 to 13000 Å. In removing the atmospheric barrier, use of the full electromagnetic spectrum permits us to widen our horizon on celestial observations tremendously. Particularly in the ultraviolet, the spectra of stars and the time varying spectral intensities will provide new scientific data and information.

The importance of measurements above the atmospheric and ionospheric layers with satellites has been accepted. Results have already contributed appreciably to our knowledge. We know that, in the long wavelength range as well

as the short wavelength range, the sun is a variable star. We will have to compare results obtained at different times; this requires instruments with proper time distinction and resolution to measure fluctuations. Other complications to add to the difficulties of satellite instrumentation are the lack of radiation standards in the far ultraviolet and X-ray regions to properly calibrate the instruments.

Let me now mention some typical measurement problems that we believe should be considered to obtain good data with future orbiting satellites and space probes: Radar measurements have contributed to the increase in accuracy of the astronomical unit which previously has been calculated from perturbations of planets and thus has been affected by the uncertainty of the planetary mass. For scientific space exploration we need to define the ratio of the astronomical unit to the unit of length on earth with high accuracy. Radio tracking of space probes such as Mariner has provided additional data and confirmed radar ranging data, but these data are not in agreement with the classically determined values. This leads to the base of all optical range measurements, the velocity of light. We must take into consideration that this "constant" is not only influenced by matter of substantial density as defined in the theory of gravity and relativity but also by the density distribution of interplanetary electrons. Therefore, despite the remoteness of measurement, the local density measured from interplanetary space probes helps in establishing corrected light velocity data and thus provides corrections for the distances involved between celestial bodies.

The other principal unit with which we deal in many measurements, directly or indirectly, is time. Time is a unit that has been determined with considerable accuracy already. Atomic clocks working with a stability of 10^{-11} are available. This is an accuracy that corresponds to an error of 1 microsecond per day. However, if we consider the speed of space probes, manned or unmanned, and the duration of missions extending to a year and more, it will be realized that we will require a time standard improved by two orders of magnitude, to 10^{-13} , to permit the accurate trajectory adjustments that may have to be performed on manned planetary excursions. Placing atomic clocks in spacecraft and comparing them with ground station clocks may contribute to the verification of relativistic predictions, such as the gravitational red shift.

Considering other instruments in the optical domain for astrophysical problems, it now appears that optical sensors have a definite role of position and attitude sensing for satellites. Sensors of this kind make use of photosensitive semiconductors, photocells, and imaging devices.

Spectrometers and spectrophotometers are also used for high resolution scanning and analysis along with interferometric techniques. Here again, the total spectral range from microwaves to X rays is employed. Many of these instruments are quite well developed because of their application in sounding rockets; however, the usual limitations as to weight and power consumption still appear to be problems for their use in planetary missions.

At present, raw data obtained by most space instruments goes through a variety of transformations such as amplification, modulation, rectification, digitization prior to data transmission, processing, or storage. All these steps increase system complexity and tend to decrease accuracy and reliability. Emphasis must be placed on transducers and sensing devices capable of providing output values in a more convenient form. A sensing device producing an output in digital form can eliminate many of the conditioning steps as schematically shown in Figure 6. The study and investigation of methods for achieving digital outputs from transducers is an urgent problem requiring concentrated attention.

These are a few of the instrumentation areas that must be explored to advance space optical technology. Figure 7 shows a summary of basic instrumentation requirements. Our current program efforts in astrophysical instrumentation emphasize the following:

1. Extension of Range: Development of high resolution instruments to cover the entire spectrum from ultraviolet to infrared. The greatest source of information on astronomical bodies and their evolution is contained in the ultraviolet and infrared portion of the stellar spectrum. We would like to see sensors developed in the laboratory making use of new discoveries in the solid-state field to cover much broader spectral ranges with uniform sensitivity. The study of photoelectric emissions from solids and thin-films will no doubt contribute to the expansion of the measurement ranges. For the ultraviolet area the need for wideband sources for calibrating these sensors is particularly apparent. Development of image tubes with long storage times with better sensitivity and resolution than photographic films for planetary investigations is needed.

2. Higher Accuracies: Nearly all instruments require better accuracy.

3. Combined Effects of Environment: The measurement of the extent of solar influence and determination of its boundary with galactic space, for example, suggests that plasma, energetic particles, and magnetic fields must be measured simultaneously so proper time correlated data can be obtained.

4. Better Standards: Particularly in ultraviolet and infrared.
5. Calibration: Absolute methods rather than relative methods are needed.

Not listed on this figure, but vital, is optimum compatibility of instrumentation for data processing.

Spacecraft Integrity	Biomedical Surveillance	Scientific Observation	Calibration and Standards
Vacuum Gages	Electrocardiograph	Magnetometers - (Inter-planetary Magnetic Fields)	Vacuum Calibration System
Leak Detectors	Respiration Rate and Volume Measurements	Telescopes (Stars, Nebulae)	Voltage Standards
Meteoroid Detectors	Metabolic and Circulatory Measurements	UV Spectrometers (sun)	Mass Measurement under zero-G
Mass Flow Meters	Gas Chromatograph for Organic Trace Components	IR Spectrometers (earth) (5-50 microns)	Accelerometer Calibration
Cryogenic Pressure Gages	Life-Support System Control	Radio-Astronomic Measurements	Black Body Reference Source
Cryogenic Temperature Gages	IR Detector for Carbon Dioxide	Charged Particles and Plasma Analyzers	Time Standard
Accelerometers (10^{-7} g)	Oxygen Partial Pressure Gauges	Diurnal Thermal Gradient Measurement	Frequency Standard
Mass Spectrometers	Water Reclamation Control Devices	Planetary Radiation Measurement	Light Flux Standard
Gas Chromatograph		Cosmic Ray Detectors	Standard Radiation Source
TV Surveillance		X-Ray Measurements	Pulse Signal Standard

FIGURE 1. TYPICAL INSTRUMENTATION FOR SPACE STATIONS

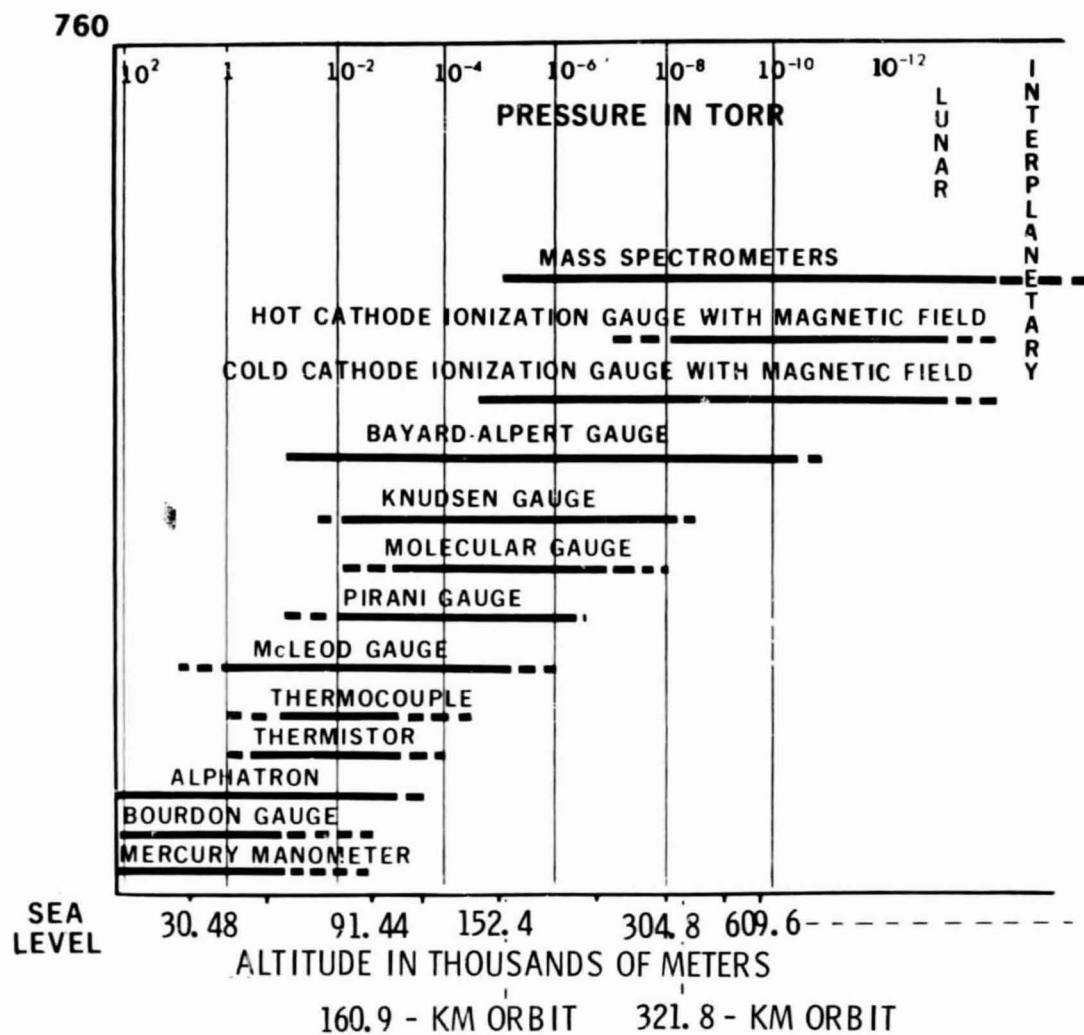
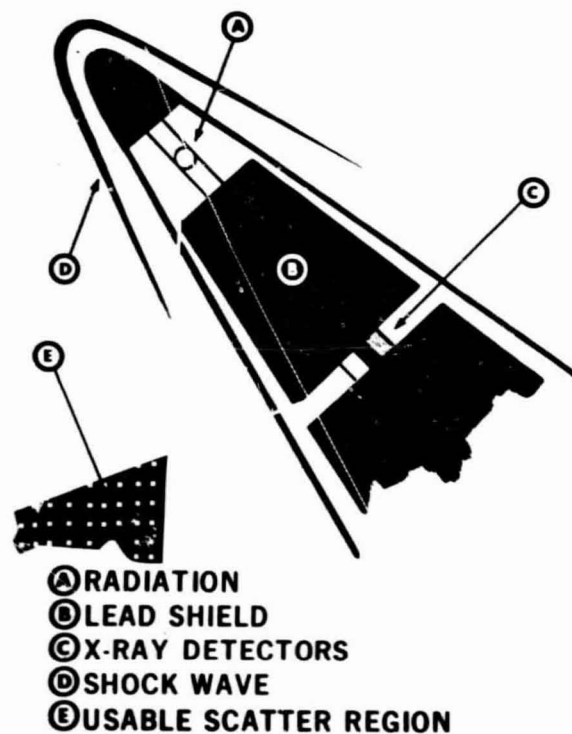


FIGURE 2. USEFUL RANGES OF VACUUM GAUGES

AIR DENSITY SENSOR SCHEMATIC



FLIGHT TEST DATA LANGLEY AIR DENSITY SENSOR

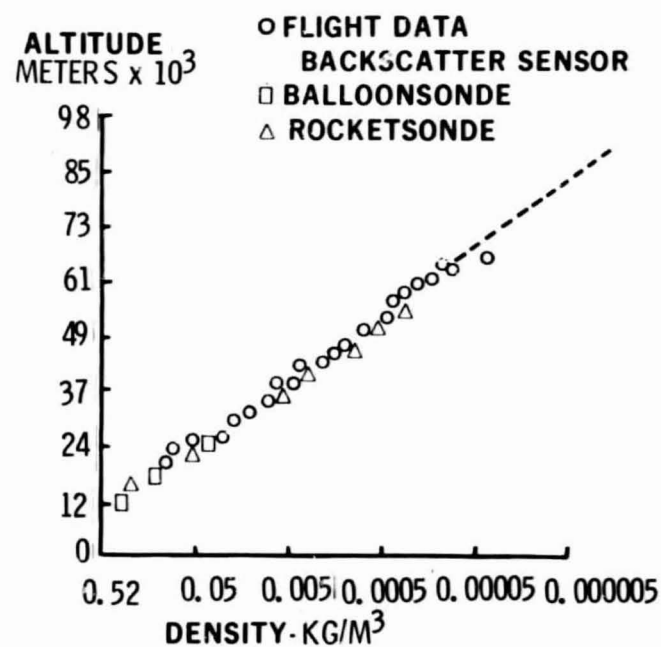


FIGURE 3. AIR DENSITY SENSOR

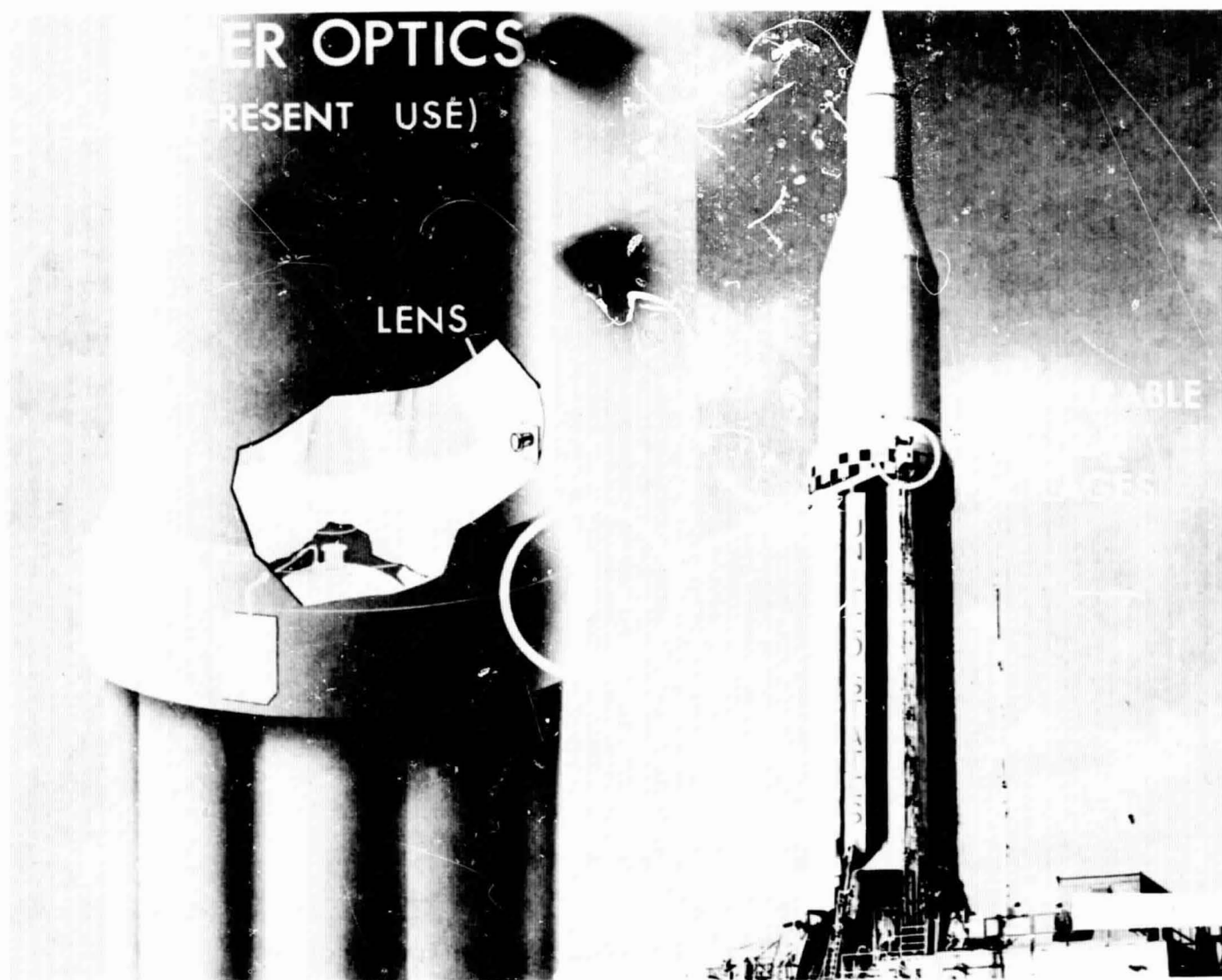


FIGURE 4. FIBER OPTICS

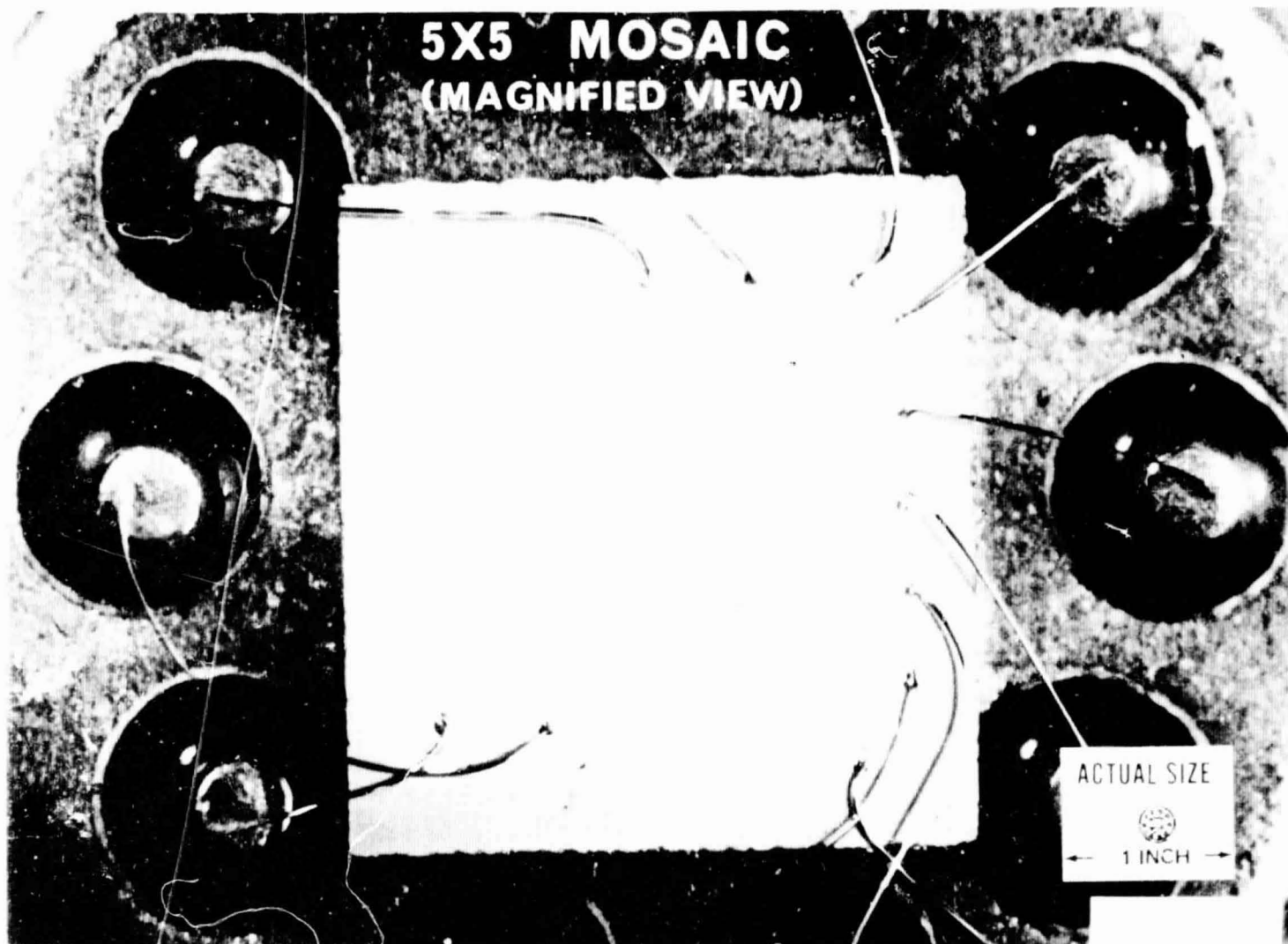


FIGURE 5. PHOTO TRANSISTOR

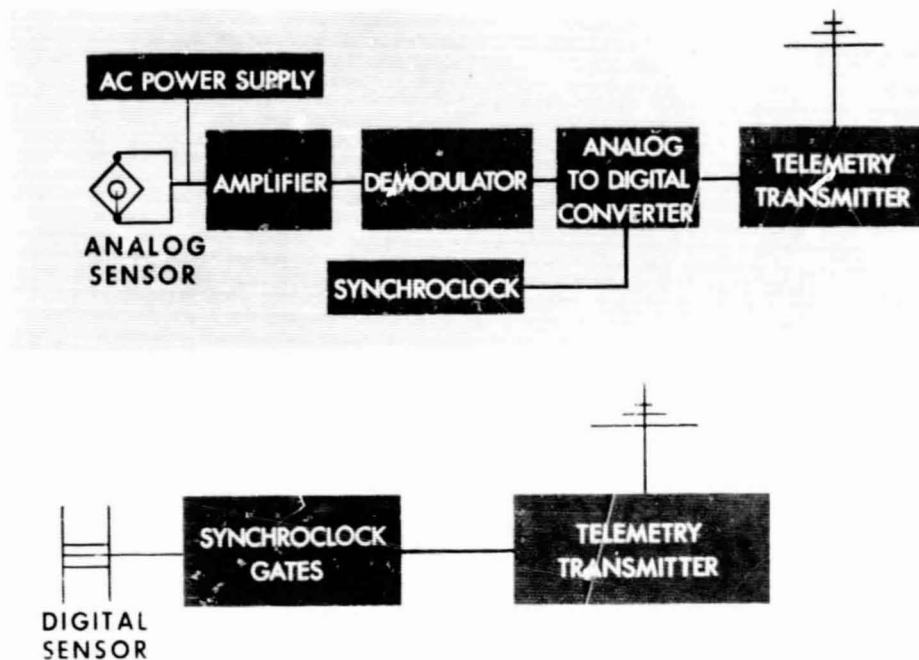


FIGURE 6. ANALOG VERSUS DIGITAL SENSING DEVICES

- EXTENSION OF MEASURABLE RANGE
- HIGHER ACCURACIES
- COMBINED EFFECTS OF ENVIRONMENTAL PARAMETERS
- DEVELOPMENT OF STANDARDS
- DEVELOPMENT OF CALIBRATION METHODS

FIGURE 7. INSTRUMENTATION REQUIREMENTS